Conformal Thinking for 3D Shaping of Bacterial Cellulose

AUTHOR: J. SMIT

Project Description

Conformal Thinking for 3D Shaping
of Bacterial Cellulose

Supervisory team

Chair: Prof. Dr. E. Karana
Mentor: E. Groutars

In Collaboration with

NextSkins
https://nextskins.eu
Joren Wierenga (BioLab, IDE TU Delft)

NEXTSKINS

Submission Date

05/03/2024

Author

Jason Smit, J.
4667654

TUDelft

Preface

Through being fascinated by designing with and for living things and my interest in 3D printing, this project emerged. Although we can not stop using the natural resources alltogether, I strongly believe that to regain our connection with nature as humanity we need to start working with living- and more regenerative materials. Keeping these materials alive forces the designer to think of ways to care for the organisms involved, resulting in a more mutualistic future.

Executive Summary

A prototype for a production method is designed that can facilitate multiple geometries of statically grown bacterial cellulose for one mould. This production method, called CelluShaping, was developed after desktop research on bacterial cellulose. Here, topics regarding the material's origin, cultural influences, its biological synthesis, material characteristics, applications and production, as well as topics regarding biodesign and conformality in design are discussed. From this research, a taxonomy is made, on which ideation on multiple principles are developed. After testing the most promising principles, a combination of two principles, where geometry is introduced through the growing bacterial cellulose sample from above the growth and from below. This principle, which is called CelluShaping, is elaborated upon and divided into its main components. From this understanding of the principle, a testing setup is designed and built. Also, a computational model, which aids in the hypothesizing of tests and is a first step in a tool to work with the production method is developed. With the testing setup and model, multiple tests are performed to test with multiple geometries and growing conditions. Finally, an overall conclusion, discussion, recommendation and reflection is given.

Terminology

|	
Bacterial Cellulose (B.C.)	Cellulose fibres produced by bacteria. In this report the cellulose is produced by the Komagataeibacter Hansenii (K.H.)
Medium	A liquid or gel-like material containing nutrients in which cells or microorganisms can be grown. The liquid medium used in this report is the CSL medium, which is similar to the commonly used HS medium.
Air-liquid interface	The top liquid layer of a liquid medium containing B.C. producing bacteria which is in direct contact with air (containing oxygen).
Conformal shaping	Being able to shape a geometry during its formation.
Vessel	The container where the medium containing the B.C. producing bacteria is situated in.

# Content

1. Introduction

This chapter starts with a short description of the project, followed by the used methodology and finally a list of research questions, related to different parts of the project.
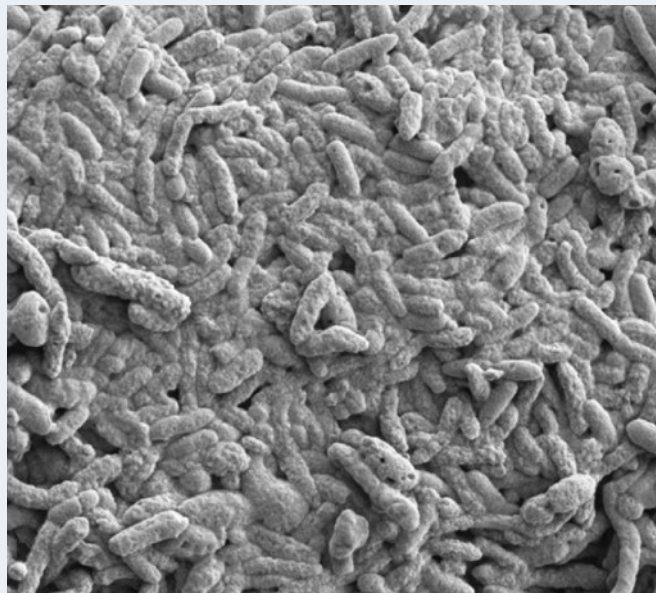
2. Literature Research

This chapter covers the literature research done on topics related to this project, answering the research questions A.1 to A.13. This being a brief history on B.C., followed by some cultural aspects of the material. Also, a more in-depth explanation is given on the formation of B.C. and what some of the current applications are of this material. Furthermore, some examples are given where cellulose was formed in 3D shapes and how the material is currently produced on an industrial scale. Finally, some explanation is given for the terms 'biodesign' and 'conformal shaping'.
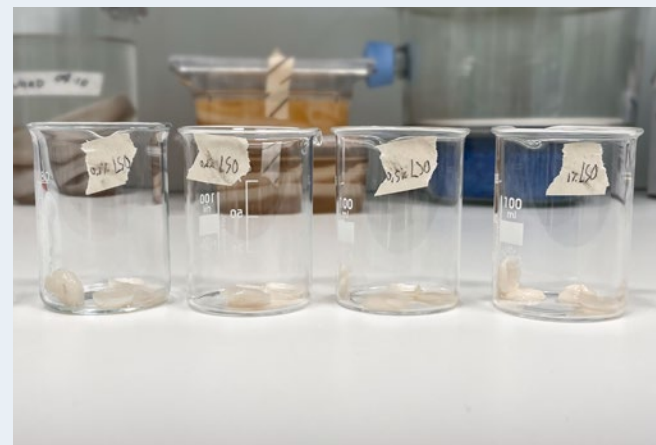
3. Material Shape Exploration

Based on the research done on the formation of B.C. and with inspiration of other projects where cellulose was shaped, new material shape explorations are conducted. In this chapter this exploration is defined into principles, which are hierarchised and tested. Finally, a selection is made from the tested principles.

4. CelluShaping

From the chosen principle, which is called CelluShaping, first the basic components are elaborated upon, answering research question D.1.. From these basic components a testing setup is designed and build (D1.1). Also, to predict the growth and to build a tool to work with the production method, a computational model is built (D.2.).

5. Testing the Setup

In this chapter, all testing of the setup is discussed. First, the performance of the setup is tested without any geometry. After this, the influence of the surface area of the profile of the geometry on B.C. growth is tested. Thirdly, the effect of conically shaped geometry versus straight geometry is tested. Finally, a more complex shape is used to test the computational model and the spacing between individual geometries.
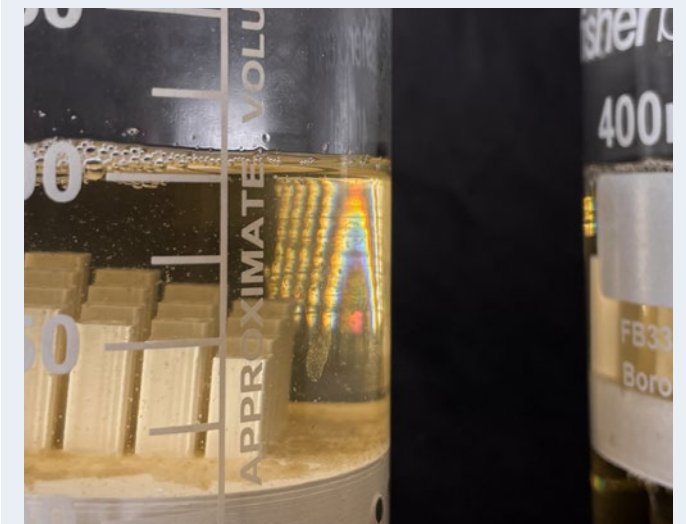
6. Discussion & Conclusion

In this final chapter, the findings of the tests performed with the testing setup are discussed. First, focus is placed upon the results regarding the B.C. samples and the testing setup. Then, some additional findings are discussed which are relevant, but do not have influence on the testing prototype. In the third part, the relevance of the findings are discussed. Next, a general conclusion is made and a recommendation on the continuation of the project is given. To close off the project, a personal reflection is made on the proces of the thesis

Introduction
TO THE PROJECT

1. Project Description

2. Methodology

3. Research Questions

This chapter starts with a short description of the project, followed by the used methodology and finally a list of research questions, related to different parts of the project.

1. Project Description

This project is carried out for the NextSkins project. The NextSkins project is a cooperation between the TU Delft, Aalto University and Imperial College. In this project, researchers come together to research and develop two new materials called the Living Therapeutical Material (LTM) and the Living Regenerative Material (LRM). The LTM is a multi-layer matrix material containing engineered micro-organisms that respond to cues excerted by the skin. This matrix material consists of B.C. and is developed to house organisms for the treatment of atopic dermatitis, also known as eczema. The LRM is a protective composite material meant for clothing that can regenerate itself when damaged. Both materials are fully biocompatible (Nextskins, 2021).

In this thesis, a new production method for the B.C. matrix of the LTM is developed. The current idea of the LTM is to produce patches which can be placed on locations of the body where for example eczema occurs. It is not defined however what geometry these patches need to be in order to fit well on the body and be unobtrusive. Also, the human skin stretches differently on different locations of the body. The patches need to be able to stretch accordingly, while maintaining its function. Furthermore, hair growth might cause the patches to come loose after some time, limiting the effective period of the LTM. Finally, to allow people to hide their Atopic Dermatitis it is considered favourable to design the patches to blend with the skin and remain imperceptible.

Currently the only options of producing B.C. is to grow it in a static- or in an agitated medium. The first solution does offer some freedom of shape, but to change the shape of the B.C. layer different moulds are needed per shape. Producing multiple moulds, that can be sterilized as well, can become a very expensive and time-consuming step in the fabrication process. Therefore, a production process that can facilitate more than one geometry per mould is needed. Researchers have also been working on FDM bio-3D printing with B.C. (Hospodiuk-Karwowski et al., 2022). This production method would allow for customizable shapes and could solve the problem.

However, scaling up with this production method to larger patches and production volume might cause problems due to the small printing volume and slow printing speed presented in the paper. A gap exists, where cellulose can not be grown in its natural microstructures from static growth, while being able to change its shape during the growing process.

Therefore, it is needed to design a new way of producing BC in a way that allows for flexibility in geometry, size and elasticity. This would not only benefit the NextSkins project, but could also benefit for example the fashion- and cosmetics industry. Bacterial Cellulose, as mentioned in the introduction, is a replacement for leather. If this new way of producing BC would exist, it would eliminate the need for additional cutting, sewing and painting.

2. Methodology

To procedurally and structurally come to a fitting result, multiple methods are followed. From the Material Driven Design (MDD) method (Karana et al., 2015) some parts are used to come to a better understanding of the material. A taxonomy, as used in a case study following the MDD method (Karana et al. 2018), was used to visualize the factors influencing B.C. growth. Also, the factors that influence each other are visualized using lines and are backed up with research papers. From these factors and the interconnections between them, design principles are created. These are hierarchized using a scoring system from the Delft Design Guide (A. van Boeijen et al., 2014). A test for proof of principle is conducted of the chosen three principles using low-fi testing methods.

For the design of a first concept of a production method to conformally change the shape of the B.C. layer in a static production, a combination of design- and scientific methodology is used. For the design of a reusable testing setup of the chosen principle, a list of requirements is made following the method from the Delft Design Guide (A. van Boeijen et al., 2014). Also, How-To's from the same book are applied in the development of elements of this setup to ideate different versions. For the use of the testing setup and the development and testing of a predicting parametric model for the B.C. growth, common scientific methodology is used where research questions are hypothesized, tested and its results discussed.

A testing setup is designed (see Figure 1), where the behaviour of the formation of cellulose can be tested in multiple shaping variations. To build strong hypothesese and work towards a tool for designers to shape B.C. using this fabrication method, a model is built alongside the tests (see Figure 2).
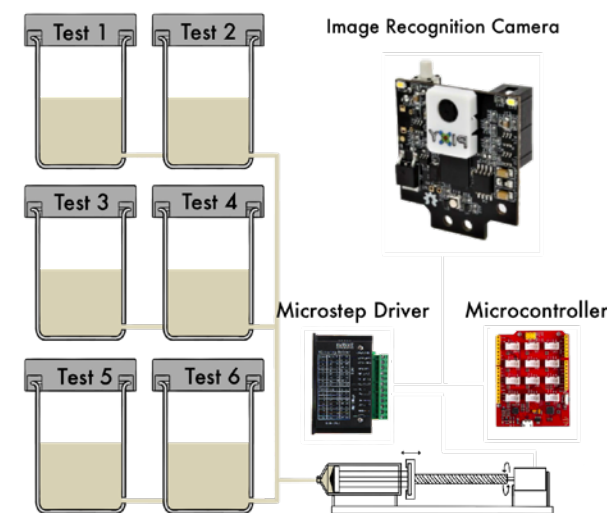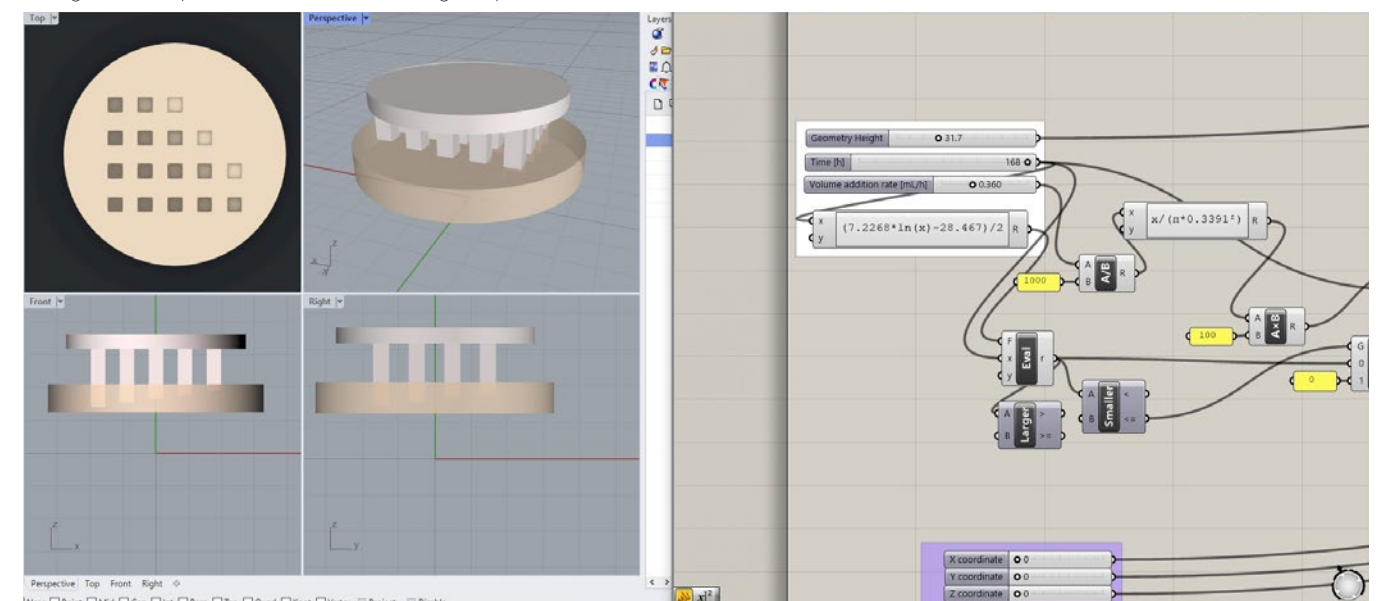

Figure 1 - Graphical overview of the testing setup

Figure 2 - Dashboard of the computational model

3. Research Questions

A. Desktop research

1. How have cellulose producing bacteria been discovered?
2. What are the cultural aspects of B.C.?
3. What biological processes are involved in the biosynthesis of B.C.?
4. How can B.C. be grown in digitally pre-designed 3D shapes?
5. What factor(s) trigger(s) the growth of bacterial cellulose?
6. What factors stimulate or inhibit the growth of B.C. and how can this be localised?
7. How do changes in growth conditions affect the mechanical properties of B.C.?
8. How can changes in 3D structures locally change the flexibility of a material?
9. What are the current applications of B.C.?
10. How is B.C. currently formed in 3D geometries?
11. How is the production of B.C. currently upscaled in industrial applications?
12. What is biodesign and how does it relate to this project?
13. What is conformal shaping and how does it relate to this project?

B. Principle testing

1. Is it possible to change the thickness of the generated shape over the x- and y-coordinates?
2. Is it possible to change the thickness variation of the generated shape over the x- and y-coordinates?
3. Is it possible to create hollow curved (shell-like) and tubular geometries?
4. Is it possible to bridge material over gaps, so air pockets can be generated within the geometry?

P1:

1. How do different types of geometry interact with the growth of B.C. when the obstruction touches the surface of the air-liquid interface?
2. How does the type of material change the behaviour of the cellulose producing bacteria when touching the obstruction?
3. How does cappilarity of the medium affect the growth when geometry is introduced above the surface of the liquid?
4. How does the level of medium over time influence the interaction between the cellulose and the obstrusion?
5. How does changing the location of an obstruction during the B.C. growth influence the resulting cellulose geometry?
6.

P2:

1. How do different types of geometry interact with the growth of B.C. when the obstruction touches the surface of the air-liquid interface?
2. Does the type of material change the behaviour of the cellulose producing bacteria when touching the obstruction?
3. How does cappilarity of the medium affect the growth when geometry is introduced above the surface of the liquid?
4. How does the level of medium over time influence the interaction between the cellulose and the obstrusion?
5. How does changing the location of an obstruction during the B.C. growth influence the resulting cellulose geometry?

P3:

1. What substances inhibit the synthesis of cellulose?
2. What substances stimulate the synthesis of cellulose?
3. How can inhibiting and stimulating substances be localised?
4. How does changing the volume of inhibiting- and stimulating substance chage the rate of inhibition or stimulation of cellulose biosynthesis?
5. What influence does surface tension have on the synthesis of cellulose?

P4

1. How does changing the location of air-liquid interfaces under the medium surface change the growing behaviour of B.C.?
2. How can B.C. layers be connected when grown in subsurface air pockets?

P5:

3. How does changing the shape of the vessel during B.C. growth affect the eventual cellulose sample?

C. Requirements Testing Setup

1. The setup needs to allow for medium addition and removal without obstructing the B.C. growth.
2. The vessel needs to be transparent.
3. The vessel and all components which are in direct air-contact with the B.C. layer need to be able to handle the circumstances in the autoclave (122 °C for 30 minutes).
4. A precision of the medium volume increase or decrease rate of at least 1.0 µl/min is needed.
5. The medium level height needs to be monitored and controlled with a precision of +-1mm (which is about +-3.4mL of volume).
6. The vessel needs to allow for the testing of multiple geometries.
7. The vessel needs to be water-tight.
8. The inside of the vessel needs to keep out micro-organisms, while allowing for air-flow from the top.

D. CelluShaping

1. How can the main principle components be defined?
1.1. How can the principle be tested in equal testing environments?

2. How can the geometrical outcome of cellulose grown on a moving air-liquid interface while being obstructed by geometry be predicted?
2.1. How does the data inserted in the model translate to the real-life shape of the grown cellulose?

3. How does the alteration of the medium volume inside the vessel of the designed testing setup alter the growth of B.C.?
3.1 How does the current testing setup affect the geometrical outcome of the B.C. sample after these medium volume changes?
3.2. How does the rate of volume added and subtracted from the vessel affect the B.C. formation?

4. How does geometry moving through the air-liquid interface affect the geometrical outcome of the B.C. sample?
4.1. In what way does the geometry in the x-y plane of the obstruction affect the B.C. growth?
4.2. What are the minimal dimensions in the x-y plane of the B.C. shaping geometry?
4.3. How does the geometry in the z-direction of the obstruction alter the B.C. formation when moving downwards through the air-liquid interface?
4.4. What is the minimal indentation the obstructing geometry can produce in the z-direction?
4.5. How does distance between geometries affect the B.C. growth?
4.6. What effect do the capillary forces on the air-liquid interface caused by obstructing geometry have on the formed cellulose layer?

5. How does obstructing geometry affect the density of the grown cellulose sample when moving through the air-liquid interface?
5.1. How does volume rate affect the density?

Literature Research

ON BACTERIAL CELLULOSE

1. History on B.C.

2. B.C. in Different Cultures

3. B.C. Formation

4. Applications of B.C.

5. 3D Shaping of B.C in current research

6. Upscaling of B.C. Production

7. Biodesign

8. Conformality in Design

This chapter covers the literature research done on topics related to this project, answering the research questions A.1 to A.13. This being a brief history on B.C., followed by some cultural aspects of the material. Also, a more in-depth explanation is given on the formation of B.C. and what some of the current applications are of this material. Furthermore, some examples are given where cellulose was formed in 3D shapes and how the material is currently produced on an industrial scale. Finally, some explanation is given for the terms 'biodesign' and 'conformal shaping'.

1. History on B.C.

Natural materials derived from plants, like wood, fabrics, rubber, and various others have been used throughout the ages. The main building block for the structure of most of these plants is called cellulose, which is the substance of which the cell wall of a plant is made of. This was discovered by a French researcher, Anselme Payen, all the way back in 1838 (Payen, 1838). 48 years later in 1896, a British professor at the University of Birmingham, Adrian John Brown, discovered that cellulose is not only produced by plants, but also by certain bacteria (Brown, 1896). In his work he first described the cellulose layer, formed by the bacterium which he named the Bacterium xylinum, which was most known as the 'vinegar plant' or 'mother of vinegar' (Brown, 1896).

This 'mother of vinegar' (see Figure 3) was a way for people to (home)brew vinegar and is created in the fermentation of alcoholic beverages like wine or cider (Bourgeois & Barja, 2009). The relevance of the 'mother of vinegar' was first demonstrated by a Dutch scientist Herman Boerhaave in the 18th century, who developed the precursor of the industrial process of the development of vinegar (Bourgeois & Barja, 2009).

In the 19th century, the 'mother of vinegar' was categorized as a fungus by Christian Hendrik Persoon and Louis Pasteur (Bourgeois & Barja, 2009) until the aforementioned professor A.J. Brown discovered its deriving from bacteria.

In the 20th century other bacterium strains that produce cellulose were discovered, where halfway this century B.C. research got traction. Hestrin and Schramm (1954) developed a glucose-rich medium and did quantitative analysis on the formation of B.C. in various conditions. In this research, it was also found that certain mutations of the Acetobacter xylinum do not produce cellulose. These mutations, as described by Steel and Walker (1957), occur in agitated or aerated medium. The occurrence of these mutants result in the decrease in efficiency of bioreactors and efforts are made to locate the DNA-sequence. In the upcoming years, multiple non-cellulose producing strains of bacteria and more efficient strains have been isolated (Park et al., 2009). Also, advances have been made in the upscaling of the production of B.C. (Zong et al., 1996) and various applications of the material rose up.

Figure 3 - Mother of vinegar

2. B.C. in Different Cultures

The use of this gel-like substance throughout the world varies a lot. While researchers are now trying to replicate human tissue with this material and already back in the 18th century it was used to produce vinegar, it is also used as a culinary ingredient in the dish called 'nata de coco', which translates to 'cream of the coconut' (see Figure 5). This dish originates from the Philippines and was developed somewhere in the late 17th century, when also vinegar production started to arise. This dish was made by fermenting coconut water, resulting in the chewy cellulose layer. This cellulose was cut in blocks and eaten as a delicacy.

Research indicates that in north-east China, around 220 B.C. (before Christ) bacterial cellulose was first used in food-production, namely in the production of the well known fermented tea beverage called kombucha (Coelho et al., 2020). It was said to have detoxifying and energizing properties and was brought to the emperor Inkyo of Japan in 414 A.C., which caused the spread of popularity of the drink to Russia and Eastern Europe. Kombucha production is the result of the fermentation of black tea leaves by symbiotic bacteria, of which commonly the Acetobacter species produces the so called 'tea fungus', which is in fact a layer of cellulose (Liu et al. 1996). This layer of cellulose, also called SCOBY (see Figure 5), is used as a starter for the fermented beverage and is passed around making it a highly shared experience, a strong cultural artefact and creating large communities of brewers and consumers.

Figure 5 - SCOBY used to brew kombucha

Figure 5 - Nata de coco

3. B.C. Formation and Material Properties

Cellulose is an organic substance which is found in abundance in nature. Mostly, it is found in plant cells, where it provides structure. There are also certain species of bacteria that produce cellulose, such as the Acetobacter Xylinum and the Komagataeibacter Hansenii . The cellulose, also called B.C., produced from these bacteria is relatively pure and free of other substances, compared to plant cellulose. However, B.C. has the same molecular composition as plant cellulose (see Figure 6).
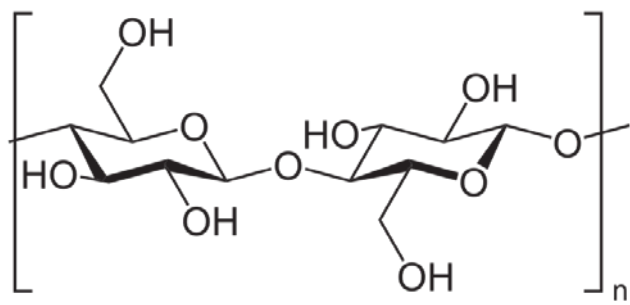
Figure 6 - The cellulose molecule

For this project, the focus is on the Komagataeibacter Hansenii (K.H.), previously called Gluconacetobacter), since this is the bacterium which is used in the B.C. production. The K.H., a rod-shaped bacterium, is a species of acetic acid bacteria and has the most efficient mechanism in producing cellulose. The bacteria are aerobic and need oxygen to survive, but also to synthesize cellulose. This synthesization of cellulose is done through a series of reactions in the cellulose-synthesizing complex (Jonas & Farah, 1998). Lahiri et al. (2021) simplified these reactions in a graphical visualization (see Figure 7).

A lot of research has been conducted on finding the optimal growing conditions for cellulose production. For the optimal pH value, multiple ranges of values are found. A common "safe" range of pH should be between 4 to 7 (Hestrin & Schramm, 1954;Fiedler et al., 1989;Masaoka et al., 1993). For the optimal temperature, a range of 25-30°C is used (Cannon & Anderson, 1991). As a culture medium, most research is done using the HS-medium developed by Hestrin and Schramm (1954).

Factors influencing the amount of B.C. synthesis are significant for this project, however the environmental factors that trigger the cellulose production are more important. Being able to turn these triggers on or off in certain locations might prove to be a solution to static B.C. production with flexibility in geometry.

A presence of oxygen is thought to be the cause of cellulose synthesis. According to the experimental research of Hestrin et al. (1947), oxygen is essential to B.C. production as the bacteria fail to successfully produce within a nitrogen atmosphere. However, this only states that oxygen is key to the chemical reactions that involve the biosynthesis of B.C. and it does not prove that it is the defining factor that triggers the reaction. Research is done on a bacterium, the Pseudomonas fluorescens SBW25, with a very similar genetic pathway, but not a strain that is used to produce cellulose.

This research indicates that the signal that triggers the synthesis of this bacterium is instead caused by a physical phenomenon, which could be surface tension and Marangoni forces (Schramm & Hestrin, 1954). "The Marangoni effect takes place when there is a gradient of surface tension at the interface between two phases – in most situations, a liquid-gas interface."(COMSOL, 2015).

When observing B.C. formation in a static culture on a microscopic level, it shows that the bacteria weave the thin cellulose fibres in very dense structures. In Figure 8 this weaving can be seen in a scanning electron microscope image of two magnifications of cellulose produced by the K.H. (a and b), a cross section image (c) and an image containing a bacterial cell (d).
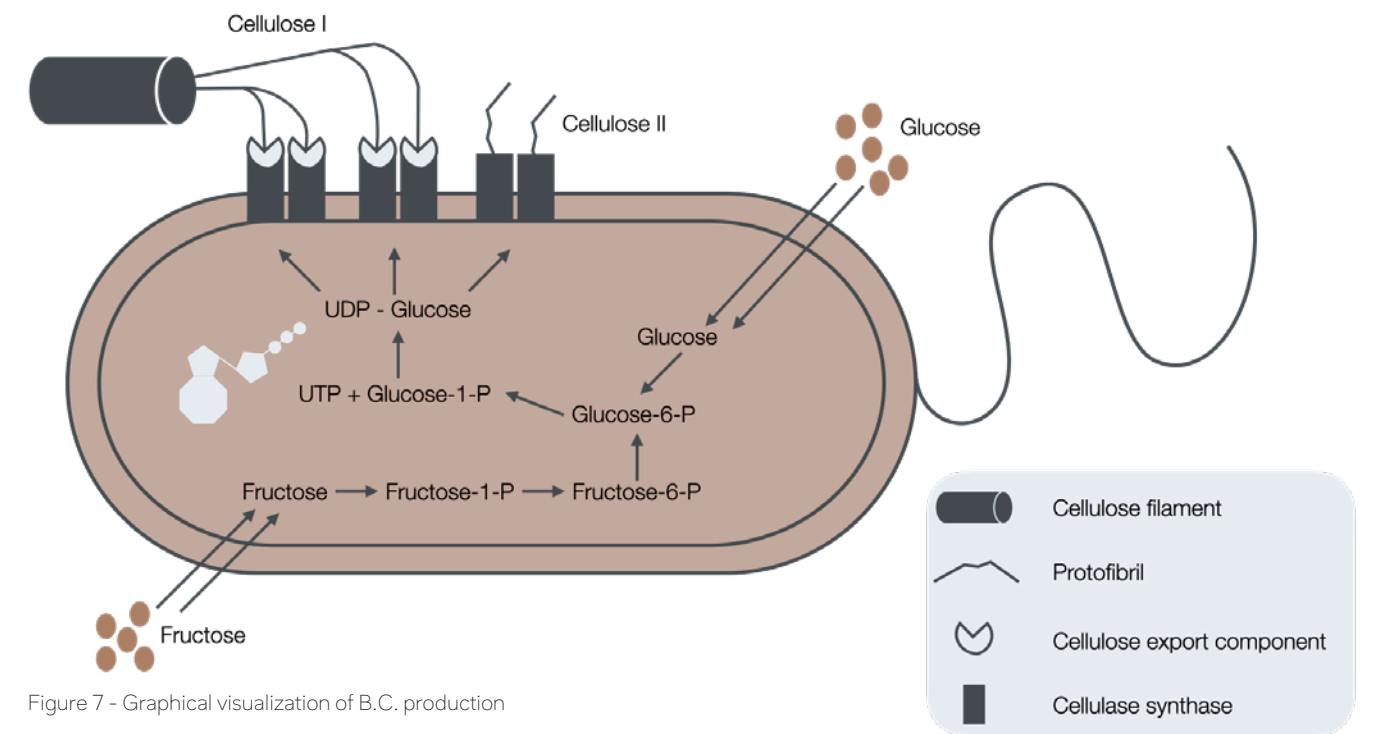

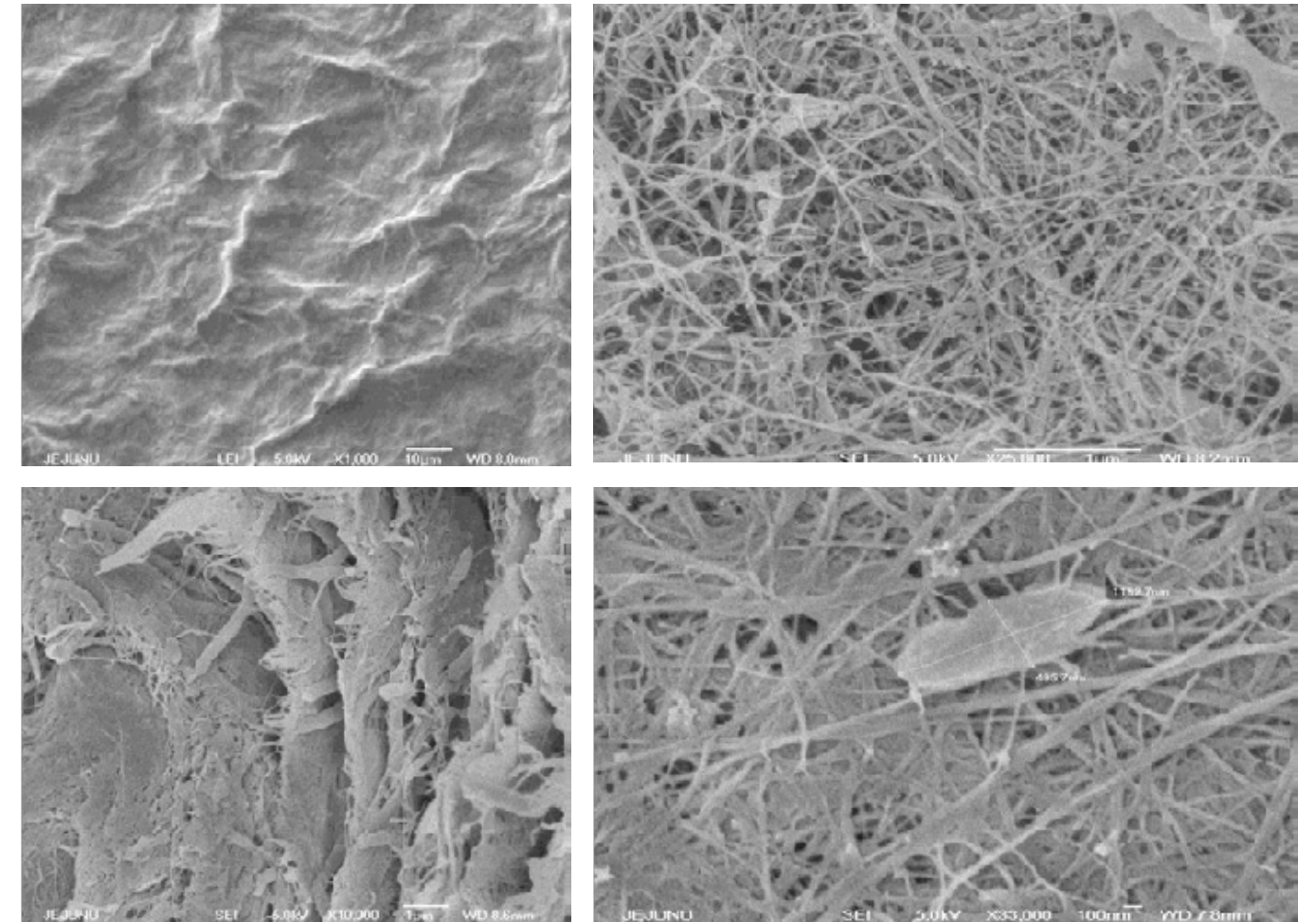Figure 7 - Graphical visualization of B.C. production

Figure 8 - Micrograph of B.C. at macroscopic level (a), microscopic level (b), a cross-section view (c) and an image containing a bacterial cell (d)

The microstructure of the grown cellulose vary significantly, due to multiple causes. For example, in Figure 9 to 11 multiple micrographs are taken of cellulose samples of different bacterial species. Here, differentiation can be seen in density, branching and length of individual fibres. On a macroscopic level, this influences the mechanical behaviour of the B.C. samples greatly.

Research by Stanislawska et al. (2016) on the mechanical properties of B.C. shows that the material has an average tensile strength of about 200-300MPa and a Young's modulus of about 15-35GPa. Due to the large differences in microstructure due to environmental differences, these ranges are relatively large. These mechanical properties are in the range of some plastics, as can be seen in Figure 12 (Ansys® Granta Edupack, 2021).

Figure 9 - Micrograph of B.C. produced by the S. enterica
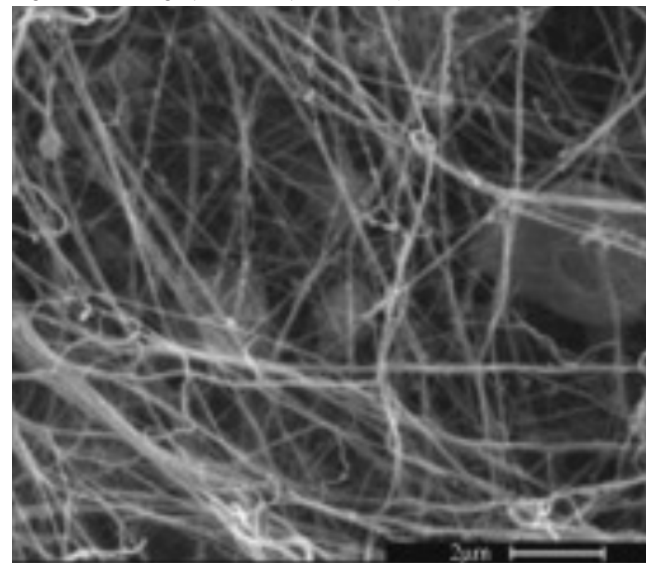
Figure 10 - Micrograph of B.C. produced by the G. Xylinus
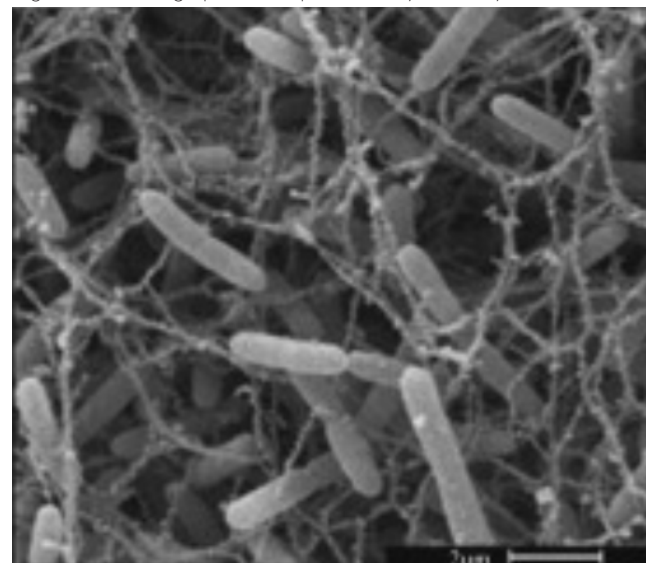
Figure 11 - Micrograph of B.C. produced by the D. Dadantii

Figure 12 - Materials in the same range of Young's modulus and tensile strength as B.C.

4. Applications of B.C.

As stated in the previous paragraph, B.C. has its applications in the food industry as a fermented beverage starter and in the delicacy from the Philippines 'coco de nata'. However, since its classification and first research, its applications became more widespread. Research by Wahid and Zhong (2021) categorized these applications in the following industries: Food, cosmetics, electronics, biomedical, water purification and others.

Within the biomedical field, B.C. is a strong candidate for internal and external body healing applications due to its high biocompatibility, which is also the reason for its applications in the NextSkins project. Portal et al. (2019) used B.C. to aid in wound healing, resulting in the same healing of the wound within 81 days, which would take 315 days in normal conditions. Other applications in the biomedical field include antimicrobial applications (Wiegand et al. 2015), drug-delivery (Abeer et al., 2014), cardiovascular grafts (Zang et al., 2015), artificial cornea and lenses (Wang et al., 2010) and bone tissue engineering (Noh et al., 2019).

In the food industry, apart from 'coco de nata', B.C. has some other applications. Since the material is not digestible, it can be used as a dietary ingredient. By adding softeners to make it easier to bite through, it can be used in the production of low-calorie desserts and salads (Ulla et al., 2016). Also, due to its fibrous texture and its ability to absorb moisture, B.C. is a good candidate to be utilized as a meat replacement (Azedero et al. 2019). Finally, it can also be used as a thickening-, stabilizing- or gelling agent and in food packaging (Wahid & Zhong, 2021).

In the cosmetics industry, B.C. is also used as a stabilizing agent to create stable oil emulsions in water (Wahid & Zhong, 2021). Also, hydrating facemasks are made of B.C. (Amnuaikit et al. 2011), replacing traditional and more sticky paper masks (Wahid & Zhong, 2021).

As an electronic component material, B.C. can be utilized in the fabrication of biosensors, batteries, and conductive membranes (Jang et al. 2017). Also, research by Zor (2018) shows that B.C. can be used as a sensor of cysteine, which is mostly used in the food industry.

To purify water, B.C. has a lot of potential. Since the material has a high absorption rate, it can be combined with purifying substances to remove certain pollutants like heavy metals, organic compounds, and dyes from water (Wahid & Zhong, 2021).

Finally, B.C. has high mechanical properties and the amount of variation in the way the material is produced allows for numerous other applications. For example, in the textile industry, some brands and artists have already utilized the B.C. fibers in the production of a leather-like material and other clothing (Chan et al. 2018).

Most of these applications ask for freedom in the shaping of the B.C. material, which also drives the conduction of this research. In the next paragraph, some examples are given of other current research on B.C. 3D shaping.

5. 3D Shaping of B.C in current research

B.C. has historically already been used in various applications, ranging from the music industry to applications in the medical field (Jonas & Farah, 1997). Shaping B.C. in 3D geometries has also been researched by various researchers and artists. One work called the 'Xylinum Cones' is created by Jannis Huelsen and Stefan Schwabe in 2015, where B.C. is produced in suspended molds (see Figure 13). These molds allow for cellulose growth on all sides, instead of only the top side where there is a direct contact with oxygen.

Figure 13 - 3D shaped B.C. called the Xylinum Cones

Figure 14 - A face molded from B.C.

Another work by Austin Chia shows how B.C. can be shaped in a 3D geometry (see Figure 14). Here, the student at Maryland Institute College of Art mixed UV-curable resin with a grown cellulose sample after which it is molded into a negative of the face of Teódula Kalaw África to keep it in shape. This work is dedicated to her, since she has advanced the scientific field of Nata de Coco, which resembles B.C. in some respects.

Both works have in common that they allow for a wide variety of geometries made out of B.C., but they are not conformally shaped. This means the shapes that are designed can not be tweaked or changed, so a new mold needs to be made to generate a new 3D shape.

However, there is some work done in the scientific field where B.C. is conformally shaped. Hospodiuk-Karwowski et al. (2022) found a way to solidify a substance partly made out of B.C. to be used in a FDM-like 3D printer (see Figure 15).

Binelli et al. (2022) researched a similar approach, but they printed the cellulose in a hydrogel (Figure 16). This way of 3D shaping offers a lot of detail in the eventual shape and has a lot of potential in the medical field.

Both of the previously mentioned ways of conformally 3D shaping of B.C. offer a lot of freedom in shape. The problem for both is their printing size and commercial scalability. For very small medical implants these production techniques would work appropriately.

However, when custom sized patches need to be made at the size of for example a person's upper leg, these production methods are lacking in their capabilities. .

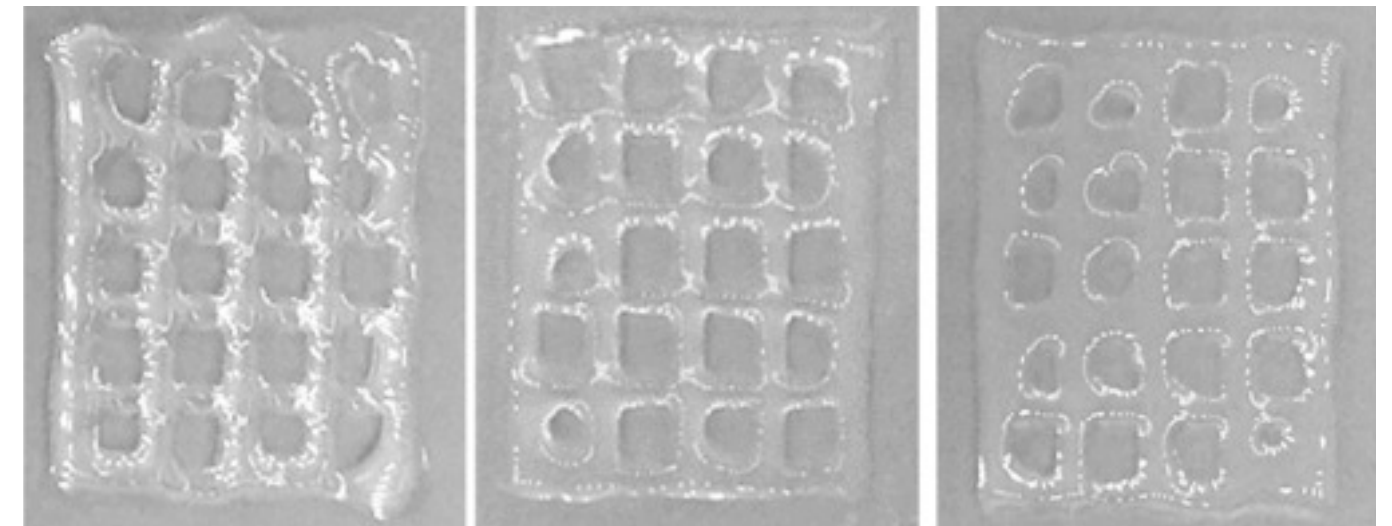There have been a lot of advances in finding new production methods for B.C. leveraging the mechanisms.

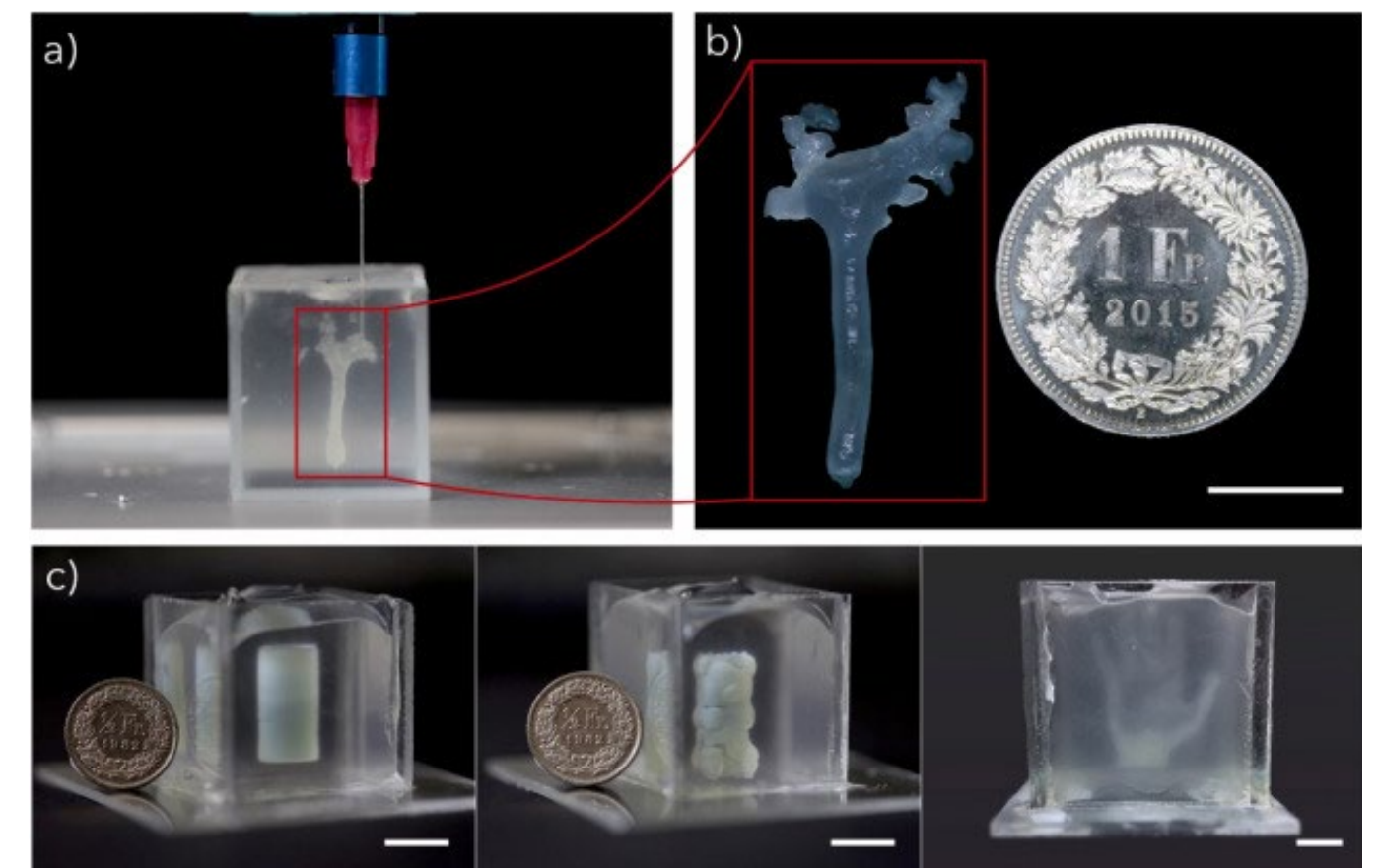Figure 15 - 3D printed B.C. samples

Figure 16 - Another example of 3D printed geometry, but in an aerogel

6. Upscaling B.C. production

To be able to commercialize cellulose produced by bacteria, numerous advances have been made in the upscaling of its production. In current industrial applications, there are mainly two types of production, which are static and agitated production. Static conditions result in a sheet of cellulose growing on the air-liquid interface, while agitated conditions lead to separate pellicles of cellulose suspended in the medium. In static conditions, common B.C. production rate ranges from 0.02 g/L per day to 0.9 g/L per day (Lahiri et al., 2021). Agitating the medium allows for oxygen to mix in the liquid, which increases the growth rate (Ross et al., 1991). However, this method also results in a higher degree of mutations to the non-cellulose producing strains, resulting in a decrease in yield (Sahni & Dahman, 2010).

The material- and mechanical properties of the cellulose obtained by static- or agitated production show some differences. First of all, the Young's modulus of static-grown B.C. is higher than that of agitated-grown B.C (Krystynowicz et al., 2002). When observing the cellulose formation macroscopically, both types seem to be highly similar (Watanabe et al., 1998). However, the same research indicates that there are differences on a microscopic level, resulting in for example this difference in mechanical strength. Also, the water-holding capacity, as researched by Krystynowicz et al. (2002) of statically grown cellulose is higher than that of agitatedly grown cellulose. Zhong (2020) argues that these differences result in a higher attractiveness towards statically grown cellulose in wound dressing and facemask applications.

Multiple methods of increasing the yield in static B.C. production have been researched. A patent by Bungay and Serafica (1999) resulted in the first very basic rotary disc bioreactor, on which multiple iterations have been made to optimize this method (Lin et al., 2013; Sharma et al., 2022). This reactor allows for more oxygen to mix in the medium, resulting in more and a semi-continuous B.C. production. Also, the additions of aerosols to the medium during B.C. growth has been researched and founded to be highly effective (Hornung et al., 2007). Finally, air-lift bioreactors have been developed for B.C. production, which were formally used in processes like waste water treatment (Chao et al., 2001; Zuo et al., 2006; Żywicka et al., 2021). Here, oxygen-rich gas is pumped into the culture, also resulting in higher yields.

7. Biodesign

Currently, in design it is common practice to use materials like plastics, metals, and wood for the fabrication of products. However, due to the ongoing climate change and the need for innovation, designers, architects, scientists and other creators started changing their practice. They started working with more regenerative and interactive materials made from or by living organisms, often being bacteria, algae, and fungi. This practice is commonly referred to as 'biodesign', of which a definition is given by Gough et al. (2021) being: "- the application of the bioaffordances of an organism." There are two types of outcomes in a biodesign process, being a result in a non-living artefact designed with living organisms, or a living artefact designed with living organisms. This 'livingness' is described as a novel material quality by Karana et al. (2020) and is supported by three principles, being Living Aesthetics, Mutualistic Care and Habitabilities. Living Aesthetics relate to how the user experiences changes of the living artefact over time. Mutualistic Care describes the relationship between the living artefact and the user. Finally, Habitabilities describes how the livingness of the artefact is conditioned by the user and other living-, and non-living entities, where the "first habitat" is the containment of the living organism and the "second habitat" is the containment during use.

For this project, concerning Habitabilities, emphasis is placed on the "second habitat". The "first habitat" for the B.C. production is a simple flask with medium containing the cellulose producing bacteria. Since I am designing a way of shaping this cellulose, a new habitat needs to be designed where the bacteria can be programmed to function in a more controlled way. In this case, I am, as a designer, the user of this living artefact. Regarding Living Aesthetics, the growth of the cellulose layer is the most noticeable type of change that can be experienced from the living artefact. The main goal of this project is to also change the way this cellulose forms as a user, directly influencing this more noticeable Living Aesthetic. Finally, regarding Mutualistic Care, the organisms provide me, the user, with the need for a cellulose geometry, while I provide them with a way to reproduce in a highly productive way.

8. Conformality in Design

In design, geometries are often defined before the fabrication process. For example, in ejection moulding, a mould is pre-made to produce a large amount of the same shape. Changing the shape of the geometry during its formation is not possible using this method and adds a lot of limitations, resulting in a production method that is mostly used at the end of a design cycle for a product. Also, when a product is bought, often times its shape stays somewhat similar and is also designed to stay that way. Shaping a form during its formation has been called conformal shaping first in a paper by McQuillan and Karana (2023).

9. Material Taxonomy

In Figure 17 the material taxonomy for B.C. is shown. Here, four categories are explored, which include parameters influencing the growth of cellulose by the Komagataeibacter Hansenii. A distinction is made between the parameters influencing the medium and those parameters influencing the environment. These two are then categorized between physical- and chemical parameters. From the found parameters interconnections are visualized by grey lines, which indicate that they have an influence on each other. The parameters and the connections between them are all backed-up by previous literature. These are listed in Appendix A.

This taxonomy and the research behind it is used to come up with design principles for the formation of B.C. in conformal 3D shapes.
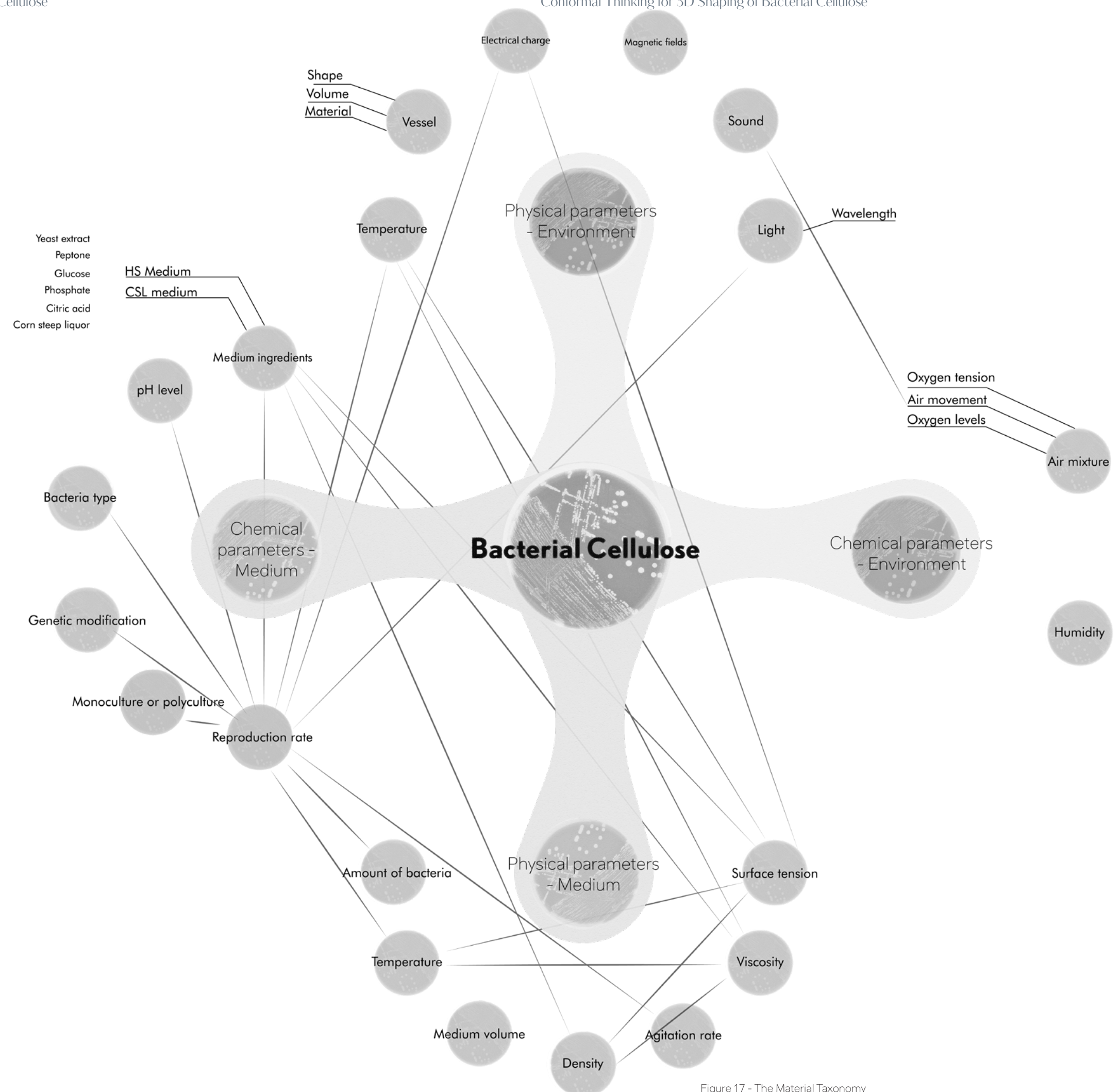
Figure 17 - The Material Taxonomy
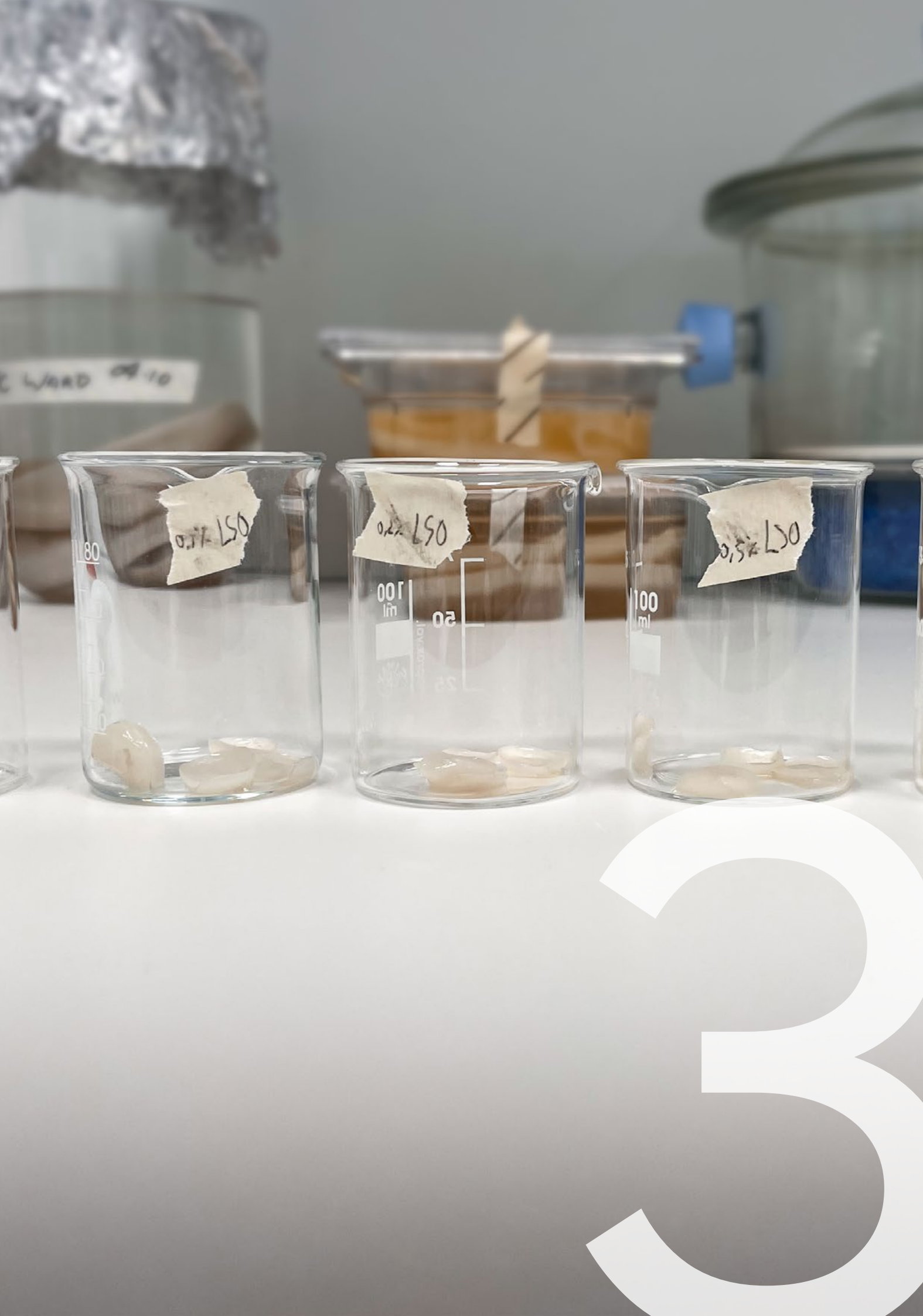
Material Shape Exploration

FINDING AND TESTING DESIGN PRINCIPLES

Based on the research done on the formation of B.C. and with inspiration of other projects where cellulose was shaped, new material shape explorations are conducted. In this chapter this exploration is defined into principles, which are hierarchised and tested. Finally, a selection is made from the tested principles.

1. Ideation for Design Principles

2. Design Principle 1

3. Design Principle 2

4. Design Principle 3

5. Design Principle 4 and 5:

6. Selection of one Principle

1. Ideation for Design Principles

From the aforementioned taxonomy, design principles are found. These design principles are abstract ways of influencing the B.C. growth with the goal of generating pre-programmed 3D shapes. From these principles multiple solutions can be thought of and thus form the backbone of further ideation to answer the main research question. Also, from these principles, multiple sub-questions are made to support the main research question.

The creative process behind finding the design principles is mostly based from the Delft Design Guide's How-To's method (A. van Boeijen et al., 2014). For every parameter from the taxonomy the questions is asked: "How can this geometrically influence the growth of B.C.?" For every parameter rough sketching is used to visualize possible answers to the question.

In Figure 19 a hierarchical overview is shown where all found principles are listed. For every principle an icon-style illustration accompanied by the description and the principle's relation to the taxonomy is made. This hierarchy is based on the feasibility of the principle and its "3D shaping potential". The rate of feasibility is based on:

- Findings from the conduct of preliminary research of this project
- Findings from research of other parties within the project
- Alignment with research from papers
- Own level of experience on the subject

All 3D shaping methods have their limitations in what types of geometries it can produce. For example, FDM 3D printing can produce complex 3D geometries. However, due to the way the material is deposited there are certain limitations when it comes to for example the maximum angle of overhang.

The 3D shaping potential of a principle is defined as what types of geometries are possible. In Figure 18 three types of geometry are identified to be critical for freedom of shape:

- Thickness variation: Is it possible to change the thickness variation of the generated shape over the x- and y-coordinates?
- Curved tubular geometries: Is it possible to create hollow curved (shell-like) and tubular geometries?
- Overhang: Is it possible to bridge material over gaps, so air pockets can be generated within the geometry?

Freedom in thickness variation in a B.C. layer can allow for multiple applications. First, localizing thinner areas in certain locations can allow for more flexibility while maintaining volume to, in the application of the NextSkins LTM, to have enough effect on the reduction of Atopic Dermatitis. Secondly, thickness variations can allow for purposely drying out of certain parts of the B.C. sample, while other parts stay in their wet state for longer. Applications for this in the NextSkins project could be a warning signal for the user to replace the patch, or, in theory, the partial drying could morph the geometry in certain shapes, which could be utilized to still create more curved geometries. Finally, thickness variations can allow for texture differences within the B.C. sample. This can be utilized to enhance the user experience of the LTM and create a user interface to communicate the product's characteristics.

Curved geometries can be used to shape the B.C. layer more to the shapes of the body. It is acknowledged that the material is flexible enough to form to the human body when shaped in a flat sheet, due to its flexibility. Facemasks for example could be produced in flat sheets, like they are made for the beauty industry. However, geometries like that of gloves or sleeves, this same production method can not be used. Curved, tubular shaped geometries would need post-processing steps like welding or stitching to be able to be formed from a flat sheet. Therefore, a production process is needed to construct these shapes out of B.C..

Like in 3D printing, the principle of overhangs or bridging allows to form geometry without the need of support underneath. It is often used to create open and closed hollow geometries and could also produce the curved tubular shaped geometries. However, this geometry type also includes closed hollow geometries, like hollow spheres or cylinders. Creating closed hollow geometries in the B.C. layer has multiple applications. Firstly, creating air pockets in the material can locally change the density of the material, allowing for potential shape morphing during drying, and flexibility and stretchability changes. Also, air pockets in the material can locally lower the7 buoyancy, resulting in the opportunity to create floating cellulose samples. Finally, adding air pockets can localize the amount of active ingredient release for the LTM.

In the next part of this chapter tests are discussed of the first five principles from the hierarchy. The first three are tested more elaborately, since they show more promise for the project. Principle 4 and 5 both are tested in a relatively simple setup.
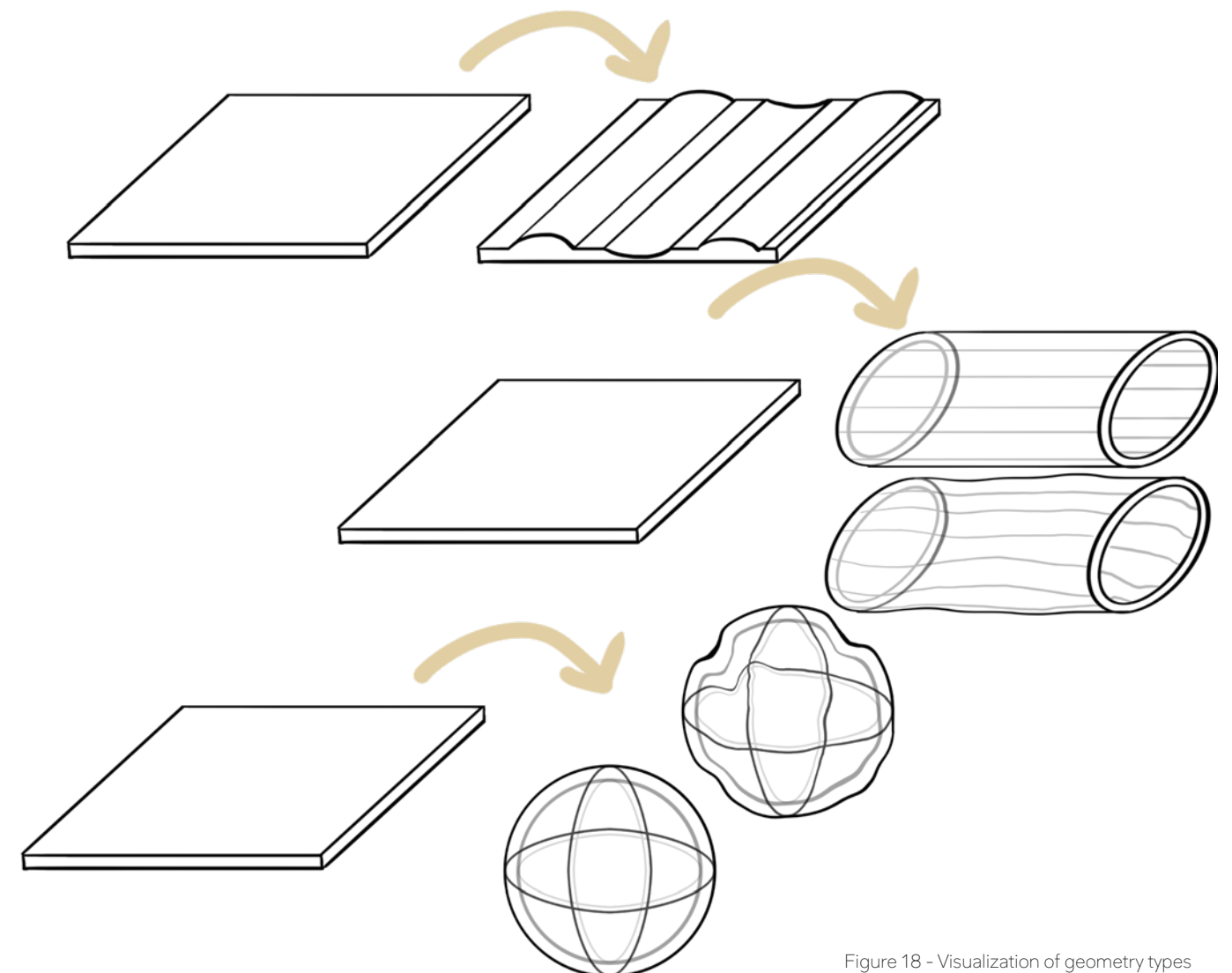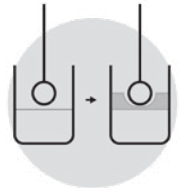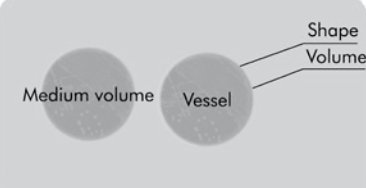

Figure 18 - Visualization of geometry types
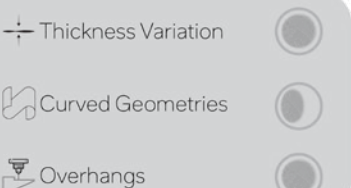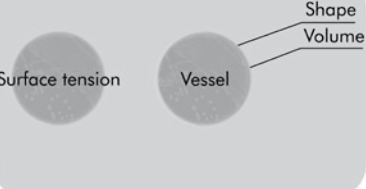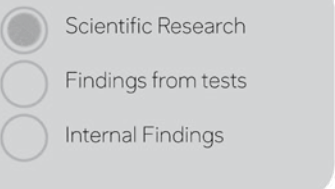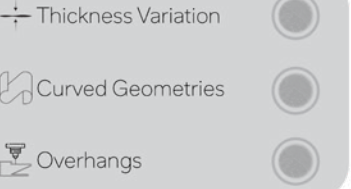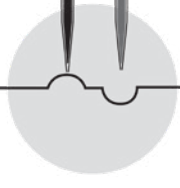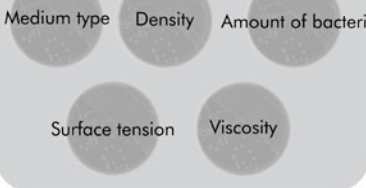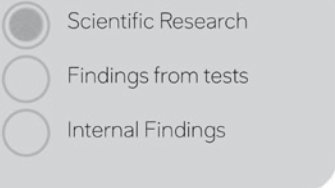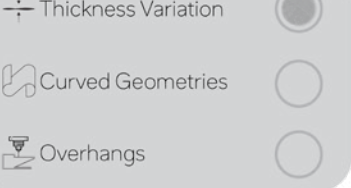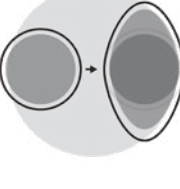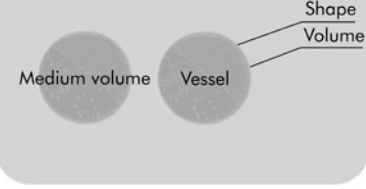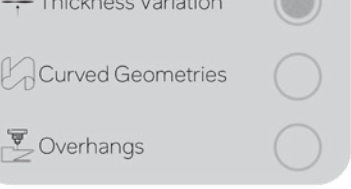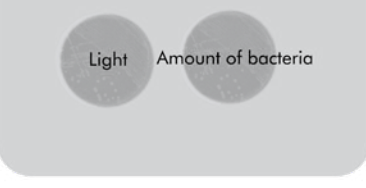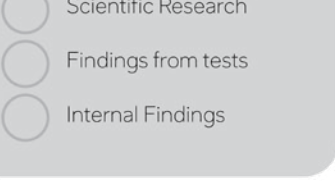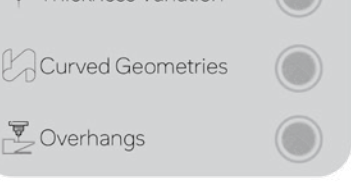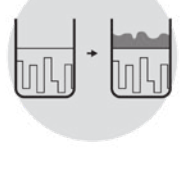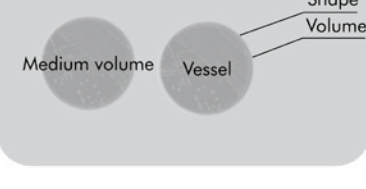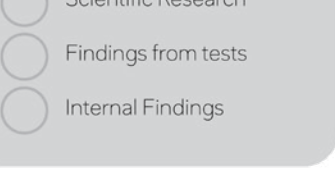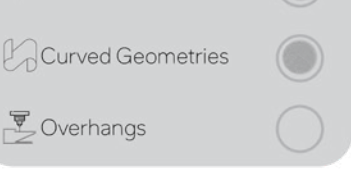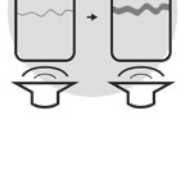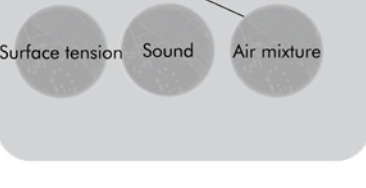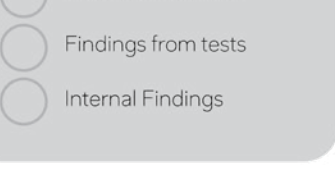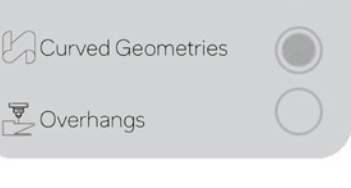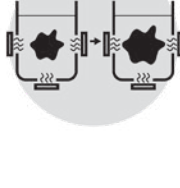
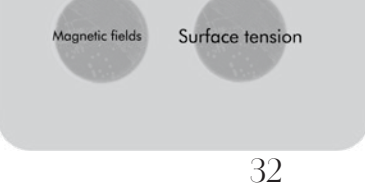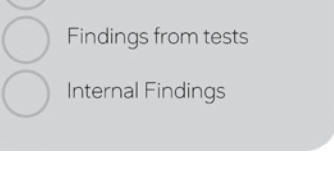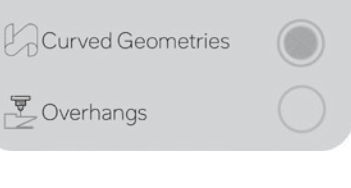|	Principle Description	Taxonomy factors	Backed up by Research	3D-Shaping Potential	Project Potential
P1	Localized obstruction of B.C. growth through the introduction of geometry above the air-liquid interface	Medium volume, Vessel (Shape, Volume)	● Scientific Research ● Findings from tests ○ Internal Findings	Thickness Variation ●, Curved Geometries ◑, Overhangs ●	This principle fits my expertise in 3D printing and mechatronics best and in theory it shows a lot of potential in the 3D shape freedom.
P2	Utilizing geometrically confined porosity to create B.C. growth within the medium	Surface tension, Vessel (Shape, Volume)	● Scientific Research ○ Findings from tests ○ Internal Findings	Thickness Variation ●, Curved Geometries ●, Overhangs ●	This principle, if it works would involve developing complex geometries and special 3D printing. While being more challenging, there is a lot of 3D shaping potential.
P3	Localized addition of growth stimulants and inhibitors to the culture	Medium type, Density, Amount of bacteria, Surface tension, Viscosity	● Scientific Research ○ Findings from tests ○ Internal Findings	Thickness Variation ●, Curved Geometries ○, Overhangs ○	This principle involves more chemical and biological knowledge, which is outside of my expertise area. However, if the right substances can be found this principle does have potential.
P4	Incremental surface area change of the B.C. growth through changing the vessel shape	Medium volume, Vessel (Shape, Volume)	○ Scientific Research ● Findings from tests ○ Internal Findings	Thickness Variation ●, Curved Geometries ○, Overhangs ○	Some basic initial tests showed that changing the shape of the air-liquid interface over time does change the eventual geometry. However, this principle does have a lot of limitation in geometry freedom.
P5	Leveraging UV light to inhibit B.C. growth in certain locations over time	Light, Amount of bacteria	○ Scientific Research ○ Findings from tests ○ Internal Findings	Thickness Variation ●, Curved Geometries ●, Overhangs ●	This principle does show a lot of potential, since it could mimic the workings of an SLA printer. However, it is expected that this principle takes a lot of testing and fine-tuning to make it work.
P6	Localized medium height change during B.C. growth	Medium volume, Vessel (Shape, Volume)	○ Scientific Research ○ Findings from tests ○ Internal Findings	Thickness Variation ●, Curved Geometries ●, Overhangs ○	It is expected that differences in thickness can be achieved in the B.C. samples, but the changes will not have enough contrast to generate well defined thickness variations.
P7	Surface shape modification through the use of static sound waves	Air movement, Surface tension, Sound, Air mixture	○ Scientific Research ○ Findings from tests ○ Internal Findings	Thickness Variation ●, Curved Geometries ●, Overhangs ○	The air-liquid interface can in theory be moved in a specific shape using static waves, however this will ask for a lot of expertise which I am lacking.
P8	Introduction of shape-changing ferrous fluid under the influence of changing magnetic fields to B.C. growth	Magnetic fields, Surface tension	○ Scientific Research ○ Findings from tests ○ Internal Findings	Thickness Variation ○, Curved Geometries ●, Overhangs ○	This idea for a principle was more outside of the box and will be too demanding to develop within the scope of the project.

Figure 19 - Principle Hierarchy
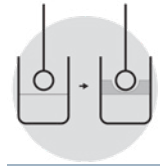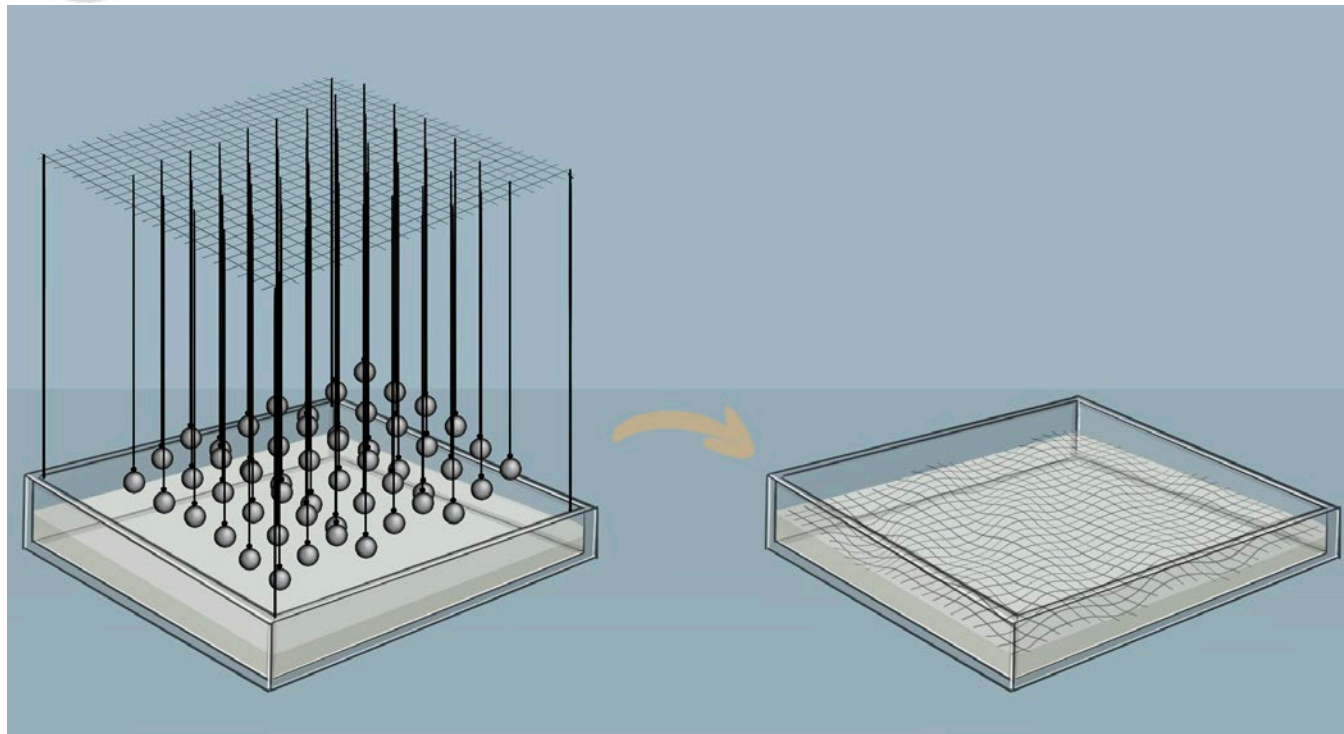
2. Design Principle 1

Figure 20 - Visualization of principle 1

"Localized obstruction of B.C. growth through the introduction of geometry above the air-liquid interface"

To test the principle as an obstruction, physical objects are used. In Figure 20 a possible final concept is depicted, where objects are hung above the medium at different heights. These would result in a varying surface height of the B.C. layer.

For this design principle multiple research questions have been listed:
1. How do different types of geometry interact with the growth of B.C. when the obstruction touches the surface of the air-liquid interface?
2. How does the type of material change the behaviour of the cellulose producing bacteria when touching the obstruction?
3. How does cappilarity of the medium affect the growth when geometry is introduced above the surface of the liquid?
4. How does the level of medium over time influence the interaction between the cellulose and the obstrusion?
5. How does changing the location of an obstruction during the B.C. growth influence the resulting cellulose geometry?

Test 1: Different types of geometry above the air-liquid interface

This test is conducted with the aim of answering the first and second research question for design principle 1:
1. How do different types of geometry interact with the growth of B.C. when the obstruction touches the surface of the air-liquid interface?
2. Does the type of material change the behaviour of the cellulose producing bacteria when touching the obstruction?

Hypothesis
It is expeced that sharply edged geometry will be directly "stamped" in the cellulose layer. Also, the porosity of the PLA material and the layer lines are expected to be translated within the cellulose. The resin 3D prints might react with the bacteria, since the material contains harmful substances when not cured properly.

Methods
To answer two of the research questions of Design Principle 1, a test setup was made. First, 150mL of HS or CSL medium is prepared and inoculated with the Komagataeibacter Hansenii bacteria. This is then evenly poured into 6 Erlenmeyer flasks. The 6 objects shown in Figure 21 to 26 will then be placed in the liquid, leaving some space around them for growth. Growth will maintain for one week, while monitoring it every day.

Materials
- 1,5L of HS or CSL medium
- Komagataeibacter Hansenii bacteria
- 6x Erlenmeyer flasks of 100mL.
- 6x objects with different geometries

Findings:
- The geometry of the cross-section of the object that moves through the growth of the cellulose is directly translated in the resulting hole.
- Sharp corners and edges are translated in the geometry of the grown cellulose.
- Not all 3D printing materials are suited for contact with the growth medium; resin from the DLP printer halted the growth significantly, but still resulted in some biomass.
- Due to evaporation of water in the medium, the waterline dropped. This resulted in the cellulose drooping over some of the objects. This effect did not affect the overall shape in the end.
- Due to the touching of the object with the inner surface of the vessel, capillary interactions caused the water level to bend. The cellulose did follow this shape and in the end resulted in a thinner geometry. This thinness could also be explained due to a smaller volume of medium accessing this surface of the air-water interface.
- The stainless steel sphere resulted in a more grey-beige coloured sample with significantly more biomass. No prior research was found to explain this behaviour.
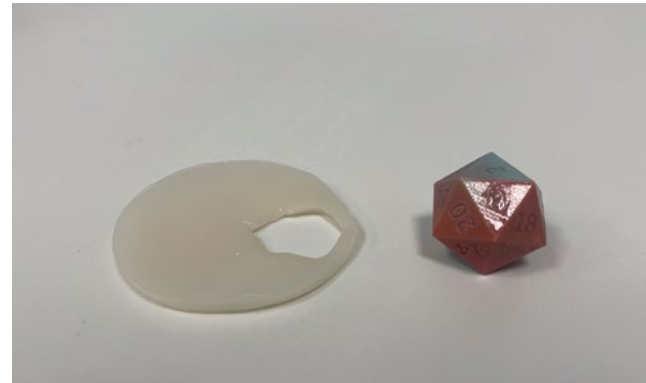
Figure 21 – P1 test 1 resulting shape of Stratasys J735 tetrahedon

Figure 22- P1 test 1 resulting shape of DLP resin sphere

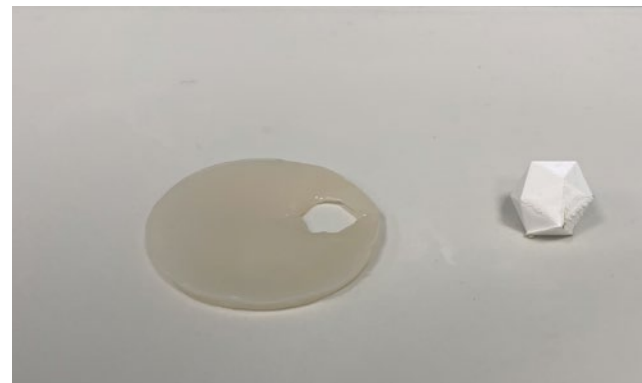Figure 23 - P1 test 1 resulting shape of FDM PLA sphere

Figure 24 - P1 test 1 resulting shape of FDM PLA tetrahedon

Figure 25 - P1 test 1 resulting shape of stainless steel sphere

Figure 26 - P1 test 1 resulting shape of casted resin tetrahedon

Test 2:   Static geometry above the air-liquid interface during growth

This test is conducted with the aim of answering the first and second research question for design principle 1:

1. How do different types of geometry interact with the growth of B.C. when the obstruction touches the surface of the air-liquid interface?
2. How does the type of material change the behaviour of the cellulose producing bacteria when touching the obstruction?
3. How does cappilarity of the medium affect the growth when geometry is introduced above the surface of the liquid?

Methods
To answer the last two research questions of Design Principle 1, multiple test setups are made. First, 600mL of CSL medium is prepared and inoculated with the Komagataeibacter Hansenii bacteria. 400mL medium is then poured into two 1L beakers and 200mL is evenly poured in two 500mL beakers. The 3D print with the height adjustable "stamp" is placed in the medium of one of the 1L beaker (setup A) (see Figure 28 and 29). The 3D printed tetrahedon from test 1, suspended in the air by the copper frame was placed in the other 1L flask (setup B) (see Figure 34 and 35). A piece of copper wire supported by a copper frame was placed in the 500mL beaker (setup C) (see Figure 36 and 37). Finally, an empty 500mL beaker with the same growth medium and bacteria was prepared as a comparison (setup D). Height of the geometry will not be changed during the first test. Growth will maintain for one week, while monitoring it every day. Also, after day 3 a timelapse is made of the growth of the height adjustable stand setup using a GoPro (see Figure 27).

Figure 27 - GoPro setup monitoring the growth after day 4

Materials
- 200mL of CSL medium
- Komagataeibacter Hansenii bacteria
- 1x Erlenmeyer flasks of 1L.
- 1x 3D printed height adjustable stand
- 1x GoPro with LED light setup

Findings:

- Evaporation of the medium causes the water level to drop faster than or as fast as the cellulose grows in height. This resulted in the stamp of setup A and C barely touching the cellulose layer and setup B to not touch it at all. For C the water level did not lower as much, since the surface area of the air-liquid interface is smaller.
- Cappilary action in setup A (see Figure 30) caused medium to "bridge" between the stamp geometry, allowing for some cellulose growth touching the stamp. This also caused for a thin arc of cellulose, as shown in the picture. This cappilary action did not occur in B and C, since the geometries did not have any other geometry in their vicinity that would allow for the "bridging" effect as for setup A. For C however the cellulose did stick to the relatively thin geometry, proving that this cappilary action is not needed for the cellulose to stick to the geometry it comes into contact with.
- As for test 1 of this design principle, drooping of the cellulose occured in setup A and C due to the fibers getting stuck to the geometry of the stamp and for setup A its stand. This drooping however did result in a geometry change for setup A. As seen in Figure 30 to 33, the cellulose has more thickness at the edges of the cellulose layer and thins out in the middle. Drooping for setup C was not as significant, since the water level did not lower as much.

- As seen in Figure 34 to 35, the cellulose shows a darker colour where the copper geometry had touched the surface throughout the cellulose layer. This same colouration was seen in test 1, where a stainless steel sphere was situated in the growth medium. In this case however, it did not change the productivity of the cellulose-producing bacteria since the biomass of setup D was not significantly more than setup C. During growth however there was some weird "fringing" situated at the bottom of the cellulose layer, which was not noticed when the cellulose was extracted after growth.
- The indent the geometry of setup C made also caused the surrounding cellulose to be thinner in a circular shape.

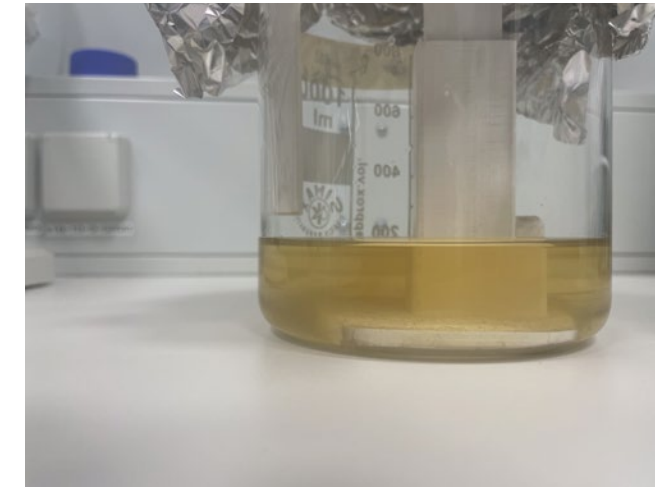# Design Principle 1: Setup A

Figure 28 - Height adjustable stand in CSL medium containing K.H.
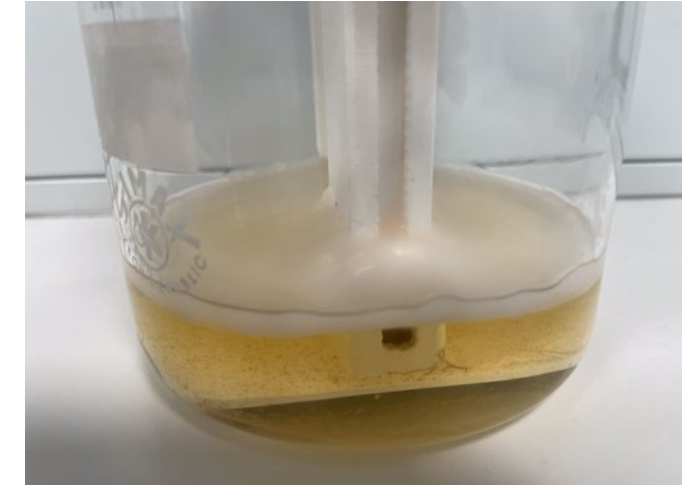
Figure 29 - Four days of growth, backside
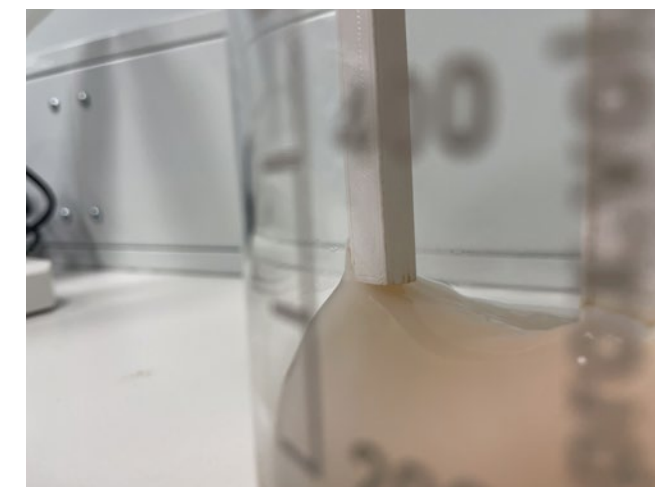
Figure 30 - Cellulose layer stuck to the stamp after 7 days

Figure 31 - Indent of the stamp in the extracted cellulose layer

Figure 32 - Four days of growth, frontside

Figure 33 - Sideview of the cellulose layer showing the effect of the drooping

Design Principle 1: Setup B and C

Figure 34 - Test setup with copper wire
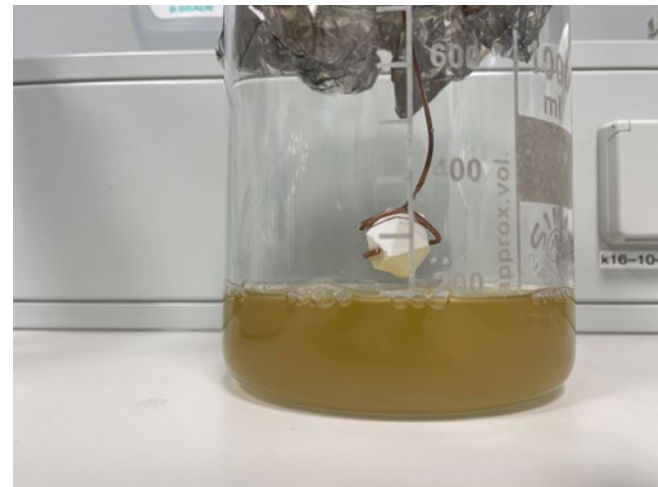
Figure 35 - 3D printed object suspended above CSL containing K.H.
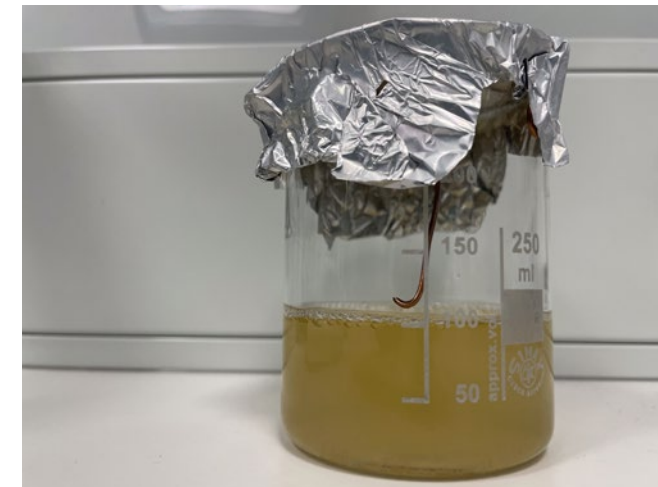
Figure 36- Copper wire suspended above CSL containing K.H.

Figure 37- Copper wire touching the cellulose layer after day 4

Figure 38 - 3D printed object not touching the cellulose after one week

Figure 39 - Two seperate layers of cellulose after addition of medium during growth
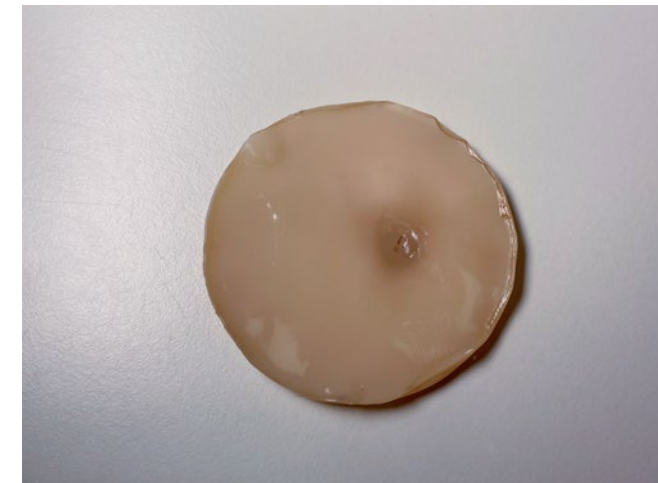
Figure 40 - Resulting cellulose sample after contact with copper wire (front)

Figure 41 - Resulting cellulose sample after contact with copper wire (back)

Figure 42 - Close-up of the cellulose sample showin the surface disturbances

Test 3: Dynamic geometry above the air-liquid interface during growth

This test is conducted with the aim of answering the first and second research question for design principle 1:

4. How does the level of medium over time influence the interaction between the cellulose and the obstruction?
5. How does changing the location of an obstruction during the B.C. growth influence the resulting cellulose geometry?

Figure 43 - Cellulose sticking to the geometry during the test

Method

To answer the last two research questions of Design Principle 1, a test setup is made (see Figure 43 to 45). Here, two 500mL beakers containing CSL growth medium with the K.H. bacteria are prepared. In one of the beakers the same geometry as setup B from test 2 was used. In both beakers a silicone tube was introduced, which end was placed under the medium surface and the other end outside of the beaker. To keep the setups sterile, aluminium foil was used to seal of the air gaps. After four days of growth, 25mL of medium is added to the medium through the silicone tube using a sterile syringe.

Findings:

- The addition of medium after cellulose growth caused medium to siple between the edge of the cellulose layer and the inner surface of the beaker. This resulted in the newly formed layer of cellulose to not stick to the previous untouched layer (see Figure 46 and 47).
- This could be prevented by adding medium at a slower rate. Also, the silicone tube going through the air-liquid interface aids in the medium leakage on top of the forming cellulose layer. A different system should be designed for this.
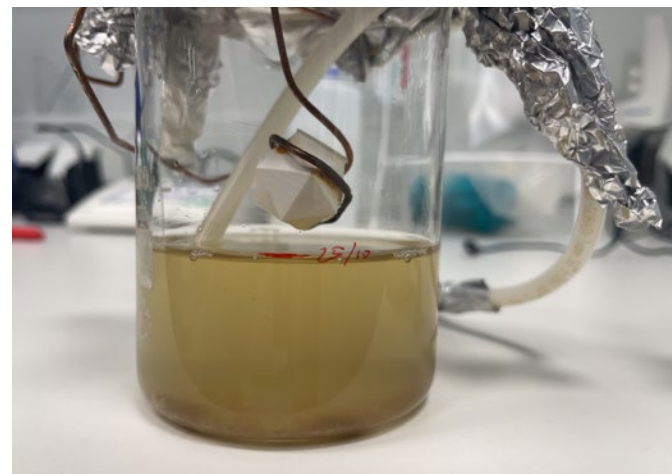

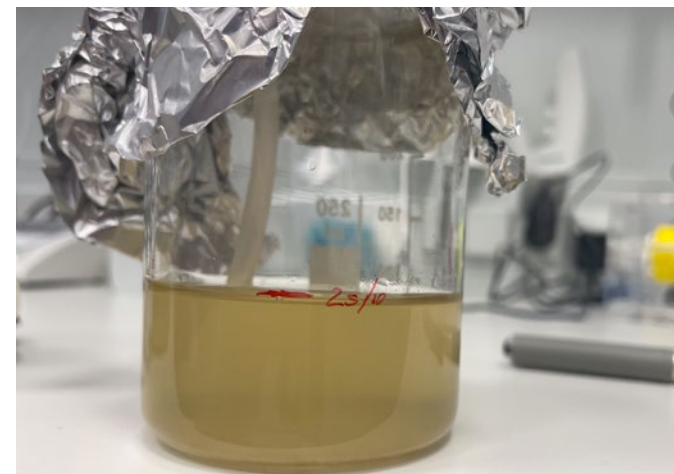Figure 46 - Object above height adjustable medium (day 7)

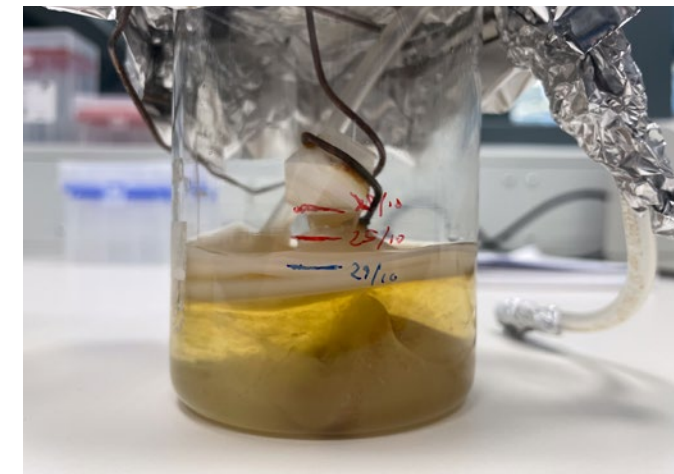Figure 47 - Height adjustable medium without object (day 7)

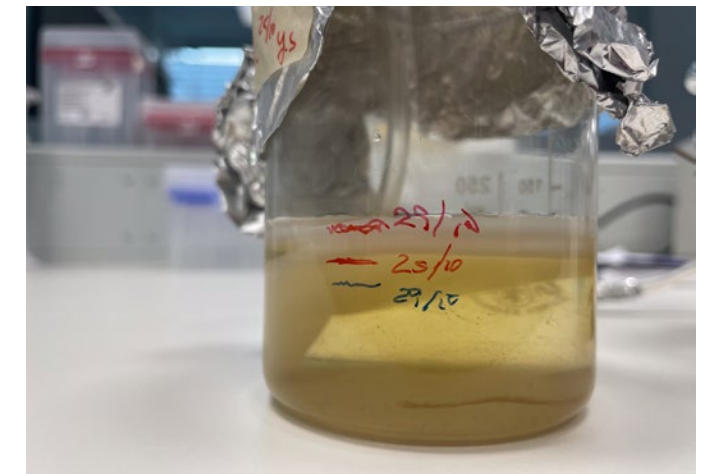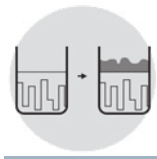Figure 44 - Object above height adjustable medium (day 0)

Figure 45 - Height adjustable medium without object (day 0)

3. Design Principle 2
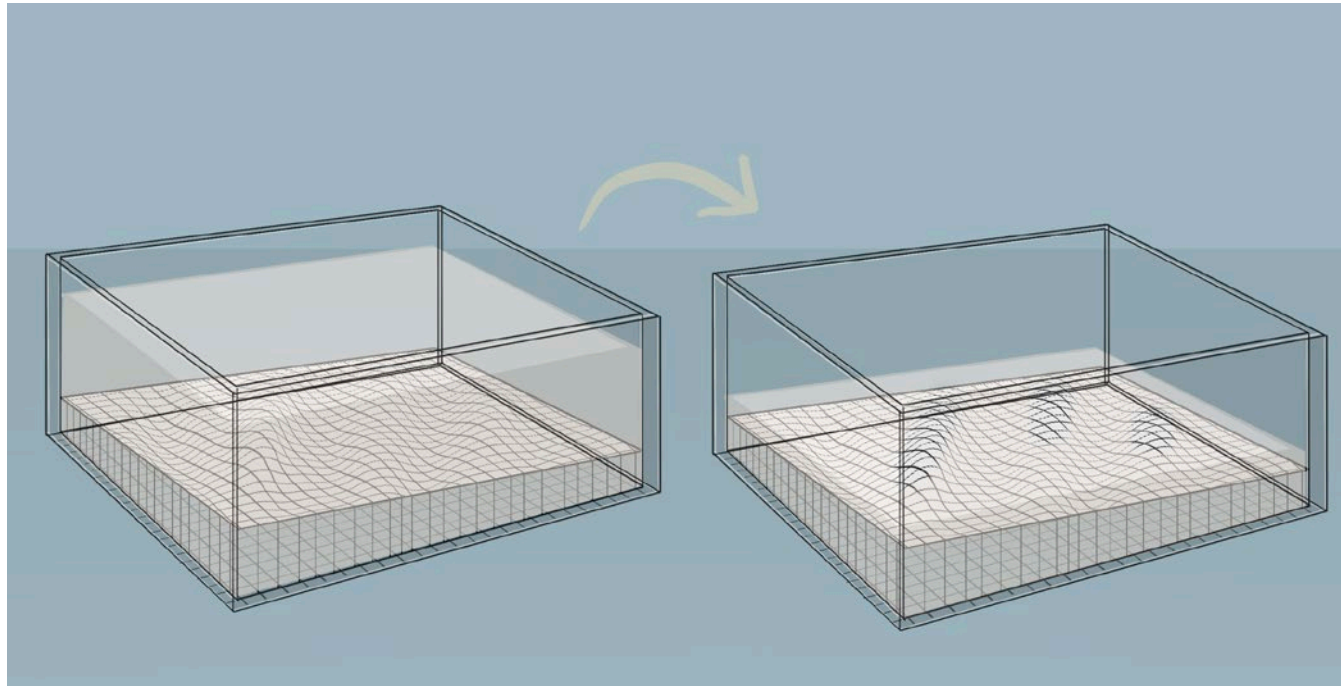
"Leveraging localized surface disturbances of the air-medium interface during the B.C. growth"

To locally disturb the surface during growth in this test physical objects are moved through the medium surface. In Figure 48 a visualization is shown of the principle.

For this design principle multiple research questions have been listed:

1. How do different types of geometry interact with the growth of B.C. when the obstruction touches the surface of the air-liquid interface?
2. How does the type of material change the behaviour of the cellulose producing bacteria when touching the obstruction?
3. How does cappilarity of the medium affect the growth when geometry is introduced above the surface of the liquid?
4. How does the level of medium over time influence the interaction between the cellulose and the obstrusion?
5. How does changing the location of an obstruction during the B.C. growth influence the resulting cellulose geometry?

Test 1: Moving sub-surface geometry through the forming cellulose layer

This test is conducted with the aim of answering the first research question for design principle

1. How do different types of geometry interact with the growth of B.C. when the obstruction touches the surface of the air-liquid interface?

Hypothesis
Moving an object through the growing cellulose layer should allow for more complex hole shapes. Movement of the object up or down should not change the behaviour of the growth.

Method
A setup is made where two objects can move vertically, using an acrylic container with holes in the bottom (see Figure 49 to 52). Two cut off syringes are used as watertight pistons. Copper wire is attached to the pistons and is used to make clamps that can hold objects. In both pistons the tetrahedon geometry from the P1 test is used. 750mL CSL medium inoculated with K.H. is added to the assembled setup. One piston holds the object above the liquid and one object is submerged. The piston above the liquid is moved down after day 4 and the other piston is moved upward, both for about half a centimeter. This is repeated after day 6.

Findings:
- Moving objects through the bottom of the vessel calls for more attention for water-tightness, increasing the complexity of the needed setup to test the hypothesis.
- Due to debris of the medium and formation of loose cellulose pellicles clogging the pistons containing the objects, it became impossible to move the object during growth. Results are therefore inconclusive.
- Autoclaving the cellulose with the pistons containing the copper arms still in it resulted in a dark colouration of the resulting samples (see Figure 53 and 54).
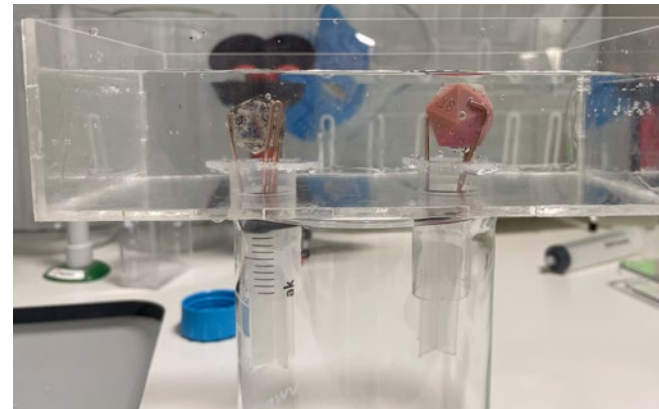
Figure 49- Test setup showing the pistons containing the objects

Figure 50 - Submerged object after 4 days of growth
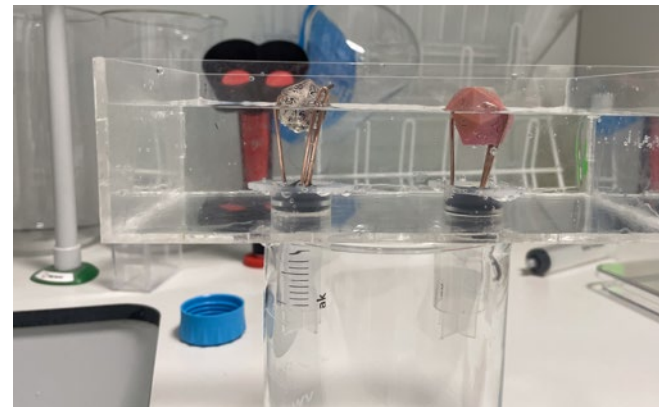
Figure 51 - Test setup showing the pistons moved upwards

Figure 52 - Object above the medium layer after 4 days of growth
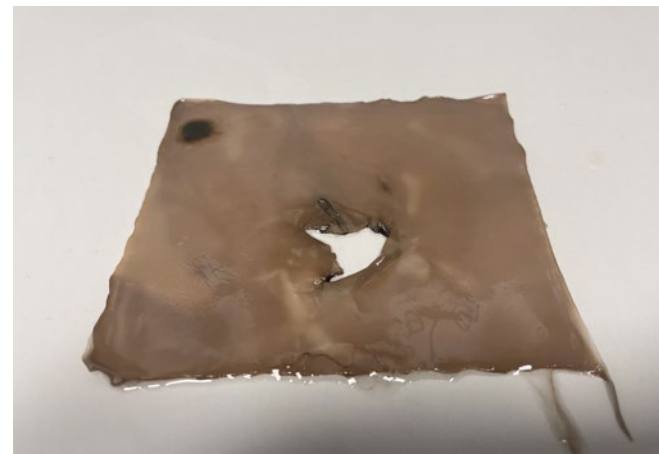
Figure 53 - Imprint of the submerged object in the cellulose sample

Figure 54 - Imprint of the copper wires in the cellulose sample

4. Design Principle 3
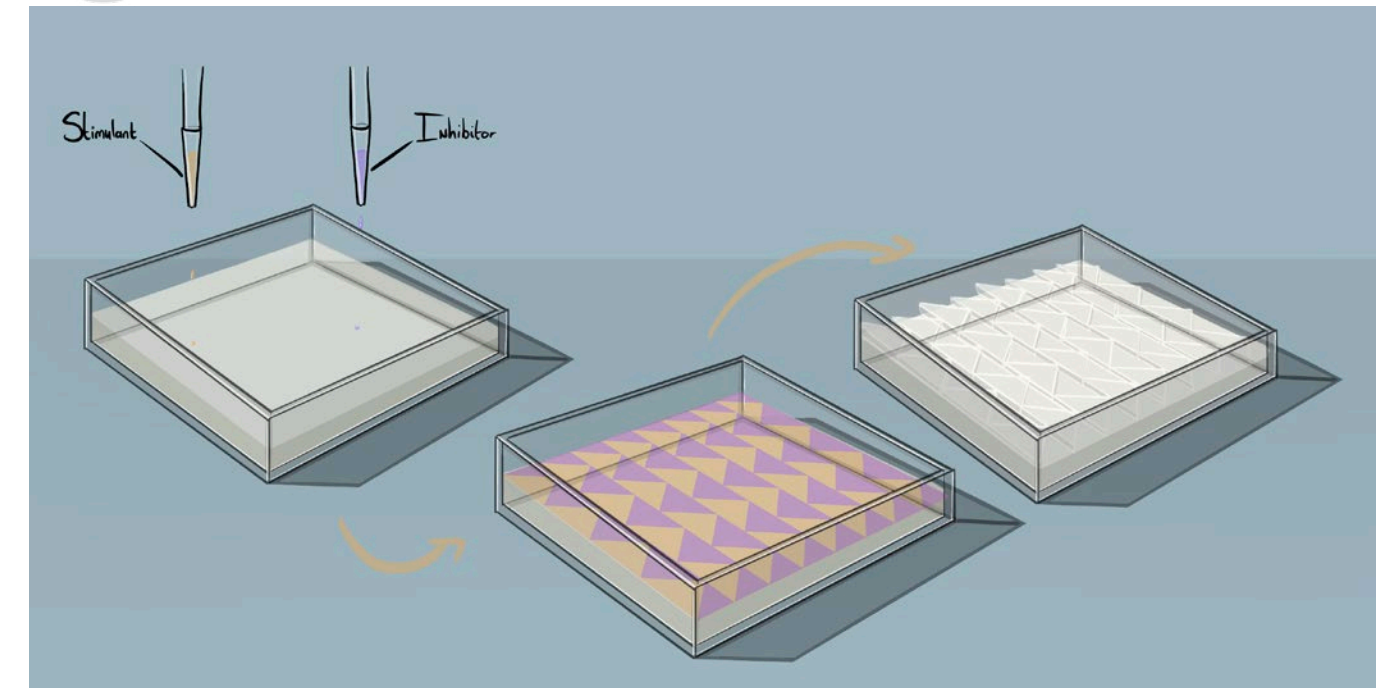
Figure 55 - Visualization of a possible final concept for Principle 3

"Localized addition of growth stimulants and inhibitors to the culture"

To locally inhibit and stimulate the B.C. growth, multiple substances are added to the medium and tested on its influence on the cellulose growth. In Figure 55 this principle is visualized.

For this design principle multiple research questions have been listed:
1. What substances inhibit the synthesis of cellulose?
2. What substances stimulate the synthesis of cellulose?
3. How can inhibiting and stimulating substances be localised?
4. How does changing the volume of inhibiting- and stimulating substance chage the rate of inhibition or stimulation of cellulose biosynthesis?
5. What influence does surface tension have on the synthesis of cellulose?

Test 1: Introducing surface tension altering substances to the growth medium

This test is conducted with the aim of answering the first research question for design principle 1:

1. What substances inhibit the synthesis of cellulose?
2. What substances stimulate the synthesis of cellulose?
3. How does changing the volume of inhibiting- and stimulating substance chage the rate of inhibition or stimulation of cellulose biosynthesis?
4. What influence does surface tension have on the synthesis of cellulose?

Hypothesis

To test this principle, two substances are added to the medium. According to research done by Żywicka et al. (2018), adding vegetable oil to the growth medium can increase B.C. yield by about 500%. Vegetable oil decreases the surface tension of water, while surfactants increase this value. From the research done on B.C. formation, this might be the trigger for producing cellulose. It is therefore hypothisised that adding oil will increase growth, while adding a surfactant will decrease (or even stop) the growth.

Figure 56 - Graphical overview of the concentrations of Tween80 and lineseed oil

Method

To answer the main research questions, a setup was made where the concentration of the substances was varied; lineseed oil and Tween80. Lineseed oil would decrease the surface tension, while Tween80, a surfactant, would increase this value. In a 24-well plate (see Figure 57 and 58) concentrations following the schematic from Figure 56 were made of both substances in the with K.H. inoculated CSL medium. B.C. was grown for one week, after which the cellulose was obtained and analysed for its thickness and shape. Two samples containg 1% of both substances were also grown in a 250mL beaker. These samples are weighed after 7 days of growth.

Findings:

- Lineseed oil addition to the medium did not alter the growth as hypothisised. The 1% addition, as stated in the research by Żywicka et al. (2018), did not correspond to the findings of this test. The paper states a 540% increase, but thickness of the obtained cellulose did not vary as significantly for all results. Weight difference was not measurable in the well plate samples. Two larger samples in the second test were weighed, which showed an increase of 115% in the oil sample compared to the Tween80 sample (see Figure 59-63)
- At 5% concentration, a ring of lineseed oil formed around the edge of the wells, resulting in a thinner outer edge of cellulose.
- For the test with Tween80 it was expected that an increase in concentration would decrease the amount of obtained cellulose. However, this was also not the case. For 1% concentration the thickness of the cellulose layer was the heighest and also higher than the samples without Tween80.

Design Principle 3: Vegetable oil v.s. Tween80

Figure 57 - 24-well plate containing CSL and oil
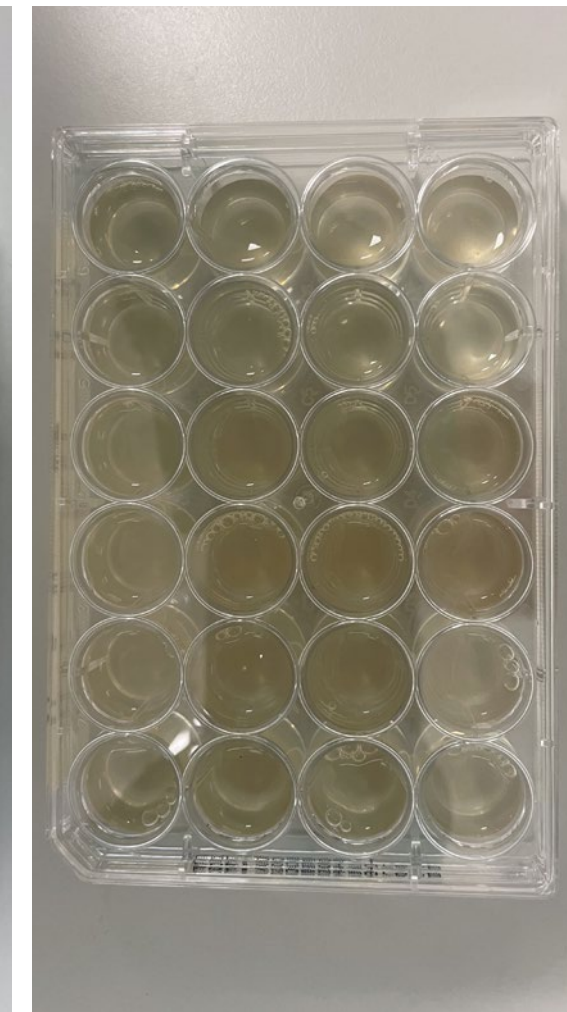
Figure 58 - 24-well plate containing CSL and Tween80
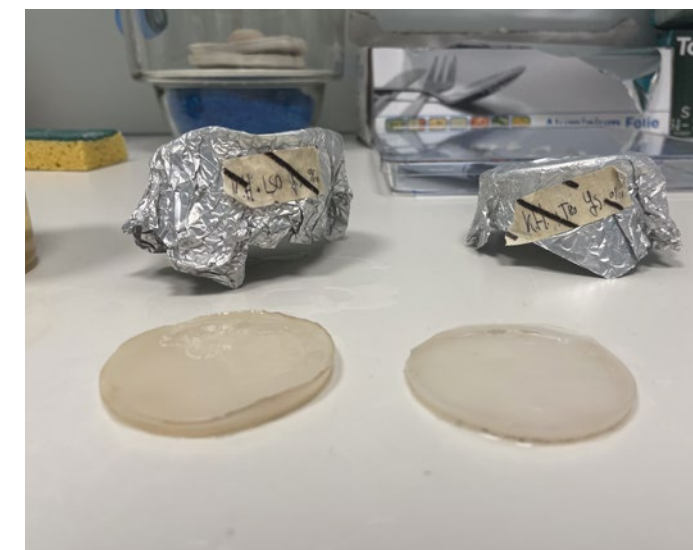
Figure 59 - Samples after 7 days of growth (left: oil | right: Tween80)

Figure 60 - Resulting Tween80 samples
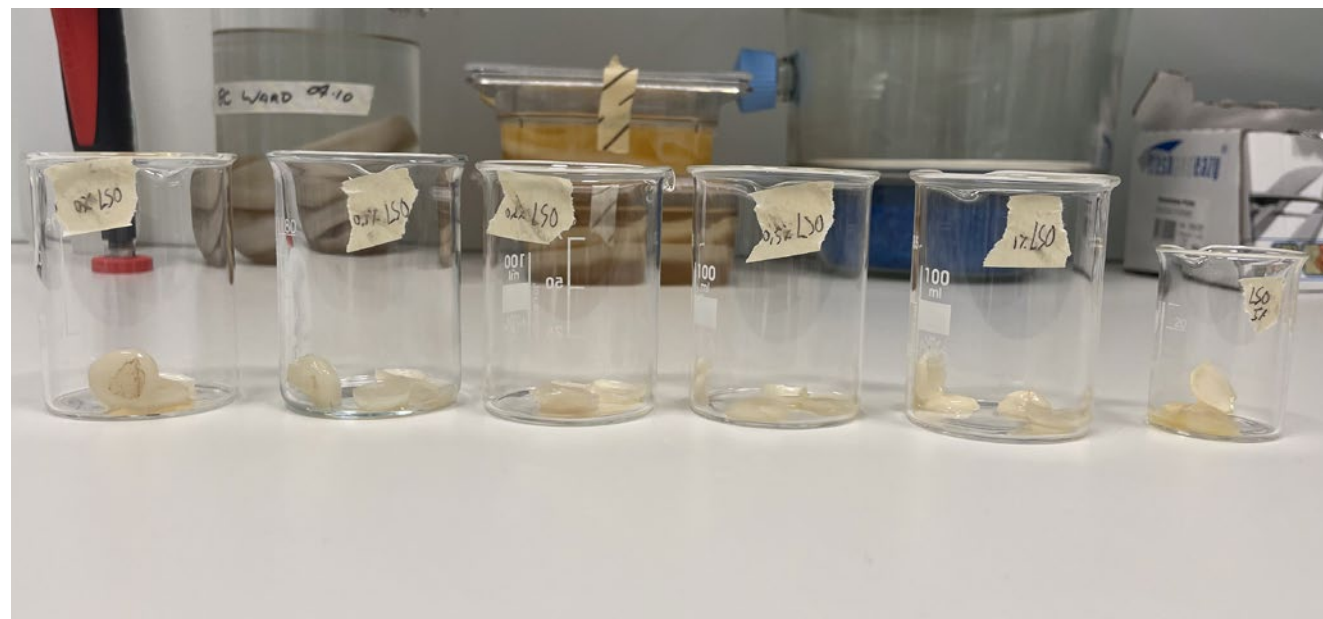
Figure 61 - Resulting samples containing lineseed oil

Figure 62 - Wet weight of the sample containing lineseed oil

Figure 63 - Wet weight of the sample containing Tween80
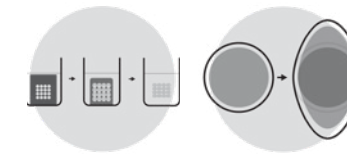
5. Design Principle 4 and 5:

"Utilizing geometrically confined porosity to create B.C. growth within the medium" & "Incremental surface area change of the B.C. growth through changing the vessel shape"

For this design principle multiple research questions have been listed:
1. How does changing the location of air-liquid interfaces under the medium surface change the growing behaviour of B.C.?
2. How can B.C. layers be connected when grown in subsurface air pockets?
3. How does changing the shape of the vessel during B.C. growth affect the eventual cellulose sample?

Test 1: Subsurface air pocket in a B.C. culture

This test is conducted with the aim of answering the first research question for design principle 4: **How does changing the location of air-liquid interfaces under the medium surface change the growing behaviour of B.C.?**

Hypothesis
A relatively thinner cellulose layer will form within the air pocket, since the amount of oxygen within the pocket is more finite.

Method
An aluminium cylinder, with a hole drilled in the bottom is situated in a 250ml beaker with CSL medium containing the K.H. bacteria (see Figure 54). Growth of the cellulose layer is monitored for one week.

Findings:
- No cellulose was formed within the air pocket. This makes this principle not suited for further development (see Figure 65 and 66)

Figure 64 - Aluminium cylinder containing an air pocket

Test 2: B.C. growth in a container with a movable wall

This test is conducted with the aim of answering the first research question for design principle 4: **How does changing the shape of the vessel during B.C. growth affect the eventual cellulose sample?**

Hypothesis
Increasing the surface area of the B.C. growth after an initial layer has formed will add a thinner geometry as an extension to the previous geometry.

Method
750mL of CSL medium is poured in the acrylic container (see Figure 67) and is inoculated with the K.H. bacteria. The wall is then placed in the culture and is moved after 4 days of growth. After 6 days of growth the wall is moved again.

Findings:
- Clear thickness alteration is generated using this method (see Figure 69-72)
- Due to cappilary forces the medium formed an arc with the movable wall, which is directly translated in the formed cellulose at this location.
- Due to the large surface area, evaporation of the medium was very strong.

Design Principle 4 & 5: Subsurface air pocket & B.C. growth in a shape changing vessel

Figure 65 - Cellulose ring formed around the cylinder

Figure 66 - No cellulose formation within the air pocket after 7 days

Figure 67 - B.C. growth after 4 days

Figure 68 - First movement of the wall (day 5)

Figure 69 - Extracted sample after two wall movements

Figure 70 - Close-up of the sample

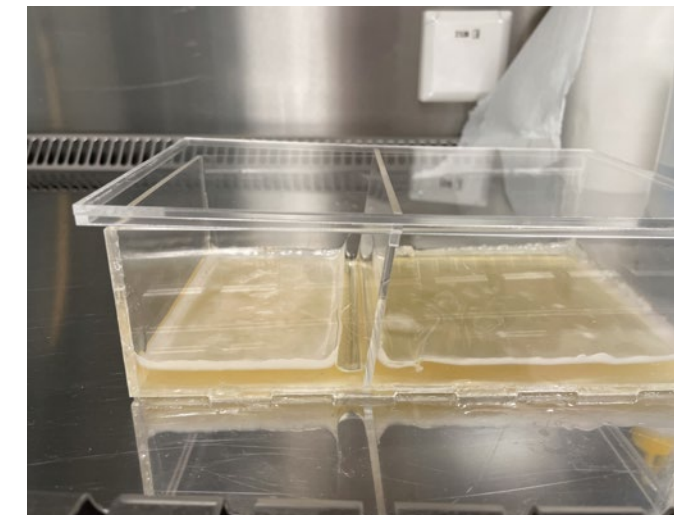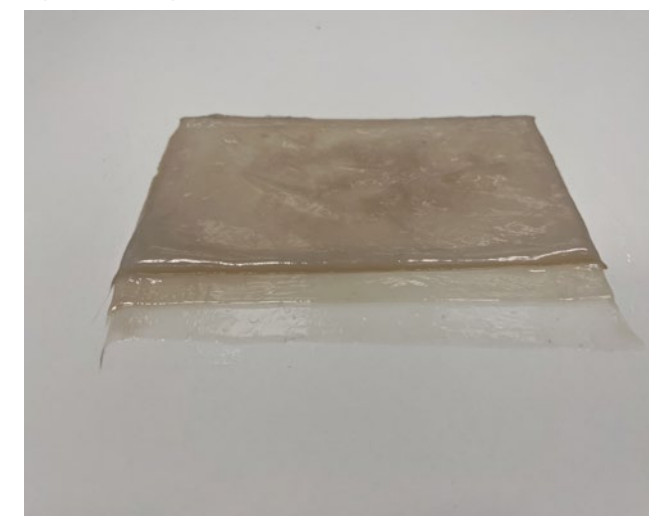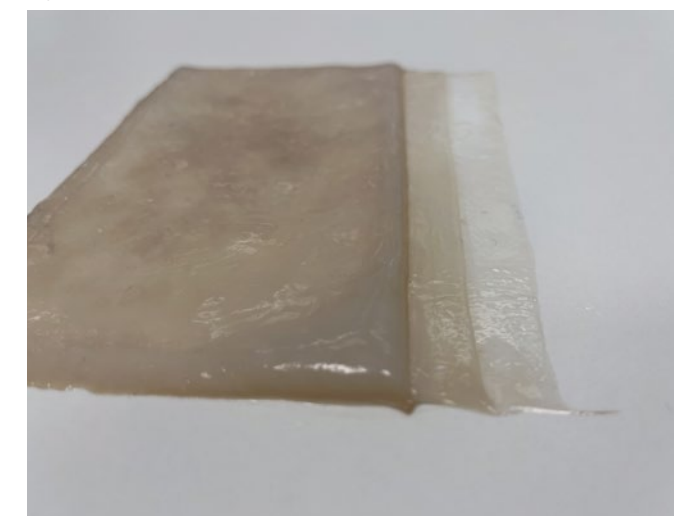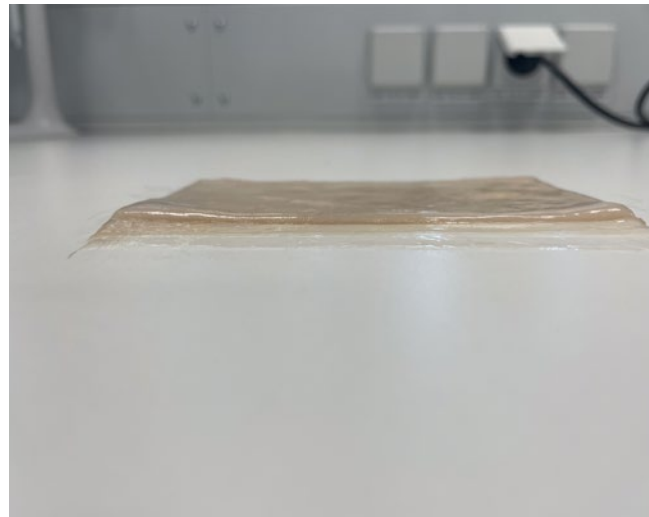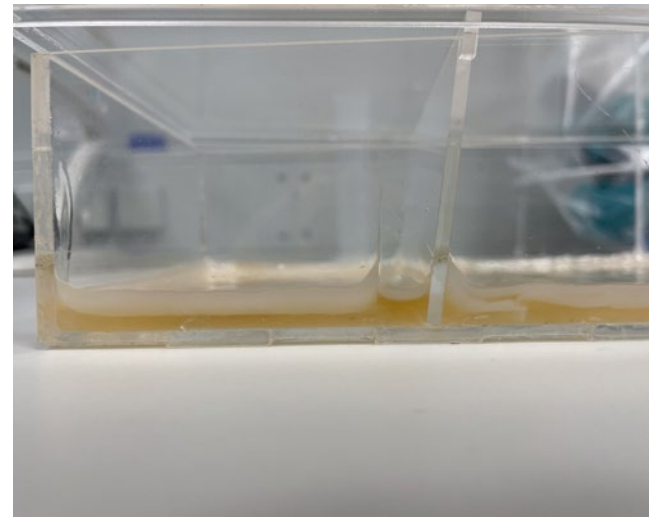Figure 71 - Side-view of the sample showing thickness variation

Figure 72 - Sideview of the first movement
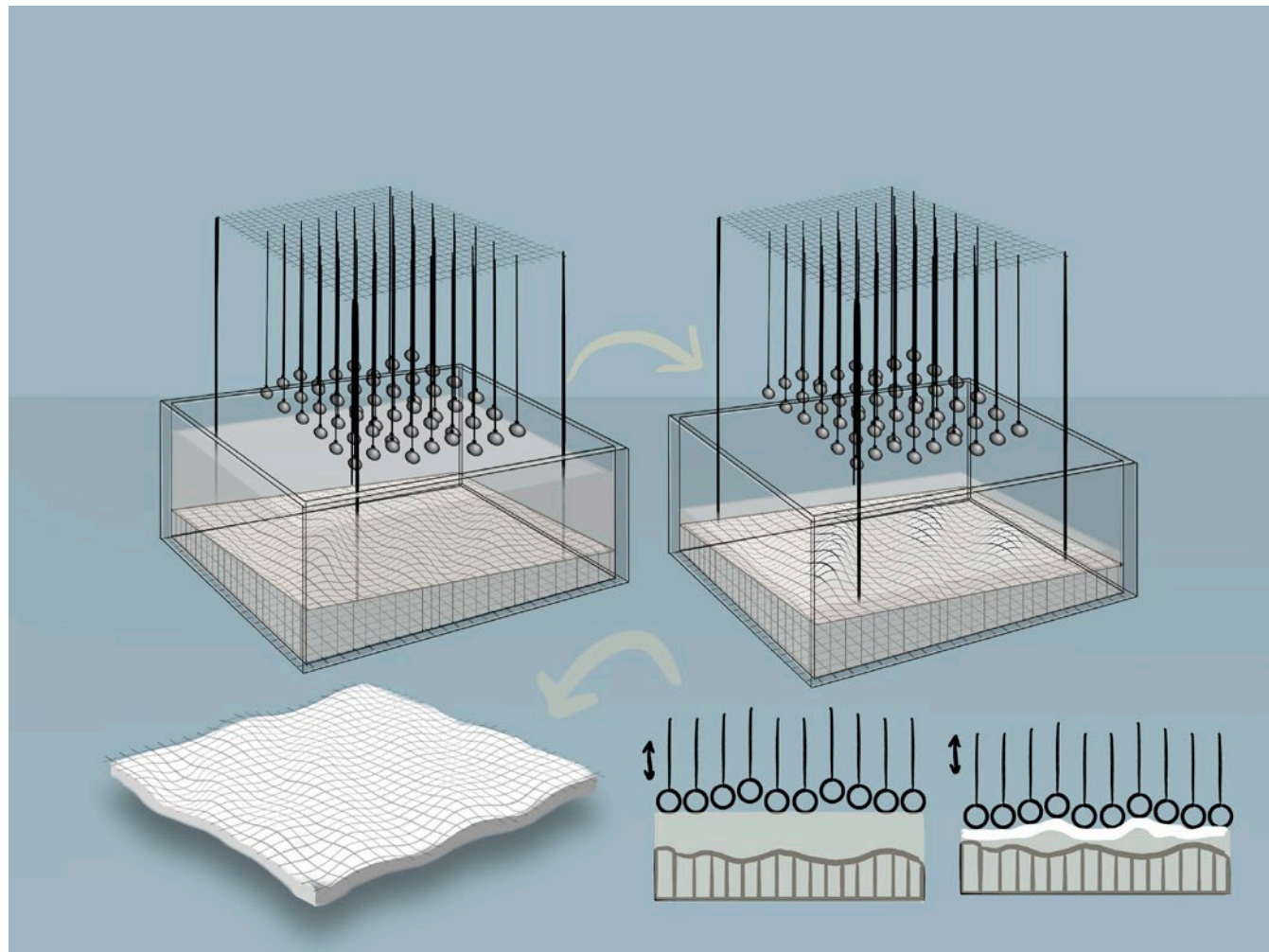
Figure 73 - Visualization of the combined principles into a possible concept

6. Conclusion and Selection of One Principle

After testing the selected principles, a selection is made for one principle for further development. Selection of this principle is, like the hierarchy of principles, based on the given feasibility and the 3D shaping potential. However, the choice is also based on the amount of ways of approaching the principles, since this increases the chance of success of finding a way to pre-program the eventual shape of cellulose.

Concluding from the tests, the choice is made to further develop Principle 1 and eventually combine this with Principle 2. For the tests of Principle 2, there was still some inconclusiveness, due to the failing of the test setup. As previously stated, moving geometry from the underside of the medium surface involves more complexity regarding water tightness. However, due to findings from Principle 1 and the potential of combining both principles, it is chosen that adding this complexity in further iterations might prove to be valuable in the end.

The combined principles are re-formulated into: "To achieve freedom in the shaping of Bacterial Cellulose by localising obstruction through the introduction of geometry above and below a moving air-liquid interface."

The choice of not further developing Principle 3, 4 and 5 has multiple reasons. For Principle 3 no substances were found to inhibit the growth substantially. Also, the substances that were used to increase growth also did not show significant enough results. Finally, it proved to be difficult to locally fixate droplets of the substances in the medium, since they moved towards the edge of the beaker over time. Solutions to these problems can be thought of, but a lack of chemical and biological knowledge will slow down the creative process and also falls outside of the scope of this project.

Principle 4 did not show any cellulose growth in the air pocket under the surface of the medium. Also, finding a way of connecting air pockets in a programmed 3D shape will prove to be a challenge.

Principle 5 was tested before making the hierarchy, to also find an easy way of tweaking the thickness of the cellulose layer and to get a grip on the B.C. growing process. The test did have the desired result, but the limit of geometry that this way of shaping cellulose can produce does not provide the desired freedom.

In Figure 73 a visualization is made of a possible solution to the combined principle 1 and 2. Combining moving geometry above and under the medium surface will allow for more complex shapes. This combined principle calls for more tests to answer the following research questions:

- How can the sticking of the cellulose to objects be controlled?
- How can geometry be moved within the medium layer, while keeping the vessel watertight?
- How can the medium volume be controlled, while keeping the cellulose layer intact?
- How can the growth rate of cellulose be controlled and monitored more precisely?
- How precise does the cellulose production need to be controlled and monitored?
- What is the exact relationship between medium volume and cellulose production rate?

To tackle the newly found design problems, multiple test setups need to be developed to individually address them. The to be further developed production method is called 'CelluShaping'. This is discussed in the next chapter.

CelluShaping

UNDERSTANDING THE MAIN COMPONENTS OF THE CHOSEN PRINCIPLE

From the chosen principle, which is called CelluShaping, first the basic components are elaborated upon, answering research question D.1.. From these basic components a testing setup is designed and build (D1.1). Also, to predict the growth and to build a tool to work with the production method, a computational model is built (D.2.).

1. Understanding the Main Principle Components

2. Designing a re-usable and adaptive testing setup

3. Building a model to predict B.C. Growth

1. Understanding the Main Principle Components

As previously stated, the description of the chosen principle says:

"To achieve freedom in the shaping of Bacterial Cellulose by localising obstruction through the introduction of geometry above and below a moving air-liquid interface"

This principle consists of four main components, being:
- The freedom in shaping of B.C.
- The localisation of an obstruction
- The geometry above and below the air-liquid interface
- The moving air-liquid interface

In Figure 74 a graphical overview is shown with all the components of the above mentioned principle

The meaning of localization is to be able to control a certain entity within a certain space. In the instance of this principle, it would mean that one or multiple objects, or obtructions, need to be positioned above or below the growing B.C. in order to generate pre-defined shapes. Full control of the X-, Y- and Z-coordinates of the obstructions is needed to have full freedom in the shaping of the cellulose.

Not only the position of the obstruction, but also its geometry is important to get the most freedom in shaping B.C.. Four categories of geometry changes are identified, each with multiple variations within the category. In Figure 75 these categories with the variations are visualised and listed in Table 1. For the variations only symmetrical shapes are listed. Combining the variations into final geometries to test with would already result in an infinite amount of variation and adding asymmetrical shapes would only make it more complex. Complexity in B.C. shape can already be achieved with the more simple shape combinations.

Finally, the movement in the Z-direction of the air-liquid interface allows for the introduction of obstructions to the B.C. growth and to localise the obstruction in the Z-direction over time. Fine control over this variable would increase the quality of the shape change and is thus important for the freedom of B.C. shaping.

Increasing the volume of medium would increase the height of the air-liquid interface, moving it towards geometry above its surface and away from geometry below its surface. This element is visualized in Figure 76.

The air-liquid interface has four states:
- State 1: No cellulose has formed yet.
- State 2: Loose cellulose pellicles have formed, covering part of the air-liquid interface's surface.
- State 3: An obstruction is situated in the air liquid interface, resulting in partial coverage of cellulose over its surface.
- State 4: The air-liquid interface's surface is fully covered with cellulose.

When cellulose forms while the air-liquid interface is in State 1 or 2 and geometry penetrates through it, movement of the air-liquid interface does not yet apply pressure to the to-be formed cellulose layer. When in State 3, the result on the forming B.C. layer after movement of the air-liquid interface can have multiple concequences depending on the geometry and location of the obstruction. Fir
When in State 4, geometry moving through the air-liquid interface will apply pressure to the cellulose layer. Depending on the type of geometry and its location on the Z-axis, this geometry can either push (part of) the cellulose layer under- or above the air-liquid interface.
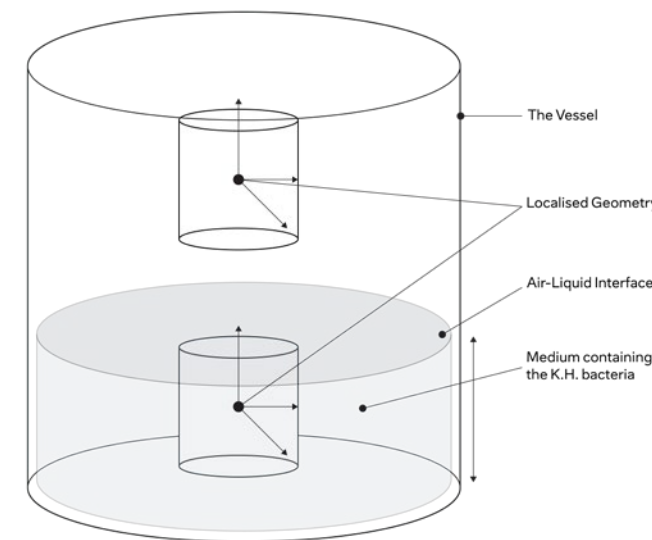
Figure 74 - Graphical visualization of the main components of the principle
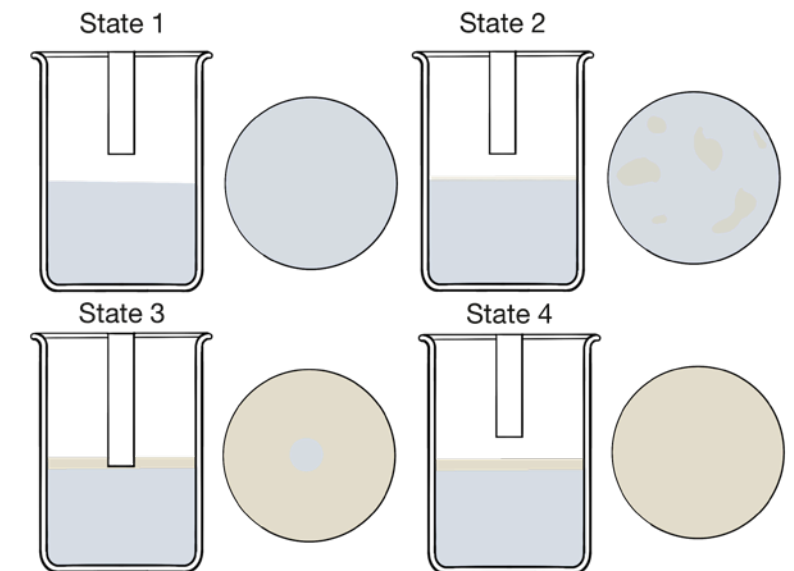
Figure 76 - Graphic visualization of the different states of the setup
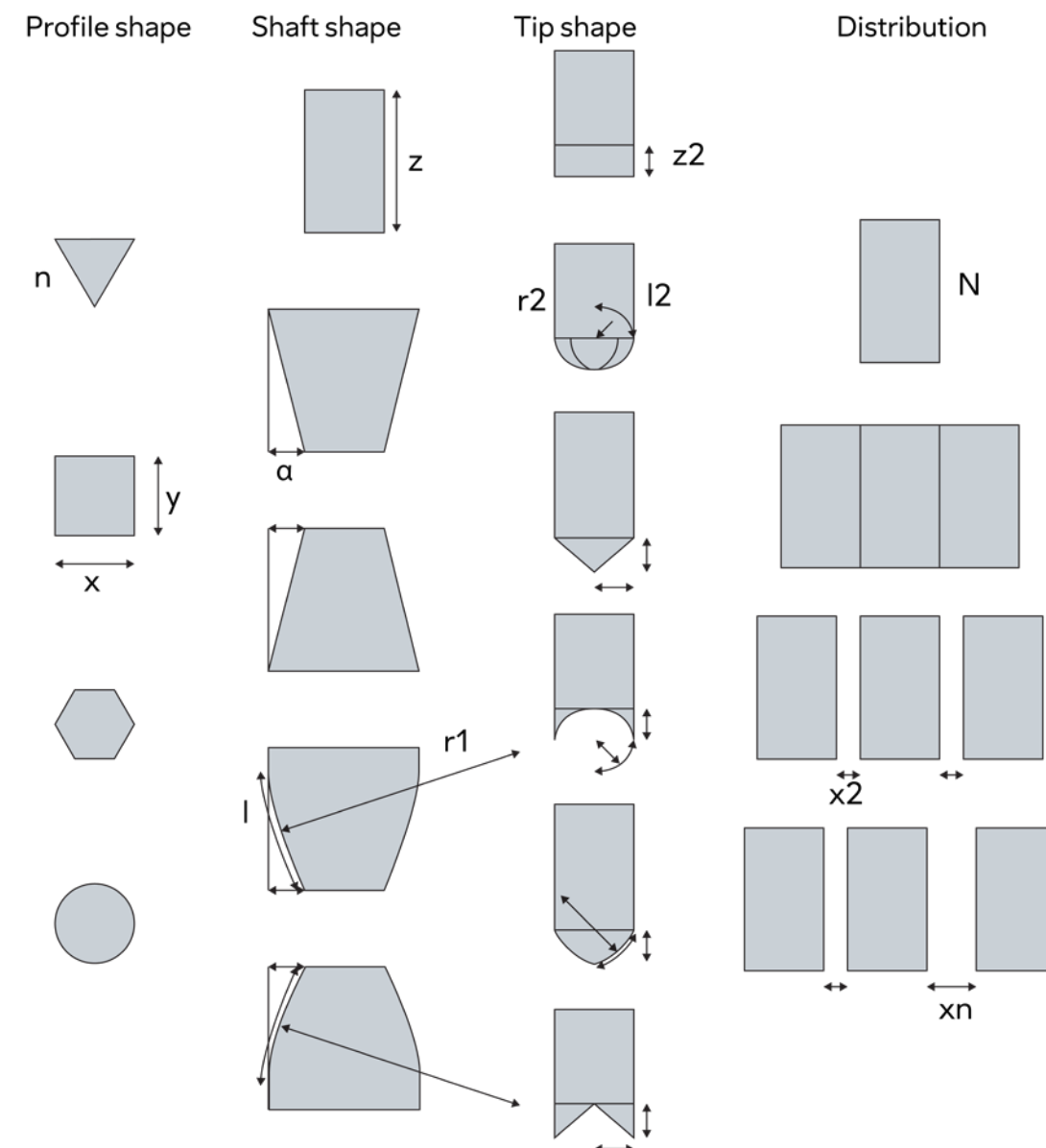
Figure 75 - Graphical overview of the shape variations of the localized geometries

	Variable	Description
n	Amount of edges of the profile
x	Horizontal size of the profile
y	Vertical size of the profile
z	Height of the shaft
α	Draft angle of the shaft
l	Length of the shaft side arc
r1	Radius of the shaft side arc
z2	Height of the tip
r2	Radius of the tip
l2	Arc length of the tip
N	Amount of geometries
x2	Distance between geometries (equal)
xn	Distance between geometries (individual)

Table 1 - Variables of the shape variations

2. Designing a re-usable and adaptive testing setup

To test with incremental parameter changes a test setup is needed, which allows for repeatable usage. Until now, random shapes are used as geometry obstrusions and the medium level was altered manually. To automate this process, a setup is designed with the following requirements:

1. The setup needs to allow for medium addition and removal without obstructing the B.C. growth.
2. The vessel needs to be transparent.
3. The vessel and all components which are in direct air-contact with the B.C. layer need to be able to handle the circumstances in the autoclave (122 °C for 30 minutes).
4. A precision of the medium volume increase- or decrease rate of at least 1.0 µl/min is needed.
5. The medium level height needs to be monitored and controlled with a precision of +- 1mm (which is about **+-**3.4mL of volume).
6. The vessel needs to allow for the testing of multiple geometries.
7. The vessel needs to be water-tight.
8. The inside of the vessel needs to keep out micro-organisms, while allowing for air-flow from the top.

For the vessel a 400mL tall borosilicate beaker is chosen. After testing on borosilicate glass, it was found that by using a diamond coated drill bit, a Dremel and enough cold water it is possible to drill small holes. A hose with a diameter of 6mm is used to make an inlet in the bottom of the beaker. The hole for the inlet is drilled at approximately 5mm, which allows for making the inlet water-tight, without the addition of glue (see Figure 76).
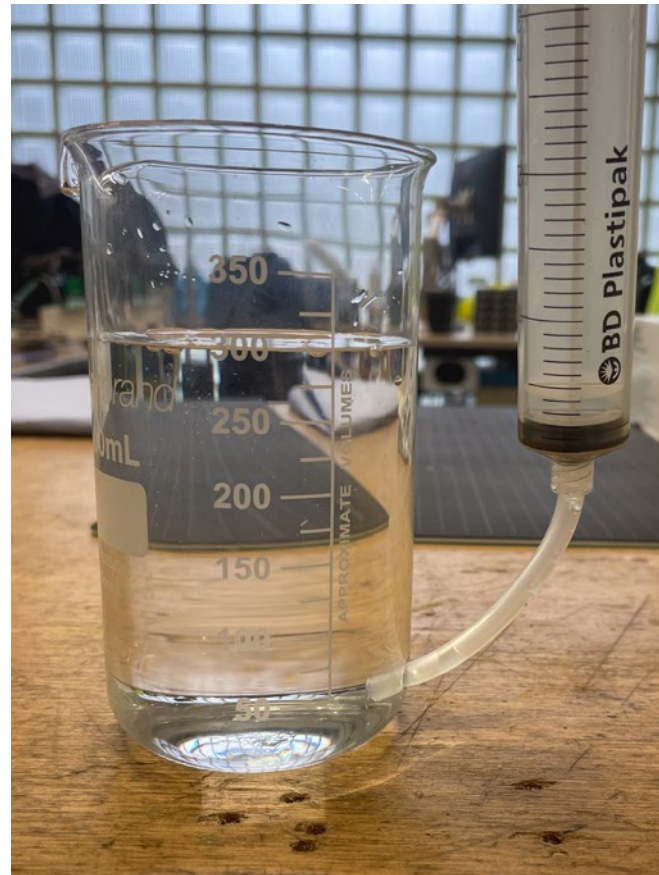
Figure 76 - The vessel connected to a syringe using silicone tubing

To increase and decrease the medium volume within the vessel, a servo powered syringe pump in combination with a TB6600 micro-step driver is used (see Figure 79). This setup is controlled by an Arduino. The micro-step driver allows for turning the servo with steps of 1/6400th of a full rotation at the lowest setting. Using the 60mL syringe, this is equal to 0.78 µL per step of the motor (see Figure 79).

To monitor the volume of the medium inside the vessel and, in the end, control this volume, multiple approaches have been considered and tested. There are a lot of solutions for liquid volume measuring, which is often done in industrial applications using sonar-, or laser-based distance measuring sensors (see Figure 78) or floating devices.

Firstly, a sonar sensor module is used to also test the written code for the addition or removal of fluid when a certain volume is too low or too high. This sensor did work for this first test setup, but the precision being +-1cm is too big to meet the requirements.

A more precise distance measuring sensor is used after this realisation. A Time of Flight sensor (the Adafruit VL53L0X), which measures the distance to the target by means of rebounded light, was tested and evaluated. Although the sensor was listed as very precise (+-1mm), there was a lot of noise in the received signal. One cause of this might be that the surface of which the distance is measured from is transparent (being water in this test), causing some light rays to diffuse in the liquid. However, when tested on an opaque, non-transparent white surface, the signal still showed a lot of noise and even drift.
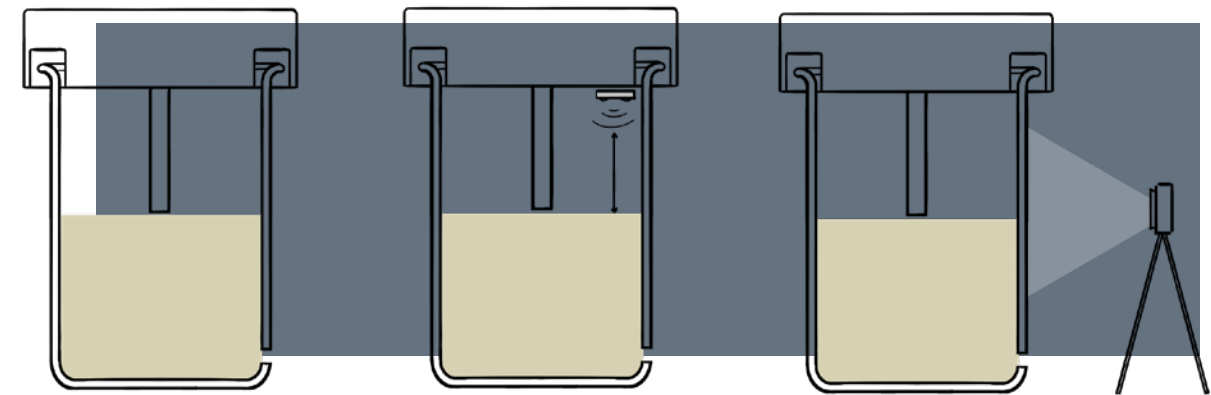
Figure 78 - Medium volume sensing methods
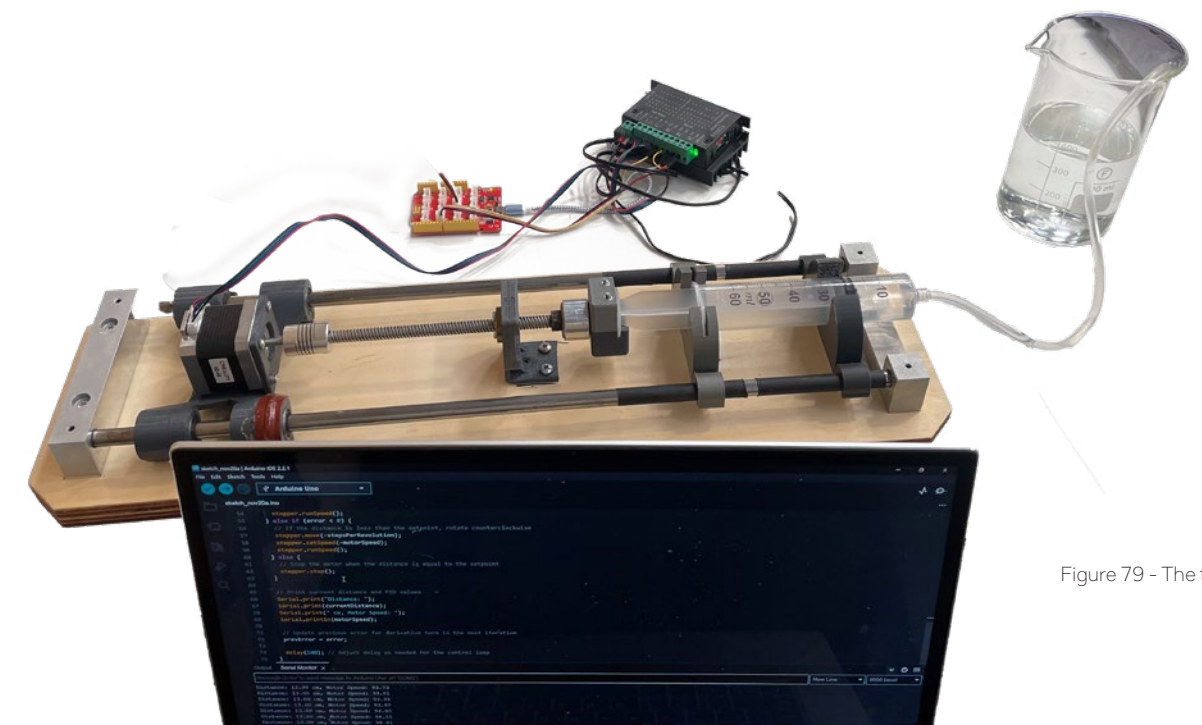
Figure 79 - The testing setup

To conform to the stated requirements, the sensor used needs to be able to handle the humid environment inside the vessel while still be operable. Also, if the sensor would be inside the vessel, like it would be the case if the sonar- or ToF-sensor was used, the sensor also needs to be able to be sterilised. This could be done by means of UV, but earlier testing with UV sterilised 3D prints showed that it does not always prevent contaminations.

Volume measuring options outside of the vessel are considered. Measuring the volume by means of a weight difference could work, but this would mean that a very precise scale would have to be placed inside the incubator. The used incubator is also used by other researchers, which means the setup undergoes a lot of vibrations when opening and closing the doors.

Finally, the volume of the medium was measured using a camera (the Pixy2 by Pixycam) and image recognition software (see Figure 80 and 81). This camera has a relatively low resolution (1296x976 pixels), but a high frame-rate. Since every pixel needs to be evaluated 60 times per second, too many pixels makes the image recognition slower. In Appendix B the code is visualized.

Figure 81 - Test setup for the evaluation of the image recognition camera

To close off the vessel, while alowing for air flow and the addition of geometry above the air-liquid interface, a lid is designed. This lid would ideally be made of a material that can withstand the temperatures and pressure in the autoclave, so the full setup can be sterilised at once after every test. In Figure 82 the final 3D model for the lid is shown. This lid has spacers at the top, so air can flow in a 180° curve and micro-organisms are kept out of the vessel. In the bottom of the lid a threaded hole is added, where geometry can be screwed in using M12 threading.
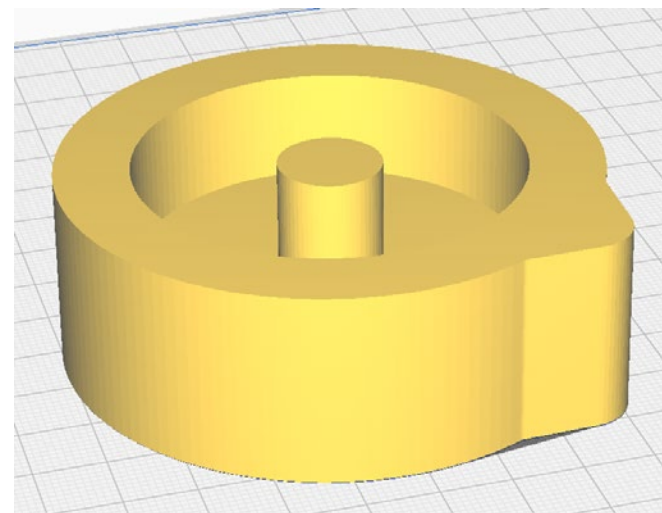
Figure 82 - Graphic overview of the full testing setup
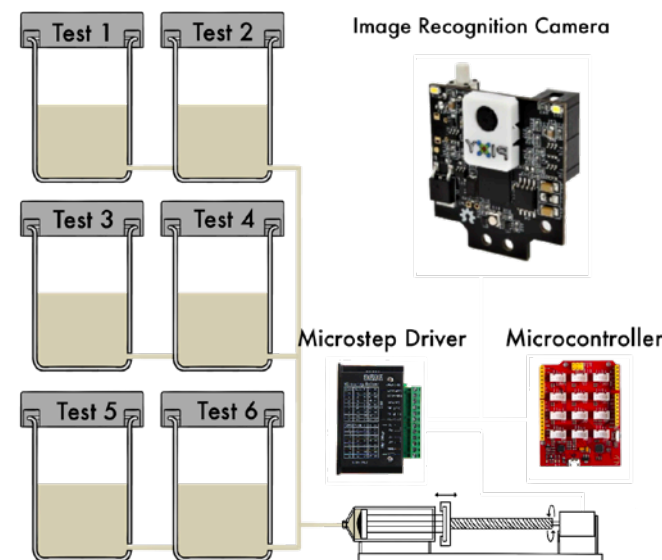
Figure 80 - Graphic overview of the full testing setup

3. Building a model towards a Designer's Toolkit to predict B.C. Growth

For the design of a toolkit for the use of the production method for shaping B.C., the data from tests and experience with growing B.C., a model for the B.C growth is made in Rhino with the Grasshopper plug-in. The goal of the eventual toolkit is to enable designers to first digitally shape a B.C. sample. This is done by inserting a standardized geometry and a volume-regulation sequence, resulting in a visualization of the outcome of the B.C. growth, a rendered timelapse of its growth and a code for the microcontroller to operate the pump. In the modelling software the test setup is mimicked in a parametric model. Here, multiple variables like the initial medium volume, the volume increase, the geometry of the obstruction, etc. are inserted (see Figure 82). This results in a final outcome of the B.C. shape, which can be used to make a more well-founded hypothesis for the tests. In Figure X the dashboard with most of the input variables of the model is shown. In Appendix C the full Grasshopper script is visualized.

To build the model, first a formula needs to be made for the increase and decrease of the medium volume. This formula states:

$$V(t) = V(0) + V_{syringe}(t);$$

Where V(t) is the volume of the medium inside the vessel over time, V(0) is the starting volume inside the vessel and $V_{syringe}(t)$ is the volume in the syringe (see Figure 83)

In the model this increase or decrease in volume translates to the movement of the starting growth plane in the Z-direction. As measured, the inner radius of the vessel in the tests is 32.91mm, which the model is set to. This results in a medium level height formula:

$$h(t) = (\Pi * 32.91^2)/V(t);$$

Figure 82 - Dashboard of the computational model

Next, a formula is needed for the thickness of the B.C. layer over time. Research by Tureck et al. (2021) shows that an average weight of 0.6 g/L of cellulose after 48 hours of growth is found when grown in CSL medium containing glucose. With an average density of 1.25g/cm³, this would translate to 0.0029mm of thickness increase per hour. This rate is used as a first estimate of the B.C. growth curve in the model and is kept constant. From experience from Test 2 of Principle 1, where approximately the same medium volume was used, it is expected that State 2 is reached at about 48 hours

Figure 83 - Graphical overview of the vessel and its dimensional parameters

Research on defining a formula for the cellulose production of a strain of K.H. by Saleh et al. (2020) gives nine variables that influence the production rate. This being glucose-, yeast extract-, KH_2PO_4-, $MgSO_4$-, ethanol-, and pH-levels. inoculum size, temperature and incubation time. Since a different medium has been used in this project, namely CSL medium, direct use of the concluding formula in the model is not possible.

Figure 84 - Method for obtaining a formula for B.C. growth

A different approach was used, where thickness of the sample over time is measured using frames of the time-lapse video of Test 3 (see Figure 84). Here, the thickness of the cellulose layer is measured per frame and added a table, resulting in graph 1. The formula for the trend-line from this graph, being:

$$h_{B.C.}(t) = 7.2268\ln(t) - 28,467;$$

is used in the parametric model, to simulate the thickness increase of the cellulose layer (see Figure X.

It is acknowledged that one case of cellulose growth does not reflect the same amount of growth when for example the medium volume is different. Therefor, a more general formula needs to be found, probably based on Saleh et al. (2020). This is kept out of the scope for now and the above mentioned formula is used as a constant.

A first attempt to simulate the forming cellulose layer moving through geometry, boolean difference is used to create a cut-out in the digital cellulose sample (see Figure 85). From experience, it is expected that bending of the cellulose layer will also occur when pressure is applied by geometry in one direction. In Figure X this behaviour is visualized.
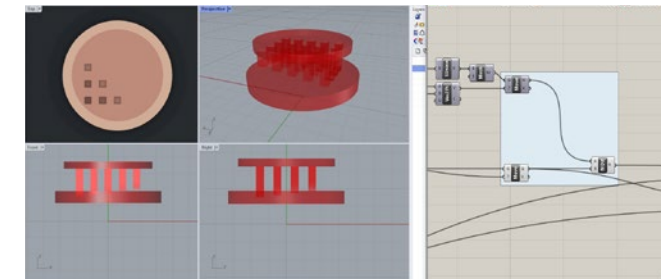
Figure 85 - Grasshopper boolean difference node inputting the geometry of the growing cellulose layer and the obstruction

The bending behaviour of the cellulose layer, seen in Test 3, can be added to the model, by adding physics models using the add-on Kangaroo2. This add-on allows for draping surfaces over objects, which can replicate the B.C. deformation in the tests (see Figure 86).

This bending can push the B.C. layer under the air-liquid interface, which could result in partial disconnecting of the formed layer to the to-be formed layer of cellulose. This also happened in Test 3 from Principle 1, where medium sipled on top of the cellulose layer (see Figure 37).
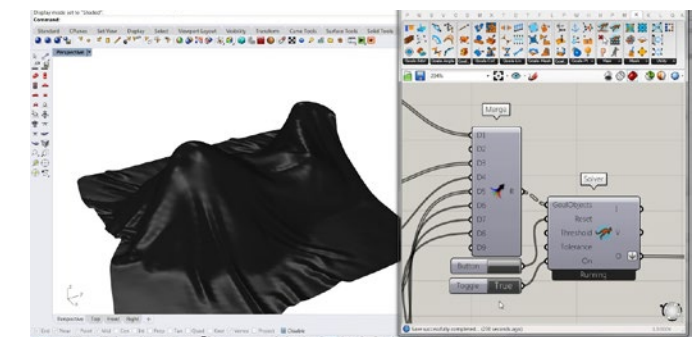
Figure 86 - Example file of the draping feature of the Kangaroo add-on of Grasshopper

B.C. thickness over time

$$y = 7,2268\ln(x) - 28,467$$
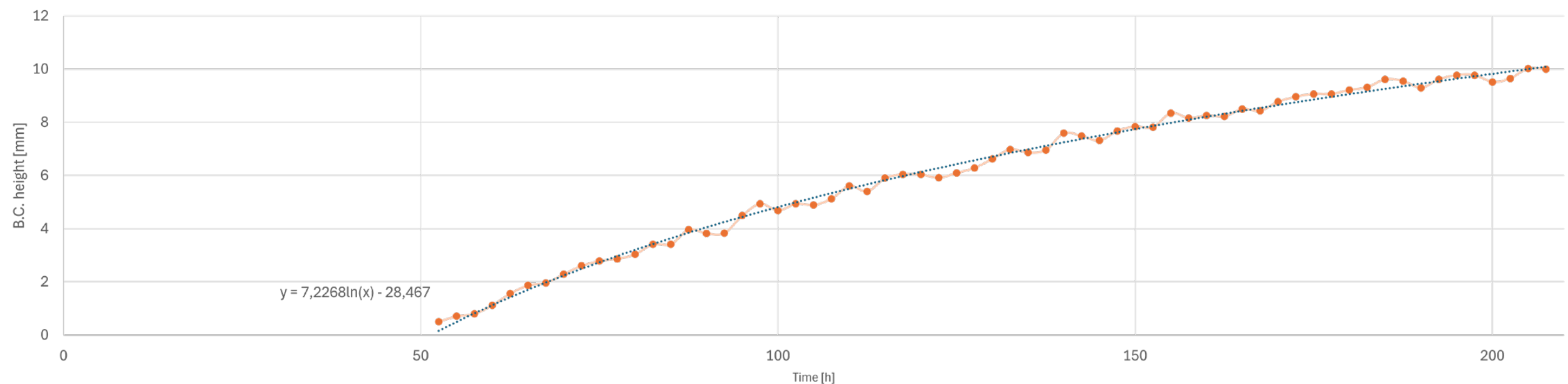
Graph 1 - B.C. thickness over time

To showcase the function and potential of the model, multiple geometries and medium volume sequence formulas are introduced as inputs. As geometries, variations are made, which are shown in Figure 87. Here, a smooth geometry, a sharply edged geometry and a more complex geometry are used. The sphere and tetrahedon are introduced after the system reaches State 4 and the hand is introduced in State 3. From experience in growing B.C., all samples will show bending, due to vertical forces being applied to the cellulose layer. Also, the model is expected to not penetrate the layer after growth.

Using the proposed model will aid in the formulation of hypothesese of the to be conducted tests discussed in the upcoming chapter.
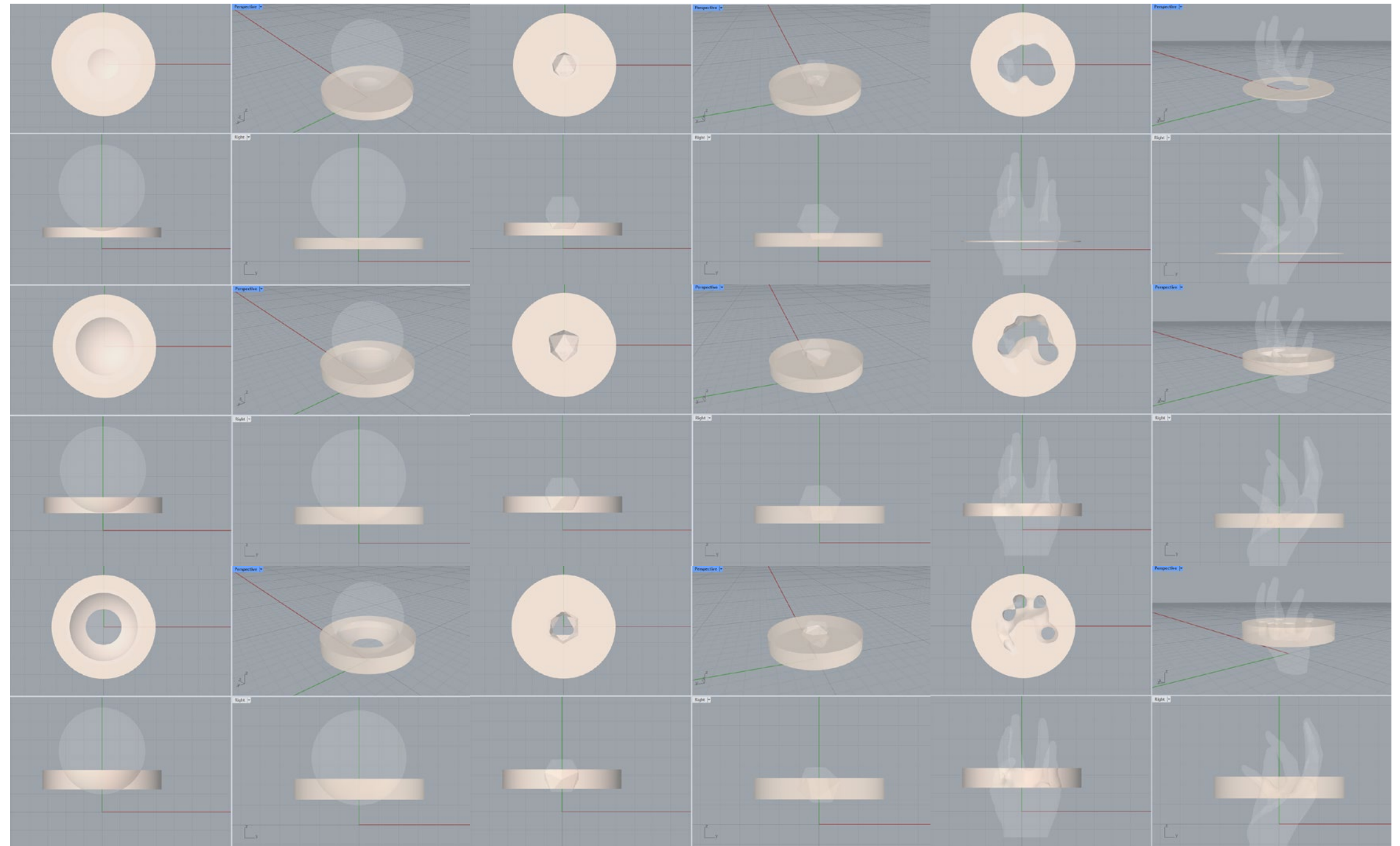
Figure 87 - Geometry variations, where a sphere (a), a tetrahedon (b) and a model of a hand (c) is inserted in the model at different time stamps

Testing the Setup

UNDERSTANDING AND TESTING THE MAIN COMPONENTS OF THE CHOSEN PRINCIPLE

In this chapter, all testing of the setup is discussed. First, the performance of the setup is tested without any geometry. After this, the influence of the surface area of the profile of the geometry on B.C. growth is tested. Thirdly, the effect of conically shaped geometry versus straight geometry is tested. Finally, a more complex shape is used to test the computational model and the spacing between individual geometries.

1. A First Baseline

2. Defining the Resolution

3. Profile and Shaft Shape Variations

4. A first conformal shape
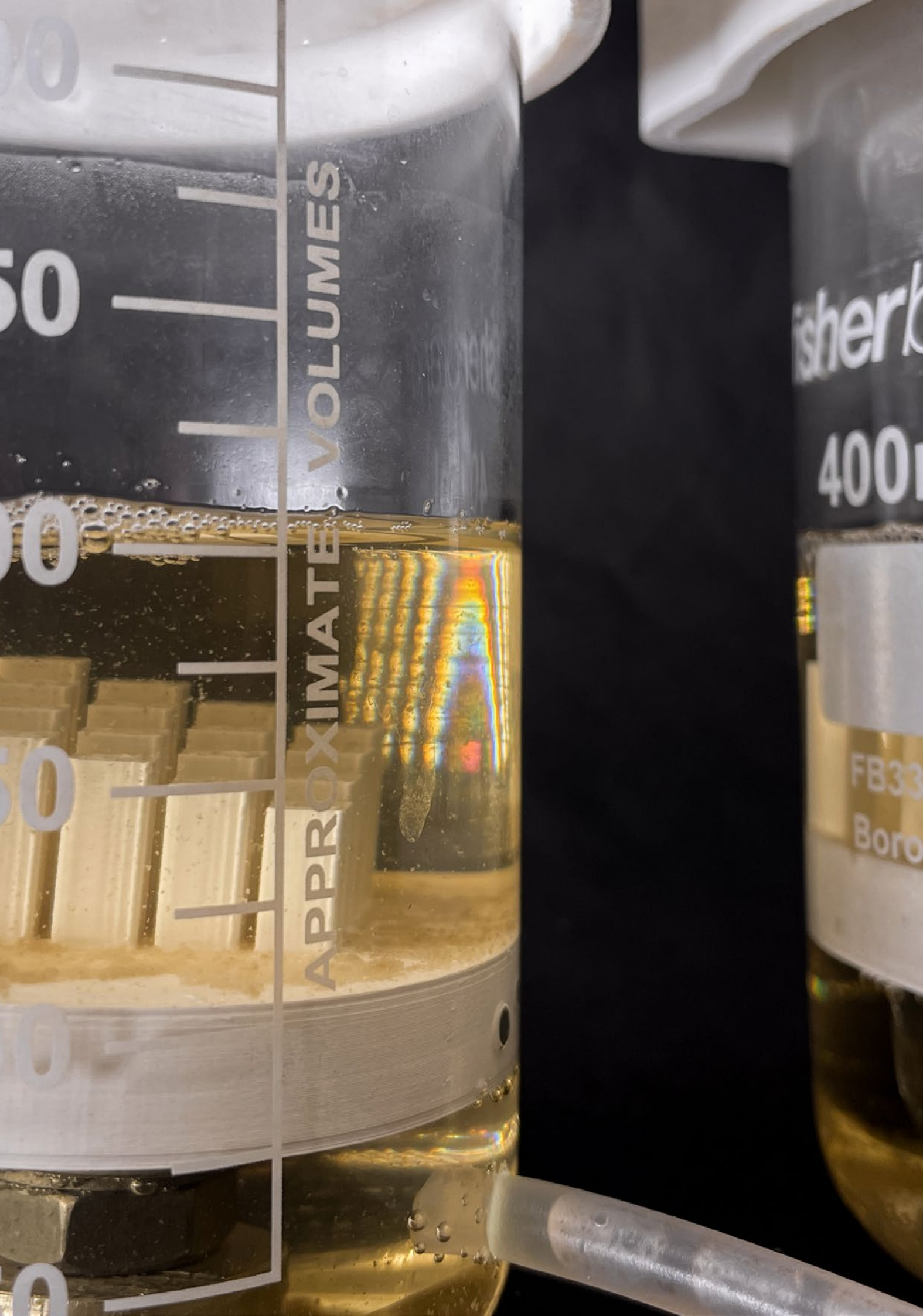
Test 1: A First Baseline

The first test partially using the test setup is done to see how the B.C. formation responds to the increase and decrease of medium volume within the vessel. Here, the lid and the camera is not used, since no geometry and medium level control is needed.

For this test the following research questions apply:

3. How does the alteration of the medium volume inside the vessel of the designed testing setup alter the growth of B.C.?
3.1 How does the current testing setup affect the geometrical outcome of the B.C. sample after these medium volume changes?
3.2 How does the rate of volume added and subtracted from the vessel affect the B.C. formation?

Hypothesis

Altering of the medium volume inside the vessel could result in different B.C. yield. This is not because of the increase of decrease of medium volume inside the vessel, since the vessel and the volume altering syringe are in direct contact. It is expected that the movement of liquid inside the vessel allows for more oxygen transportation in the medium, increasing the growth rate.

Also, loose cellulose formation in the medium could cause clogging in the syringe and tube, stopping the flow of liquid.

Finally, by adding medium volume to the vessel too fast could result in medium sipling alongside the edge of the forming cellulose layer, resulting in the separating of layers like in Test 3 of Principle 1 (see Figure 46).

Method

In Figure 88 the test setup is shown. A Go-Pro is used to monitor the growth of the cellulose layer. Before inoculation the vessel is filled with 260mL of CSL medium of which 60mL is initially pumped in the attached syringe. Medium is then added to the vessel from the syringe for one week every 24 hours in 10 second bursts of 8.6mL using the Arduino operated pump. After one week of growth the same amount of liquid is removed from the vessel at the same rate for another week.
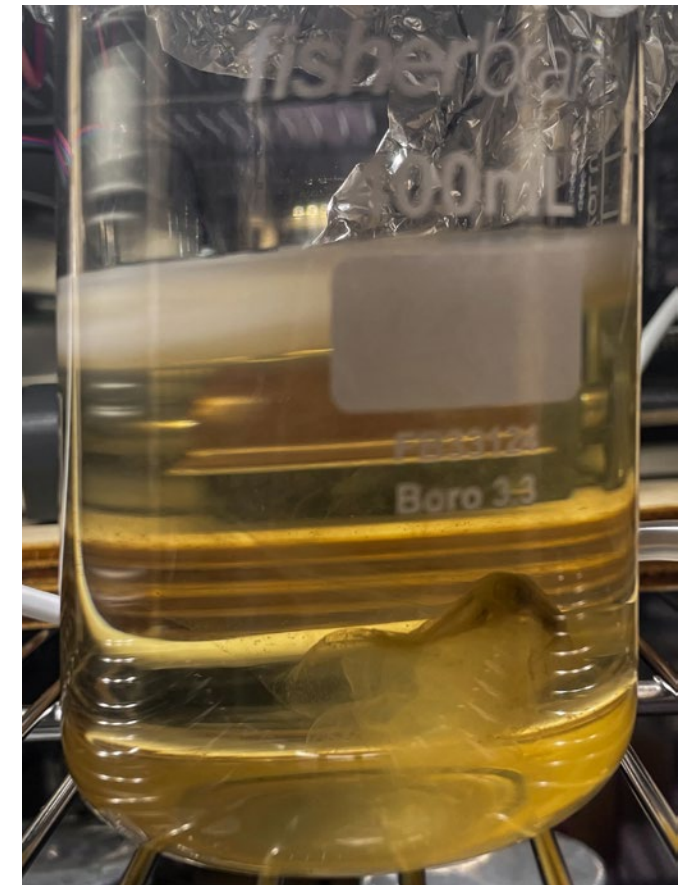
Figure 90 - Slanted cellulose growth after 14 days
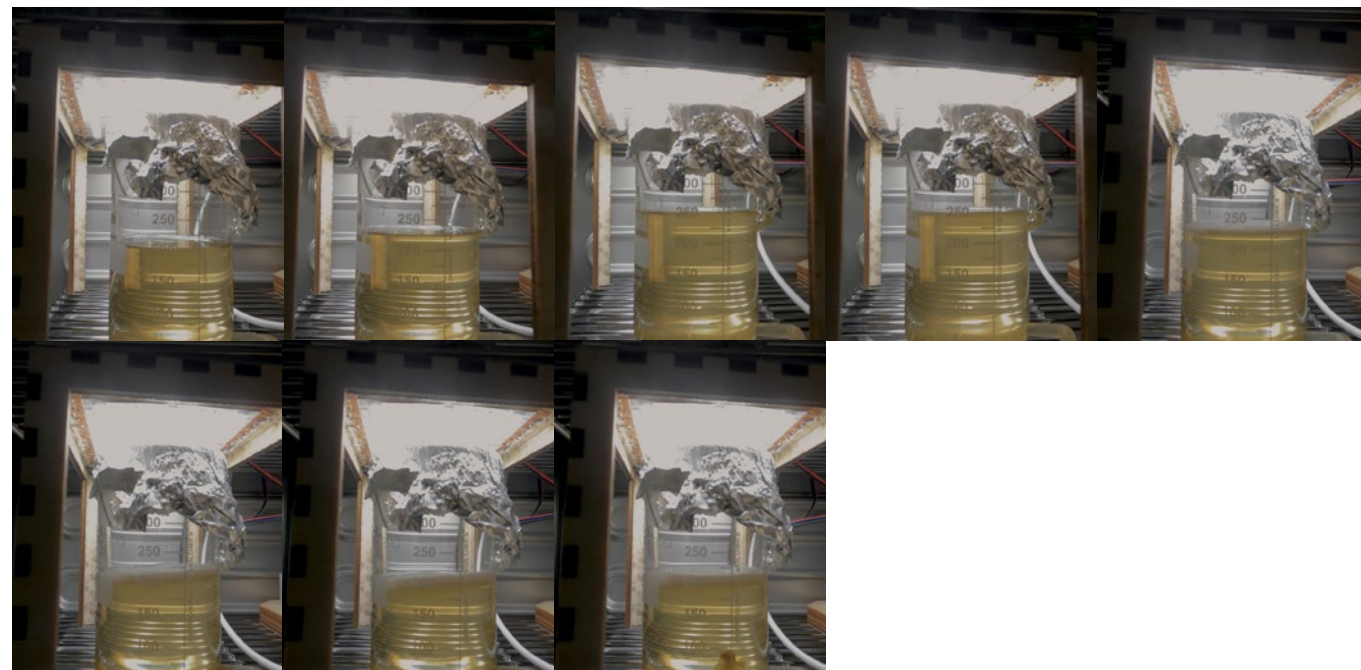
Figure 89 - Frames of the timelapse of 14 days of growth, where a) is day 1 and the next frames all have 2 days inbetween

Figure 88 - The testing setup for Test 1

Findings

Older K.H. stock was used for this test (dating from about two months), resulting in a relatively slow start of B.C.. Growth of the B.C. layer started at the 6th day, resulting in a relatively thin cellulose sample for 14 days of growth (see Figure 89). Gel-like cellulose growth on the underside of the layer on the air-liquid interface was sucked into the inlet after about 9 days of growth. This resulted in the partially submerging of the cellulose layer, due to the fibres being stuck to the sample.

This slanted growth (see Figure 90) resulted in a difference in geometry of the final sample compared to the control sample. The thickest part of the sample is about 7.4mm and the thinnest part is 4.9mm. The control sample had a thickness about 5.2mm at 14 days. The sample weighs 14.31g

During the 14 days of B.C. growth, because of the slow start, no testing of the growth could be done when the air-liquid interface moves up during cellulose formation. Therefore, medium volume addition is reversed after the 14th day so the volume in the vessel increases again at the same rate for 6 days. This resulted in long strains of cellulose to be pumped into the vessel. These B.C. strains are formed against the wall of the tubes and slowly as hypothesized, causes clogging (see Figure 91). Increasing the volume in 10 second bursts of 8.6mL did not result in alterations in the formation of B.C. on the air-liquid interface. Simple addition of medium volume without any geometry should not influence the growth geometry of the B.C. layer, but no proof of an increase or decrease of production has been found.

Figure 91 - Frames of the timelapse of 6 additional days of growth, where a) is day 15 and the next frames all have 1 day inbetween

5. Defining the Resolution

To find out at what resolution the B.C. can be shaped, a test is conducted varying the x and y variable listed in Figure X. In this first test the medium volume is not regulated, meaning the liquid level inside the vessel will drop during the test due to evaporation and the usage of substances in the medium by the K.H. bacteria. A second test is performed using the same geometry, but with an increasing medium volume.

For these tests the following research question applies:
4.   How does geometry moving through the air-liquid interface affect the geometrical outcome of the B.C. sample?
4.1.   In what way does the geometry in the x-y plane of the obstruction affect the B.C. growth?
4.2.   What are the minimal dimensions in the x-y plane of the B.C. shaping geometry?

Method
A geometry holder is 3D printed in which aluminium rods are attached (see Figure 93). These rods have different diameters and lengths, as seen in Figure 92. This holder is then screwed in the lid, so all rods are about 10mm submerged in the CSL medium. The vessel contains 200mL of medium.

4.0mm
l: 15.2mm

5.0mm
l: 16.2mm

2.0mm
l: 14.7mm

6.0mm
l: 18.2mm

1.0mm
l: 14.2mm

0.6mm
l: 13.5mm

0.3mm
l: 13.3mm
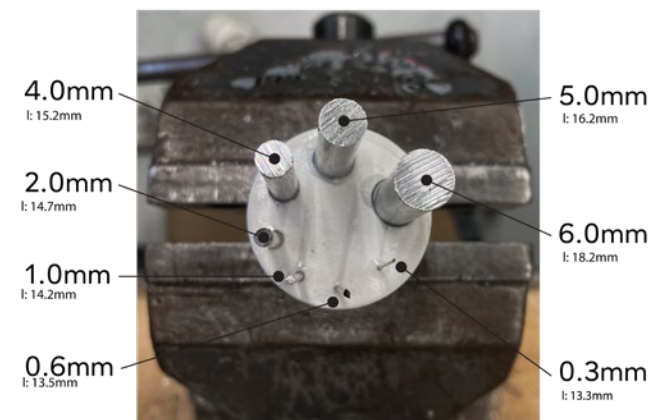
Figure 92 - Annotated overview of the tested geometry

The B.C. layer is then grown for one week, after which the obtained cellulose layer is measured and compared to the hypothesised shape. In the second test the same geometry is used. However, a syringe containing 60mL of medium is added to the setup. To the 200mL of medium in the vessel, the contents of the syringe are pumped at a rate of 0.36mL/h. This rate was chosen based on findings from the previous test. Due to a Christmas break the growth of this test could not be monitored.

Figure93 - The used geometry for Test 2

Figure 94 - The used geometry for Test 2

It can be concluded from the first test that geometries of 0.3mm in diameter can be translated in the cellulose layer. However, due to internal compression when laying the sample flat this is result is not very visible at first sight (see Figure 97). Also, a lot of 'spottiness' is visible in the sample. These clumps of cellulose are only visible in the top of the sample. The cause of this phenomenon might be due to the large amount of water drops on the inner surface of the vessel, which is caused by evaporation. These drops slowly fall onto the air-liquid interface, causing the bumps. No footage is made to support this claim and the same phenomenon has only been noticed in smaller amount seemingly randomly located, like in Figure X from Test 2 of Principle 1. The bumps around the formed holes are both a cause by capilar action of the air-liquid interface, which can be noticed in Figure 95, and cellulose sticking to the aluminium rods while the air-liquid interface lowers slightly due to evaporation (see Figure 96).

The overall thickness of the obtained B.C. sample is about 6.5mm and its wet weight is 12.63 grams. Dry-weight is yet to be measured after freeze-drying.

Figure 74 - The resulting shape for Test 2 (Front)

Figure 97 - The resulting shape for Test 2 (front and back)

Figure 95 - The setup has reached State 2 at 48 hours, where loose clumps of cellulose are forming and capilary action is highly noticable.

Figure 96 - B.C. growth at day 5. A high amount of moisture drops are visible on the inside of the vessel and the bumps in the sample are starting to be noticable.

In the second test (see Figure 98), using the same geometry but by moving the air-liquid interface through the geometry, the indentation are more subtle (see Figure 99). Where in the previous sample there were holes, in this sample cellulose formed caps in these holes. The setup reached State 4, so full coverage of cellulose on the air-liquid interface, before the geometry touched the surface of it. This caused the cellulose to slowly be pushed under the air-liquid interface. This pushing speed of the cellulose layer is thought to be close to the rate of formation of cellulose, since new cellulose formed above the 'first layer' of cellulose sticking to this layer. Since no timelapse was made of this behaviour and due to the Christmas break no in between pictures were made, this behaviour is visualized in Figure 100.

The obtained sample shows a less dense structure of cellulose, being about 5.43mm thick on average (after measuring thickness at 10 points) and weighing 11.2g in a wet state. This results in a density of about $0.61g/cm^3$ which is below its average of $1.25g/cm^3$. This difference in structure was thought to originate from a difference in the CSL medium, but from the same bottle a more dense sample was also produced in Test 3. It is hypothesised that by decreasing the volume addition rate to better match the formation rate of the cellulose, a higher density sample will form. This would also imply that volume addition of medium, with the added geometry to move the forming cellulose under te air-liquid interface, can regulate the density of the obtained sample. Further testing is needed to support this theory.

The thickness of the cellulose formed in the holes is measured to be around 2.5mm. Not visible in the images is that the smallest radius of the geometry, being 0.3mm, also resulted in a small indentation. The length of this rod (13.3mm) was the shortest, resulting in the shallowest indentation.

Figure 98 - Cellulose formation after 7 days of growth inside the vessel.
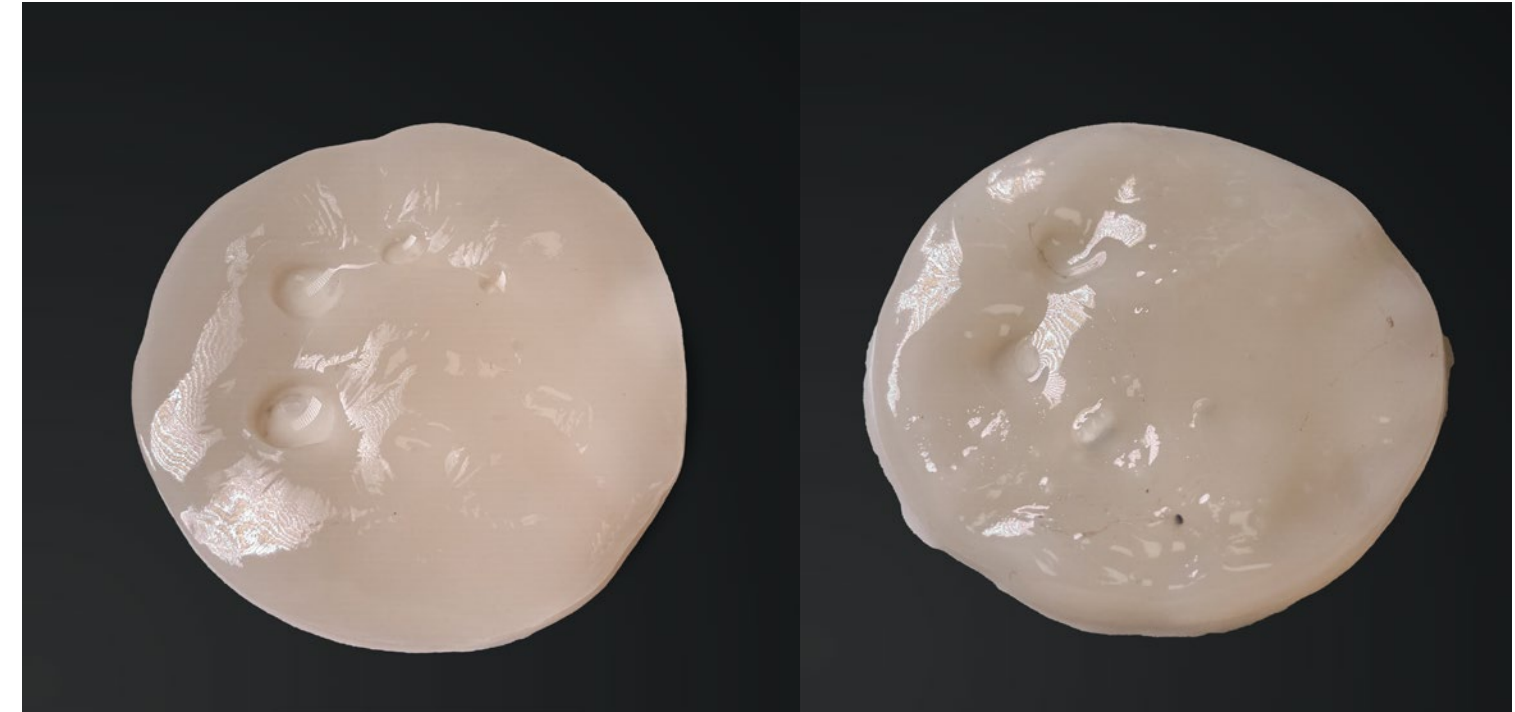
Figure 99 - Cellulose sample from Test B (front and back)
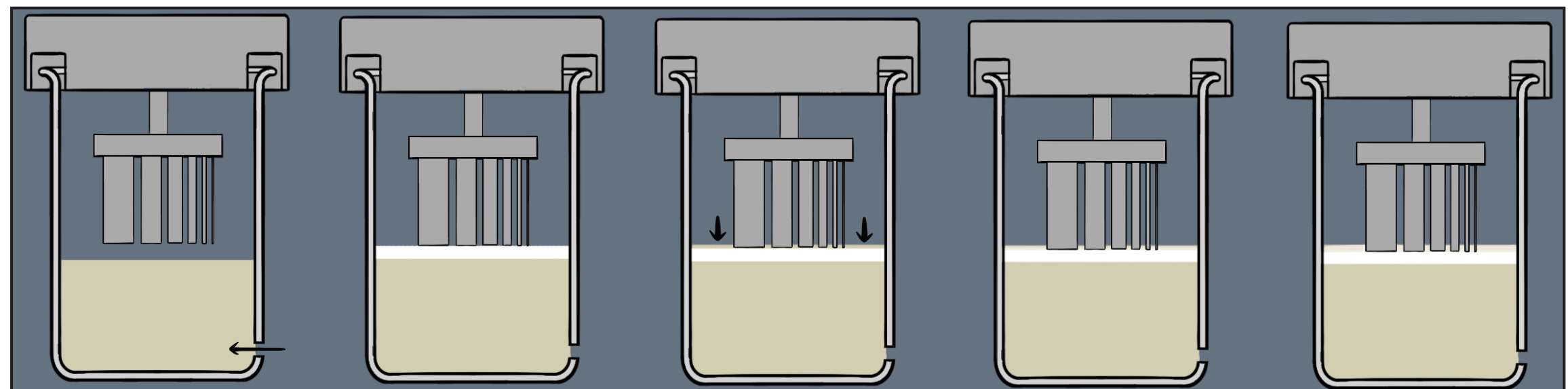
Figure 100 - Graphic visualization of the pushing of the cellulose layer under the air-liquid interface, allowing for semi-attached new layers of cellulose to be formed

6. Profile and Shaft Shape Variations

In order to test a set of geometry variations from Figure 75, two tests were performed. For these tests the geometry variations are visualised in Figure 101. Both tests use the same geometry variations, but in test A medium volume is increased and in test B medium volume is decreased.

For this test the following researchs question apply:

4.   How does geometry moving through the air-liquid interface affect the geometrical outcome of the B.C. sample?

4.1.   In what way does the geometry in the x-y plane of the obstruction affect the B.C. growth?

4.3.   How does the geometry in the z-direction of the obstruction alter the B.C. formation when moving downwards through the air-liquid interface?

4.6.   What effect do the capillary forces on the air-liquid interface caused by obstructing geometry have on the formed cellulose layer?

Figure 101 - Visualization of the four shape variations

Figure 102 - Milling of the geometry for Test 3

n	x	y	z	α	l	r1
∞	5	5	20	0	(-)	(-)
∞	5	5	20	5	(-)	(-)
∞	5	5	20	-5	(-)	(-)
4	5	5	20	0	(-)	(-)

r2	z2	l2	N	x2	xn
(-)	0	(-)	1	5	(-)
(-)	0	(-)	1	5	(-)
(-)	0	(-)	1	5	(-)
(-)	0	(-)	1	5	(-)

Table 1 - Variables for the geometry of Test 3

Figure 103 - The four geometries for Test 3

Hypothesis Test A

In Figure 104 the resultant shapes of a first version of the model is shown. In this model the formula, being:

$$h_{B.C.}(t) = 0.0029*t-0.14;$$

is resultant from desktop research and experience, as described in Chapter 3.3. It is expected that the conical shape could result in the partial pushing of the B.C. layer under the air-liquid interface, due to downward pressure from its geometry. This might result in the less dense formation of B.C. in the middle of the sample, like seen in Test 2B.

Hypothesis Test B

The shapes visualized in Figure 104 resulting from the model are also the expected resultis for this test. However, it is also expected that using an inverse conical shape will add pressure to the forming B.C. layer when medium volume is added. This would result in the partial lifting of the B.C. layer above the air-liquid interface, resulting in a bump or even some lifting of the entire forming sheet. If the second option of an outcome would take place, the density of the cellulose layer should resemble that of the result of test 1B. The straight shapes are expected to also show this behaviour, due to frictional forces with the forming cellulose layer. This should not be the case for the conical shape.
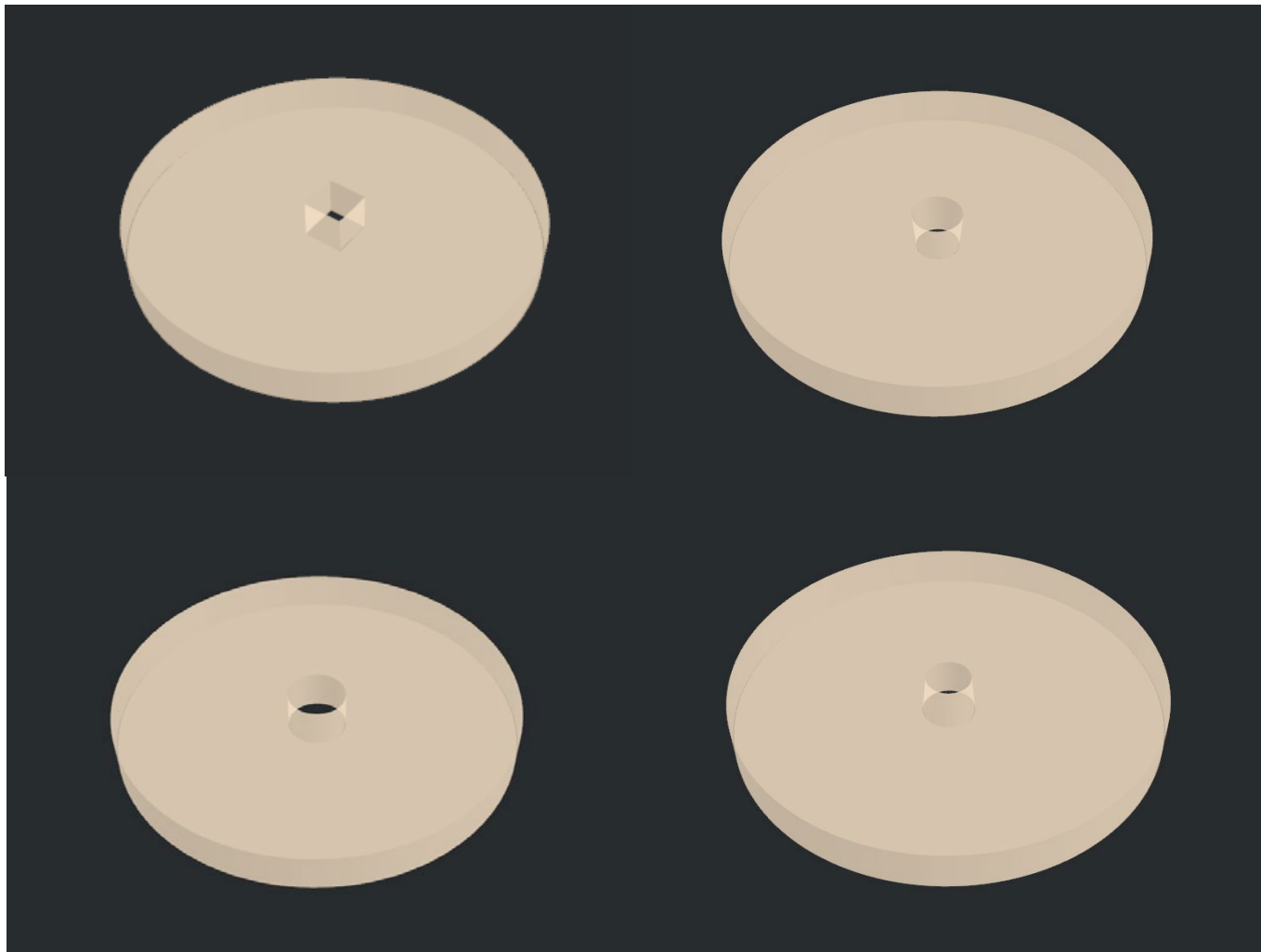
Figure 104- The predicted shapes generated by the model

Method

In test A 60mL of CSL medium was added to the 250mL of medium in the vessel within 7 days (averaging to 0.36mL per hour). In test B 60mL was removed from the 220mL of medium in the vessel at the same rate. A difference in starting volume is used and the square geometry is left out in test B due to a shortage in medium.

In Table 1 the data for the shape variables is shown. These geometries are then fabricated in aluminium using turning and milling (see Figure 79 and 80). Using this fabrication method allowed for more precise dimensioning than 3D printing, resulting in more equally sized geometries. Also, 3D printing thread in parts offered some difficulties and the warping of the parts and rough layer lines resulted in too much difference with the original model.

Four vessels are filled with CSL medium. Each inlet is connected to a singular syringe filled with 60mL of CSL medium. Divided by four vessels, this would mean that the medium in each vessel would increase with 15mL. The four geometry variations are then inserted into the lids and placed in the four interconnected vessels (see Figure 105 and 106). By screwing it into the lids, the height of each geometry is set equally so that 5mm of the geometry is submerged, leaving 15mm above the air-liquid interface. This initial ratio of geometry above and below the air-liquid interface was also used in the second test.

Figure 105 - Side view of the four geometries penetrating the air-liquid interface 5mm deep

Figure 106 - The test setup for Test 3
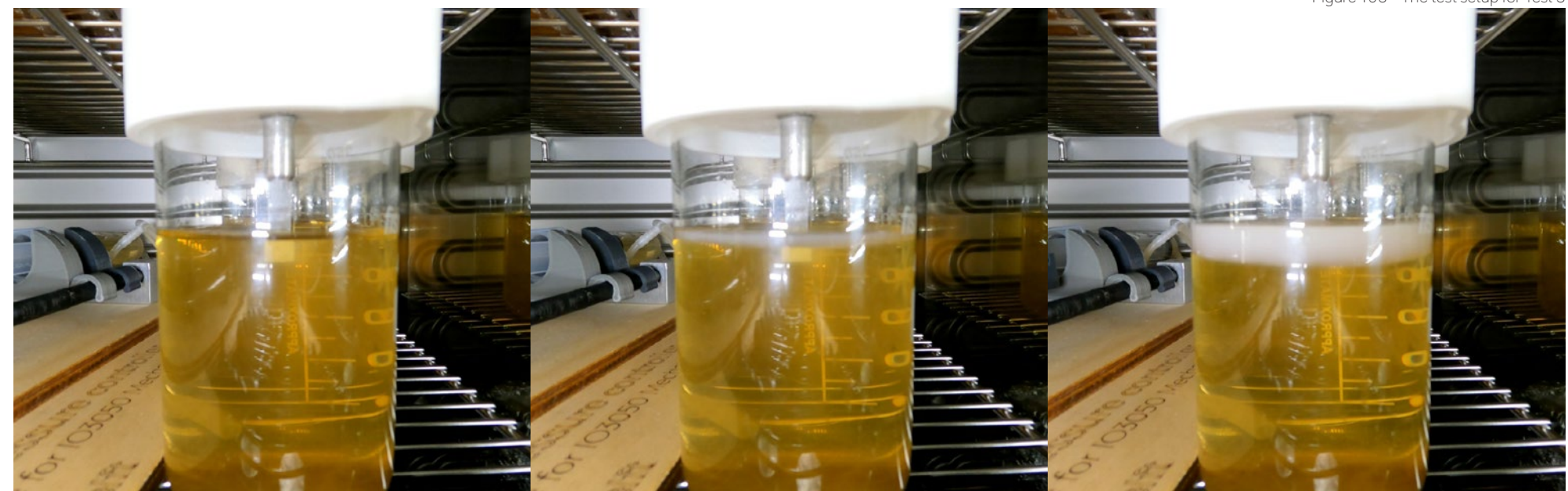
Figure107 - Timelapse frames from test A showing day 0 (a), day 2 (b) and day 7 (c)

Findings

In Figure 108 the results of test A and B are shown and in Figure 107 some stills of the timelapses can be found. The lighter coloured samples, which is the result of cleaning, are from test A and the darker coloured samples are from test B. Both tests showed cellulose formation at about 110 hours and all samples have the same thickness.

There is some similarity in the hypothesized B.C. geometry and the final samples. For test B it was not hypothesized that there would form a thin layer of cellulose on top of the hole. Almost all samples do not show this, except for the conical geometry. Here, the layer of cellulose deattached from the geometry more easily due to less frictional force, resulting in some medium inside the hole which caused the bacteria to form the thin layer.

In the samples from test B, all samples show a bump at the location of the hole on the front side. This bump is the result of the cellulose sticking to the geometry, which lifted it up and resulted in a difference in geometry with the hypothisized samples. This bump is less noticable in the picture of the straight circular geometry, however this is not the case.

Thickness of all samples of Test A are 4.7mm on average and weigh 19.4g on average in a wet state. This would result in a density of 1.21g/cm³, which is close to the average.

Thickness of all samples of Test B are 3.5mm on average and weigh 15.1g on average in a wet state, which is about 22% less yield than from Test A. This would result in a similar density of 1.27g/cm³.

The lower amount of cellulose produced in Test B is as expected, since the amount medium volume was 12% lower. A 22% decrease was not expected, but can be used to find a more accurate formula for the B.C. formation.

The results from this test are used to change the cellulose growth curve in the Grasshopper model to the formula described in Chapter 3.3. Also, the tests show that to release the cellulose from the geometry, when lowering the medium volume, a more slanted shape of the shaft is needed, being in this case at least 5 degrees.
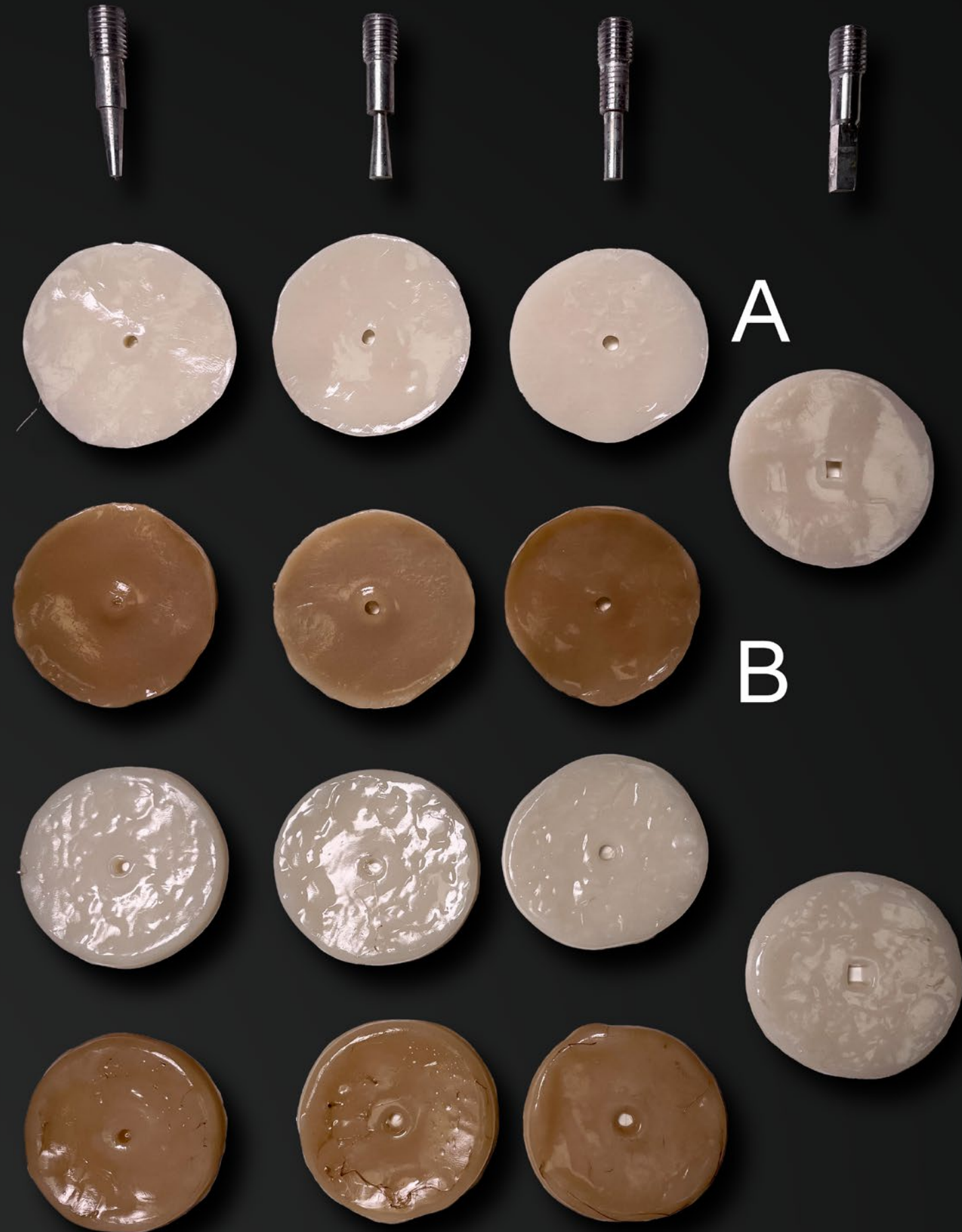
Figure 108 - Resulting samples of Test 3

Validating the Model

To combine the research done from the previous tests, a 3D model is made of a more complex geometry. Different from the previous tests, the Grasshopper model is used as a template of which the final outcome of the cellulose sample should resemble, making the shaping of this cellulose sample conformal.

Figure 109 - Predicted outcome of Test 4

For this test the following research questions apply:

2.1. How does the data inserted in the model translate to the real-life shape of the grown cellulose?

4. How does geometry moving through the air-liquid interface affect the geometrical outcome of the B.C. sample?

4.1. In what way does the geometry in the x-y plane of the obstruction affect the B.C. growth?

4.3. How does the geometry in the z-direction of the obstruction alter the B.C. formation when moving downwards through the air-liquid interface?

4.4. What is the minimal indentation the obstructing geometry can produce in the z-direction?

4.5. How does distance between geometries affect the B.C. growth?

4.6. What effect do the capillary forces on the air-liquid interface caused by obstructing geometry have on the formed cellulose layer?

5. How does obstructing geometry affect the density of the grown cellulose sample when moving through the air-liquid interface?

5.1. How does volume rate affect the density?

Figure 110 - The input geometry into the model

n	x	y	z	α	l	r1	r2	z2	l2	N	x2	xn
4	5	5	10-20	0	(-)	(-)	(-)	0	(-)	20	5	(-)

Table 2 - The input variables for Test 4
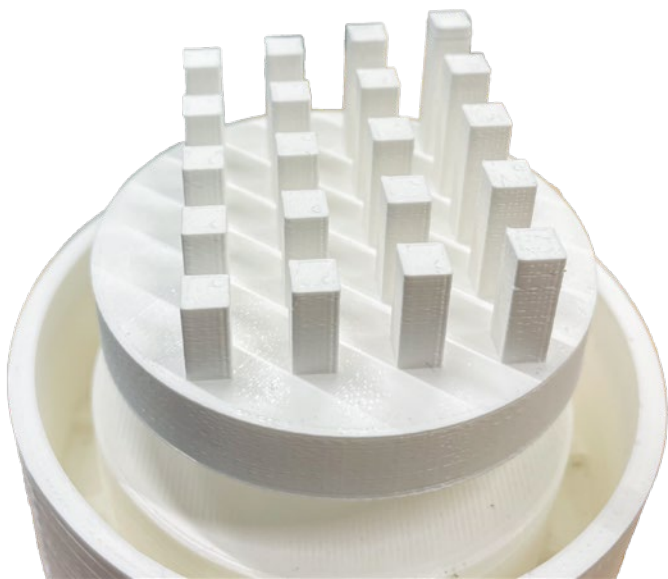
Figure 111 - The 3D printed geometry for Test 4
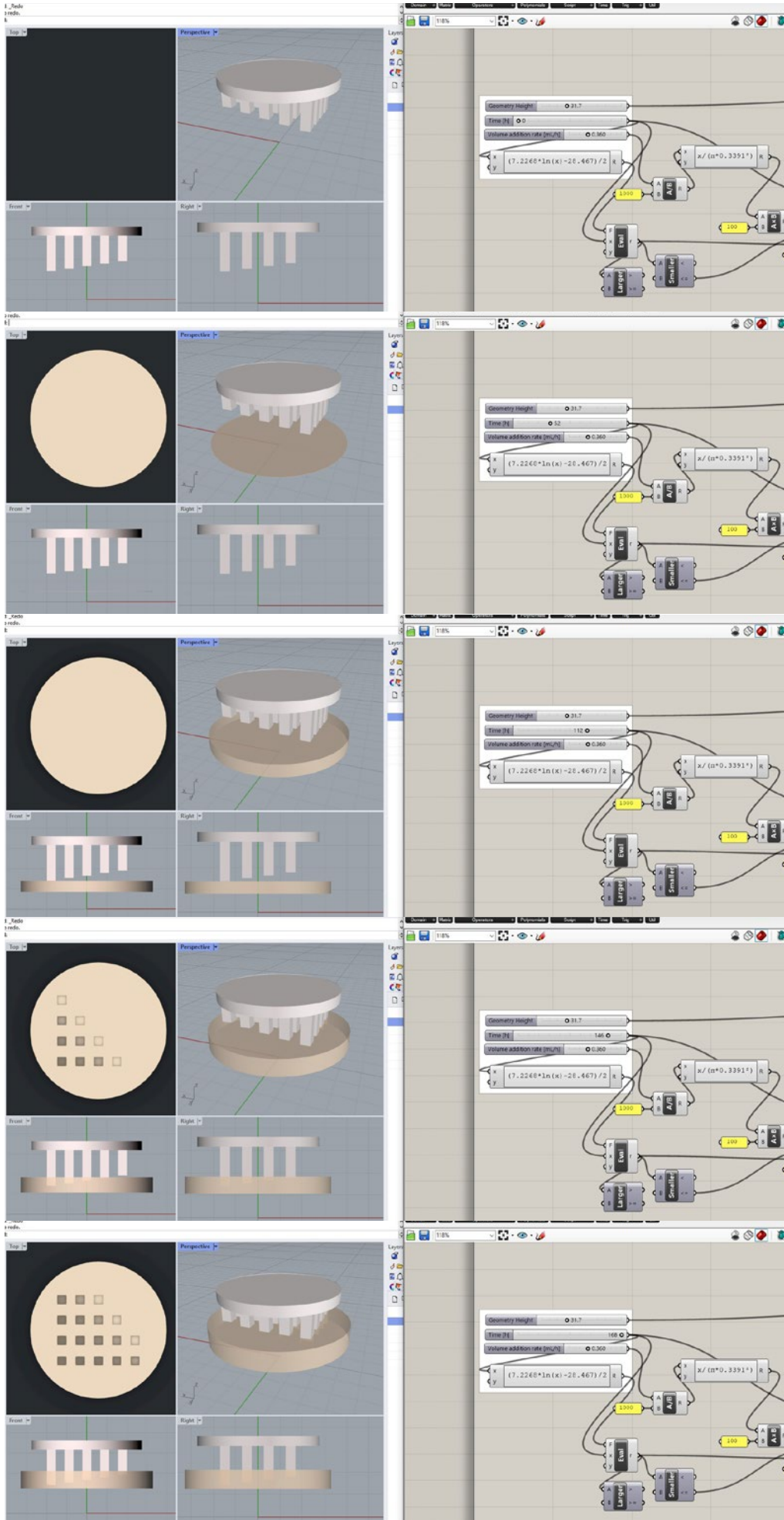
Figure 112 - The dashboard for the model showing different time inputs
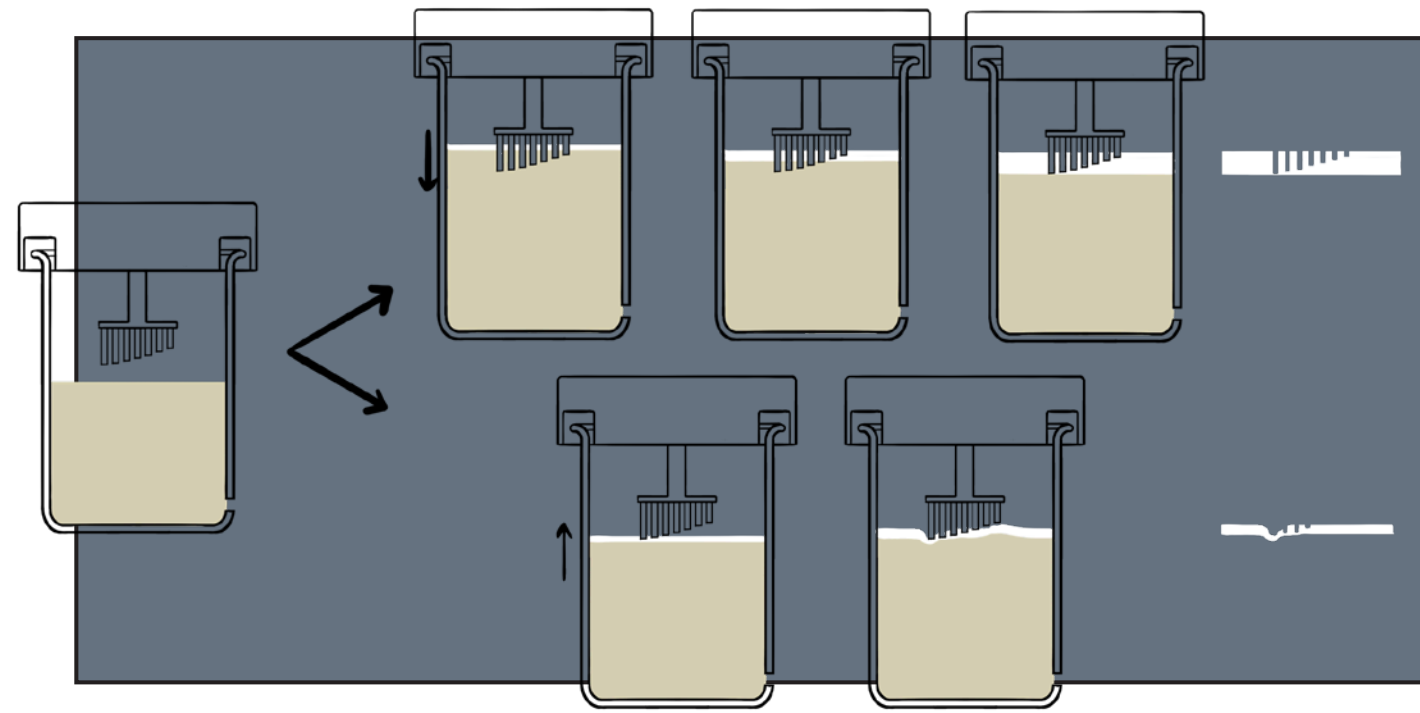
Figure113 - Graphic visualization of the bending of the cellulose
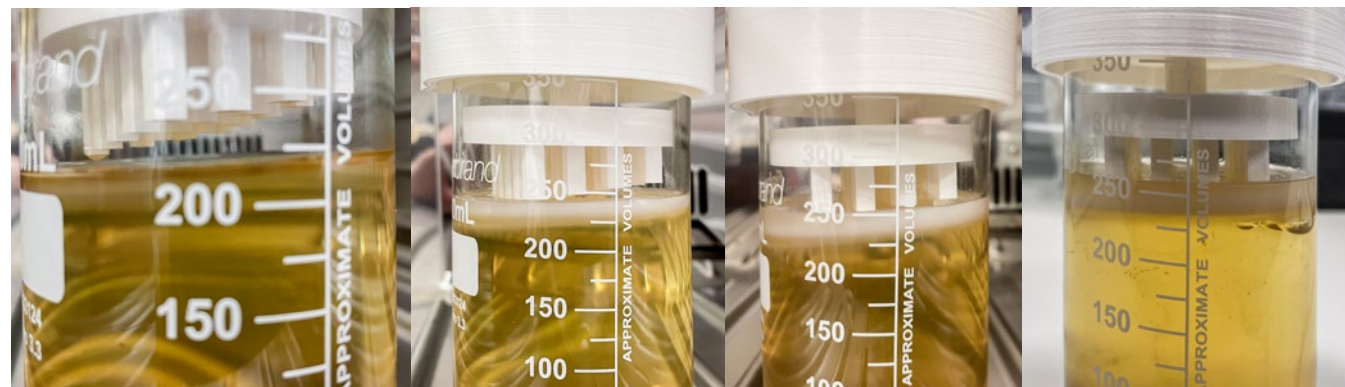
Figure 114 - B.C. growth after 2 days (a),5 days (b), 6 days (c) and at the 7th day (d) where the formed cellulose layers are pushed under the air-liquid interface
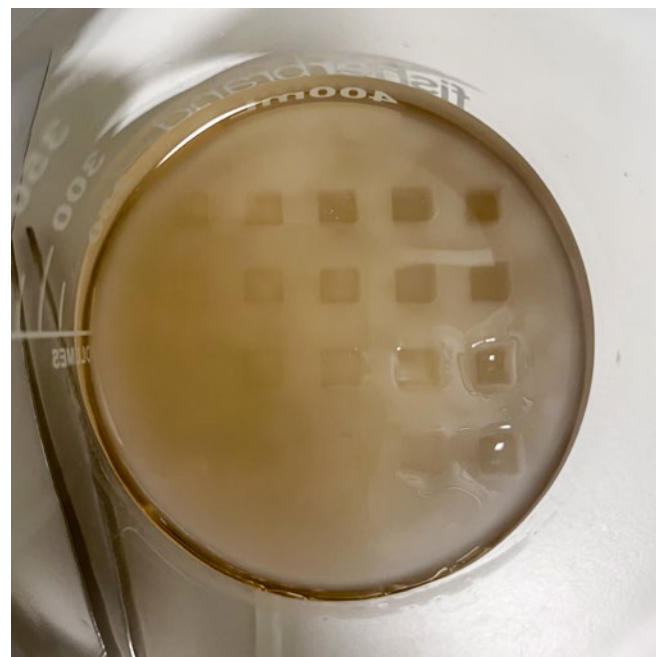
Figure 115 - Top view of the formed B.C. in the vessel

Figure 116 - The resulting B.C. sample of Test 4

Method

A square profile shape is chosen, which is repeated in a rectangular evenly spaced pattern (see Figure 110 and 111). The length of every shaft is varied, ranging from 10mm to 20mm. This is then made into a 3D print and inserted into the lid. The initial height of the 3D print and the air-liquid is set to the height used in the model, being 5mm from the lowest point of the model.

The liquid pump for this test is replaced by a more reliable and accurate Prosense syringe pump (the PSNE1000). For the flow-rate the pump is set to 0.36mL per hour, being the same as Test 2B to test its findings. This would mean the air-liquid interface would rise up to about 17.63mm in 7 days.

Hypothesis

Inserting this in the model using the growth curve resulting from Test 3 (see Figure 112), the shortest three pins of the model should not touch the cellulose layer if no bending of the B.C. layer would occur (see Figure 109). However, it is expected that bending will occur, since the pins should exceed a downward force on the forming B.C. layer. A visualization of this is made in Figure 113. How much bending occurs and how this will translate into the outcoming B.C. shape is to be tested. The sample is expected to have a thickness of about 8.6mm.

Findings

In Figure 114 it can be noticed that the bending did in fact occur. In Figure 115 and 116 the final shape of the B.C. sample of this test is shown. Here, it can be seen that there is a lot of similarity between the hypothesised shape and the final outcome. However, the bending of the sample and the pushing under the air-liquid interface did cause some alterations. Where there should not have been any touching of the geometry there is a very slight indentation in the cellulose. This can not be seen or photographed, but you can feel a small difference in thickness in the sample. Also, some of the squares in the sample are a bit stretched.

The indentations of the squares lack the sharp edges the 3D print has when the sample was removed from the vessel. This sharpness of the edges was visible in Figure 115, but due to the relatively less dense structure of the cellulose, when laid flat the indentations are stretched out. Also, capilarity of the medium partly explains the more soft appearance of the indentations. The sample, being about 4.5mm at it thickest and 2.5mm at the thinnest part (3.95 on average), weighs about 13.4g in its wet state. This translates to a density of about $0.997g/cm^3$, being below average but more dense than Test 2B. This same decrease in density can be explained by the same mechanism that was seemingly appearant in Test 2B, being the partial pushing of the cellulose under the air-liquid interface.

All in all, the shape did behave as it was intended and the curvature during the growth of the sample can be added to the model. A second test is set up where the same geometry is used, but introduced from the bottom.

5. Introducing Obstructions from below

In this test, instead of above the air-liquid interface, like in the previous tests, geometry is placed below it. Also, in this test, the same geometry is used as the previous test, as well as a variation on this geometry where the distance between the rods is made smaller.

For this test the following research questions apply:
- How does geometry below the air-liquid interface change the growth behaviour of the B.C. layer?
- How does the distance between spacing of multiple geometries translate to the grown B.C. sample?

Method

For this test, two geometries are modelled and 3D printed, using an FDM 3D printer with PLA as printing material (see Figure 117). Geometry A has square rods of 5x5mm with even spacing of 5mm at both sides. Geometry B has the same size, length and amount of rods, but the spacing is changed to 2mm. These two 3D prints are attached to two weights, which consist of an stainless steel screw with some washers. This is done to counteract the floating of the 3D prints, due to air pockets in the prints, while also increasing the height. Height of the geometries is increased by 25mm.

The two prints are then placed in the testing setup, where two of the vessels are filled with 200mL of CSL medium each (see Figure 118). This initial medium volume resulted in the two geometries being fully emerged, with 8mm distance between the highest point of the geometry and the air-liquid interface. After 48 hours of growth, the medium is removed from the vessel at the same rate as the previous tests, being 0.36mL per hour. This would mean that the medium level would decrease with a distance of approximately 17.63mm in 7 days. In 48 hours, the geometry would penetrate the air-liquid interface, which is expected to be in State 4 (so the air-liquid interface should be fully covered with B.C.).

Figure 117 - The used obstructing geometries
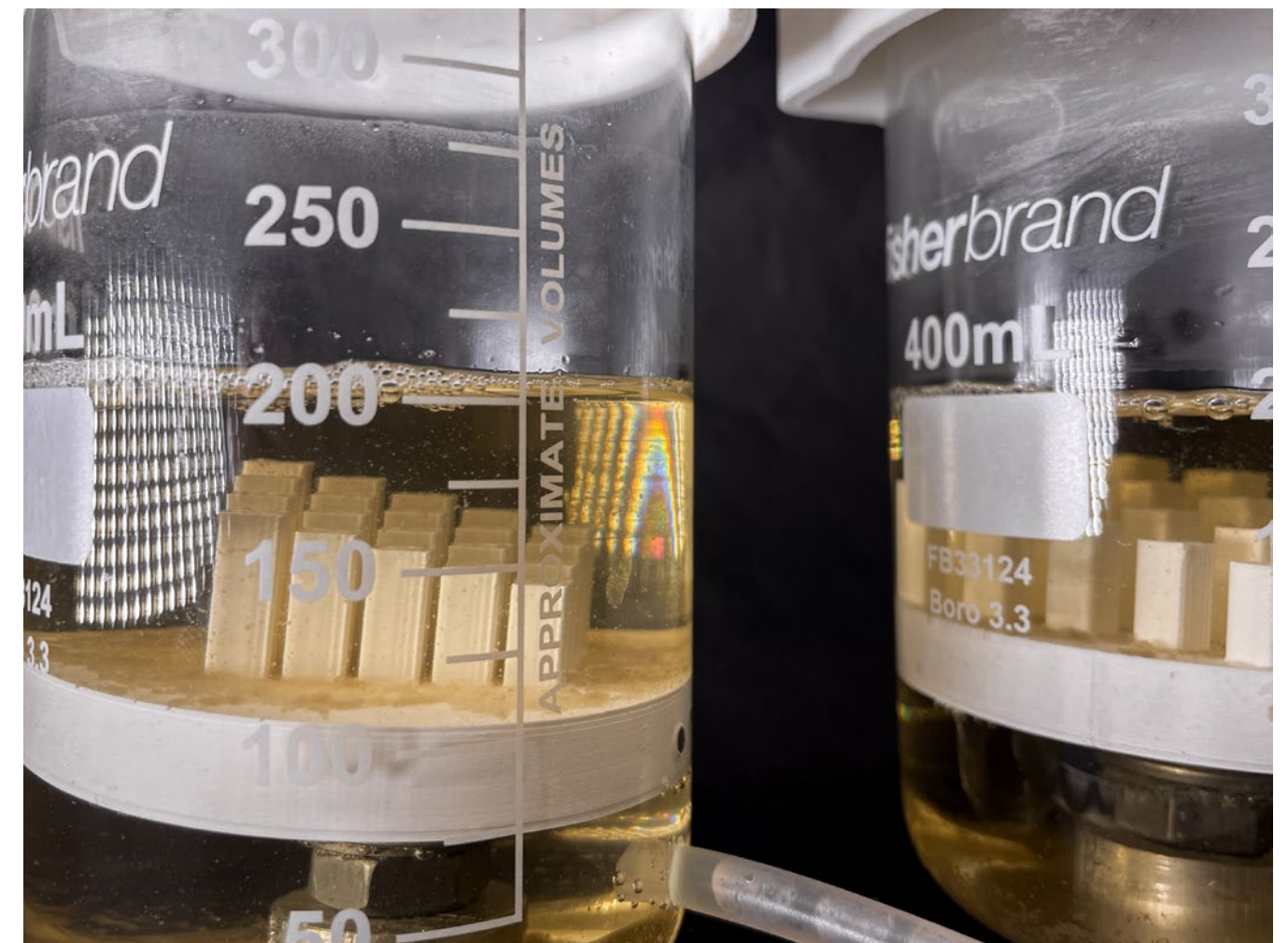
Figure 118 - The two models submerged in both 200mL of medium

Hypothesis

In Figure 119 some stills of the computational model is shown where both 3D models are introduced through the expanding cellulose layer. Here, overall the results show a similar resulting pattern as the test of the previous chapter. However, some differences are expected. In Figure X a visualization is shown of the geometries partially pushing the growing B.C. layer above the air-liquid interface. This would cause the formed cellulose layer to drape over the edges of the pillars, while new cellulose is expected to grow at the lowering air-liquid interface. This would cause a thinner sheet of cellulose at the highest point of the geometry and a thicker piece at the lowest point. This should be appearant for both geometry A and B. For geometry B it is expected that due to cappilary action no cellulose will form in between the rods. An overall thickness of 8.6mm is expected, based on the obtained formula for B.C. growth.
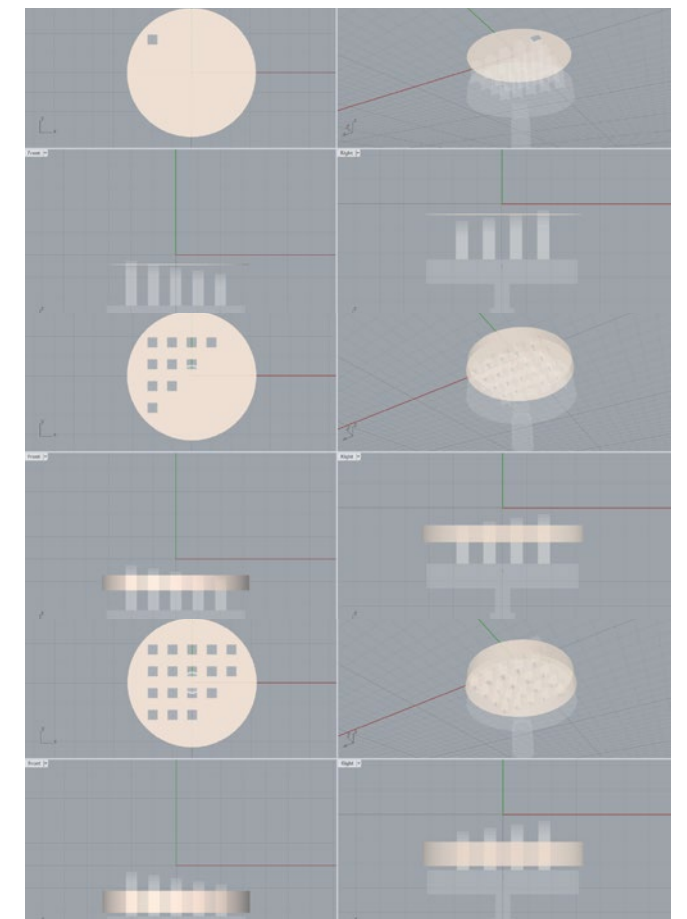
Figure 119 - Results from the model and settings inserted into the model
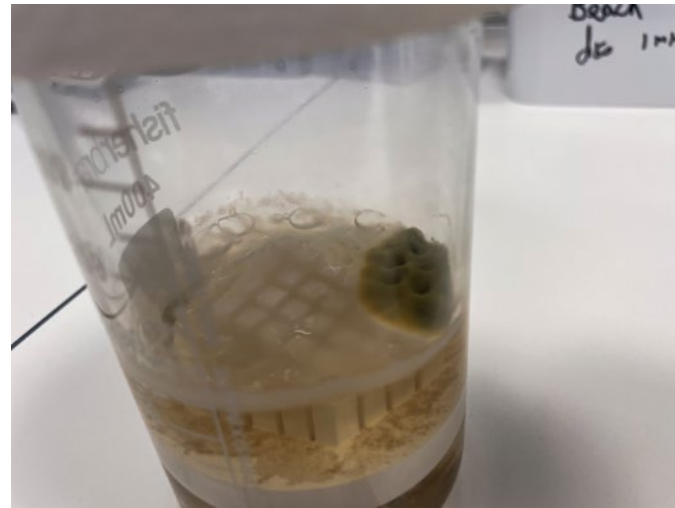
Figure 120 - Contamination of test B

Figure 121 - Growth in test A after 7 days

Findings

Due to a contamination in the vessel containing geometry B, the tests are deemed invalid and a new test should be set up (see Figure 120). However, some minor conclusions can be drawn from this test.

It can be concluded that contaminations in separate vessels are not transferred to the other vessel after 7 days (see Figure 121). This is in the case of this fungal contamination. The vessel for geometry A was separated after 7 days from the pump and vessel for geometry B. Growth was continued for 5 additional days. In Figure 121 growth after 7 days and in Figure 122 after 12 days can be seen. Cellulose growth was minimal and did not increase significantly after 7 days. The obtained sample has a thickness of approximately 1.8mm and weighs 3.5g. It is expected that most nutrients from the medium are used by the fungal species from vessel B. Also, by disconnecting the vessel from the system, the amount of nutrients available is lowered by more than 50%, resulting in the low amount of biosynthesis of cellulose.

In Figure 122 to 124 the obtained sample from vessel B can be seen. Here, the square profiles are translated in the growth, but no significant growth is found in between the square rods. Also, the hypothesized thickness variation from the highest to the lowest rod is not observed, but this is to be expected at this growth rate. In Figure X some thickness variation, apart from the indentations by the square rods can be observed. Air bubbles are formed underneath the cellulose layer at some locations around the geometry. At these locations, the formed cellulose layer is thinner, due to the new forming cellulose not sticking to this layer.

Figure 122 - Growth after 12 days
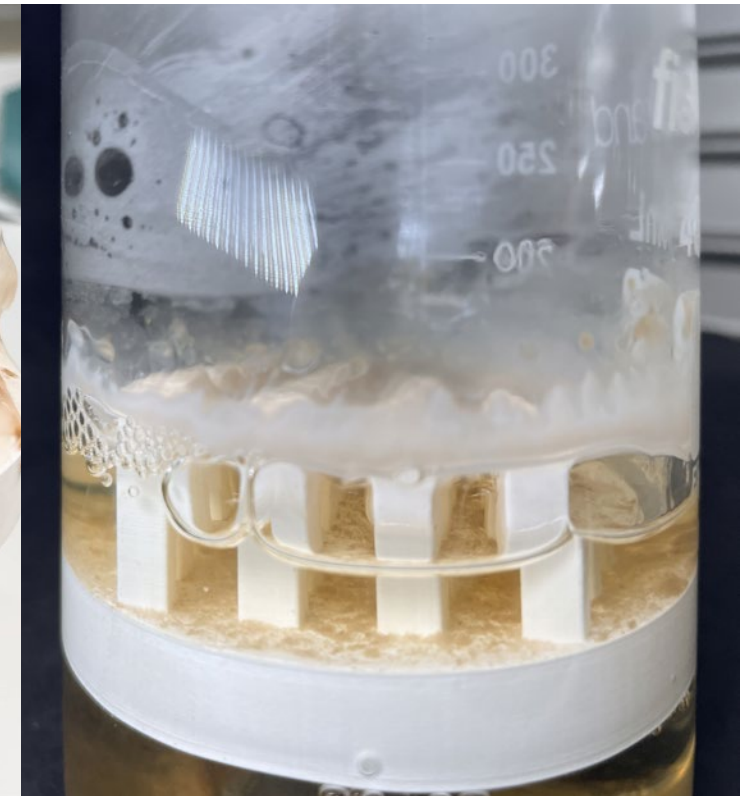
Figure 123 - Air bubbles formed underneath the cellulose layer
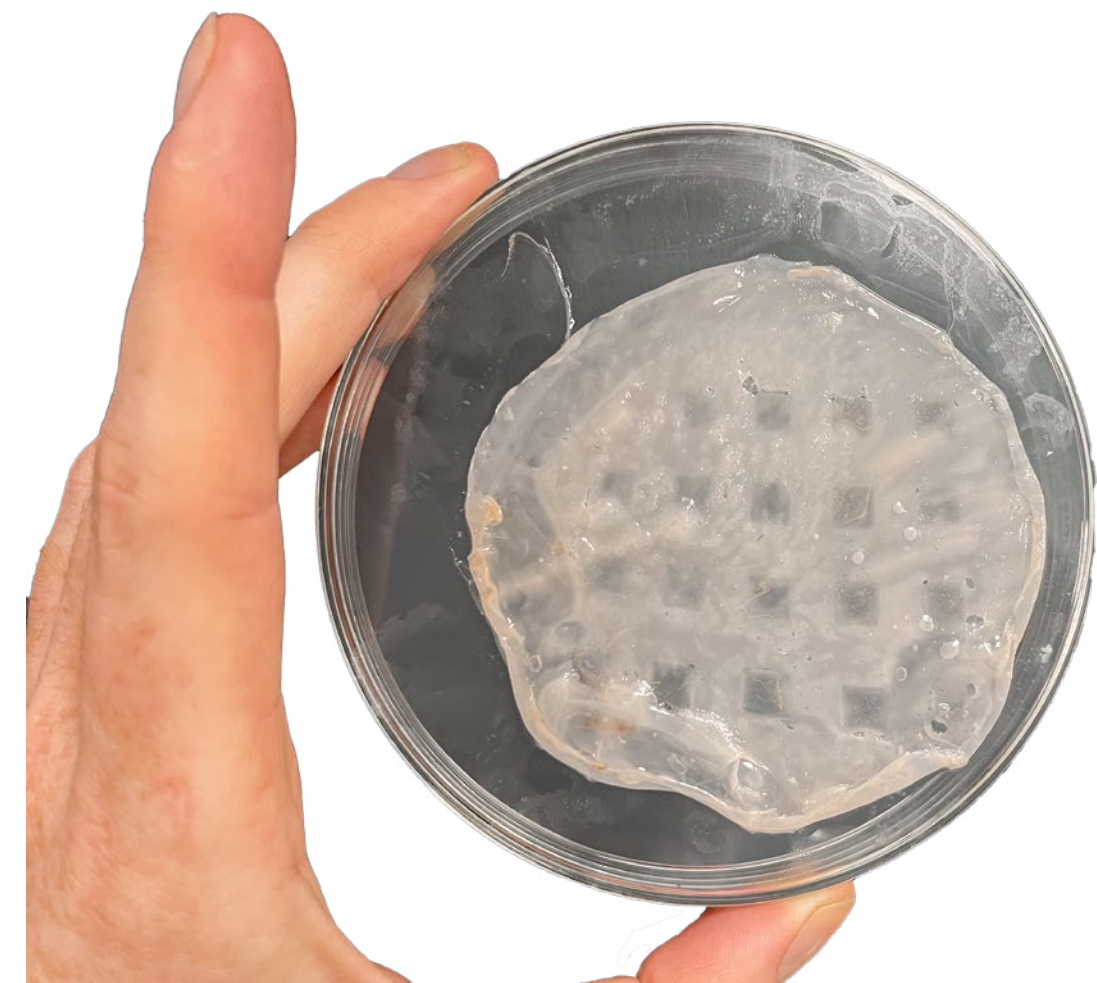
Figure 124 - The obtained sample from test A

Discussion & Conclusion

ON THE FINDINGS OF THE TESTS

In this final chapter, the findings of the tests performed with the testing setup are discussed. First, focus is placed upon the results regarding the B.C. samples and the testing setup. Then, some additional findings are discussed which are relevant, but do not have influence on the testing prototype. In the third part, the relevance of the findings are discussed. Next, a general conclusion is made and a recommendation on the continuation of the project is given. To close off the project, a personal reflection is made on the proces of the thesis

6

1. Discussion

In this paragraph, the results of the tests are discussed. First, the results regarding the produced B.C. samples are discussed. In the individual chapters of the performed tests, results are already discussed, however in this paragraph a more general and combined overview is given. In the second part the performance of the testing setup is discussed, on which in Chapter 6.4 recommendations are made.

Discussion on the B.C. samples

When looking at the sample of the first test, moving the air-liquid interface up and down can have an influence on the geometry of the grown cellulose layer. From this test no evidence could be found on a difference on the amount of cellulose synthesis compared to a normal static growth. However, from the other tests it can be said that there is no significant difference in synthesis performance between normal static growth and when the medium volume changes. More in depth study is needed to substantiate this finding. A more appearant difference in geometry is found from the first test. When substracting medium volume from the vessel, the loosely hanging cellulose fibres on the bottomside of the sample got pulled into the feeding tube. This caused partial slanting of the B.C. sample, resulting in a thickness variation over the sample. This finding was not repeated in test 3B, since not as much loose cellulose was formed. The formation of these loose hanging fibres was different per test and its cause

From the second test, it was concluded that geometries with a thickness of 0.3mm can be directly translated into the forming B.C. layer. This works for both a static medium volume as well as for an increasing medium volume. Smaller geometries could still be tested to have a better understanding of the resolution of the material using this production method. It is acknowledged that only thickness variation in the x- and y-plane does not fully define the resolution.

In test 4, 5 and 6 the results also offered more understanding of the resolution in the z-direction. Accurate measurements of the depth of the indentations are still needed. These were left out of the scope of the project, due to the soft and flexible mechanical behaviour of B.C. and the high precision needed to accurately measure the depth of the indentations that are not even visible to the naked eye.

From the third test it became appearant that using sloped geometry is needed for the release of the growing cellulose layer when the air-liquid interface loses the physical connection with an obstruction. In the samples where the B.C. layer sticked to the geometry, bumps were formed. This behaviour could either be unwanted, since it is rather unpredictable, but when controlled this can also be used to localize these bumps. Slope angle of the performed test is limited to two values, resulting in the drawing of a more general conclusion that sloped geometry is needed for the release from the obstructing geometry. This sloped geometry was not noticibly translated in the grown sample, when compared to the non-sloped geometry tests. In the fourth test this sloping angle was not incorporated. However, this was also deemed unnecessary, since the medium volume was only increased and no releasing from the obstructing geometry took place.

Discussion on the Performance of the Test Setup

Overall, the CelluShaping test setup functions as expected. However, there are some issues with the current version. First of all, the designed lid for the beaker does fit on the beaker with small tolerances. However, this meant that when sterilizing in the autoclave, the glass expands faster than the lid, generating clamping forces which shattered the beakers. Thus, it was not possible to sterilize the whole test setup before and after growth, resulting in additional steps in the growing process. Also, the used connector pieces of the silicone tubes are made of polypropylene, which warp in the temperatures inside the autoclave. The additional steps needed resulted in more risk of contamination of the medium. The highest risk of contamination however was found to be the usage of PLA 3D prints, which could not be sterilized in the autoclave and were sterilized with UV light and 70% ethanol. It is hypothesized that the porosity of the material leads to organisms being trapped in the 3D prints, which were released in the vessel when submerged in the medium. Due to time restrictions it was decided to opt for the quicker prototyping of FDM 3D printing, which led to multiple contaminations.

The usage of the beaker with a hole in the bottom, allowing the connection to silicone tubing did function as intended. However, in some cases it was observed that clogging of the silicone tubing caused issues with the flow of medium. The clogging was in some cases caused by loose floating cellulose fibres, which are resultant from the pumping of the medium. This agitates the medium slightly, resulting in oxygen transport, which causes loose cellulose pellicles to form. Also, it is hypothesized that while being in State 2 (so when loose pellicles form on the air-liquid interface) the shaking of the vessel can lead to the formed pellicles to submerge and also clog the inlet. The current testing setup was placed in an incubator which was used by other students and researchers and opening and closing this incubator causes it to shake. This resulted in differentiation from the intended and modelled medium volume sequence, changing the final outcome.

To have fine control over the medium volume height, a camera was used alongside image recognition software to track the medium level. This method of volume tracking was tested, but it was decided to be left out for the tests performed in this project. This meant that evaporation of the medium was not counteracted in the system, resulting in a slight loss in medium volume per test. This loss however was deemed neglegible, since the performed tests were run for only one week, where evaporation caused a decrease in medium level by less than 0.1mm. When scaling up the production method, so by increasing the surface area of the air-liquid interface and by increasing the growth time, it is expected that this evaporation will become more important to counteract.

Finally, the used pump, where a syringe is placed inside of a pushing mechanism operated by a stepper motor, did allow for fine medium volume control. However, the total amount of maximum volume, being 60mL, to be pumped in and out of the vessel is too low, resulting in a limitation in medium level height differences. This is especially the case when operating multiple vessels with the same pump, resulting in dividing this maximum volume in even smaller parts.

2. Relevance of the Findings

The results of the tests show that the principle "to achieve full freedom in the shaping of Bacterial Cellulose by localising obstruction through the introduction of geometry above and below a moving air-liquid interface" can achieve geometries that are impossible using other conformal techniques. The production method allows for precise thickness variation and the addition of texture to the B.C. sample, while leaving the grown cellulose network intact. The same geometry would be possible by for example CNC milling with a very fine mill, but this would partly destroy the structures made by the bacteria. As stated in the Material Research chapter, 3D printing at these sizes with the methods developed by Hospodiuk-Karwowski et al. (2022) and Binelli et al. (2022) is not yet possible. Also, it is expected that the size of the sample using this production method allows for scaling up.

This localisation of thickness variations in the grown sample has relevance for the NextSkins project and general advances in the biodesign field in multiple ways.

Firstly, the thickness variation will allow for the customization of flexibility and stretchability of the L.T.M. patches by adding cellulose to the parts where more rigidity is needed and removing cellulose where more flexibility is needed. This is important for patches made for moving parts of the body, like armpits or elbows.

Secondly, as stated by Zeng (2023), texture for the L.T.M. is needed to express livingness, act as an interactive interface and emotional avelliation. This production method allows for generating these textures, as well as fine tuning them to the user's needs.

Also, this production method allows for defining the drying time of the patch in every location. This could have multiple benefits. For example, this could aid in providing a location for the L.T.M. where the user can notice that the patch is starting to dry out and that it needs re-wetting or replacement. Also, local drying of B.C. could morph the material in curved shapes, allowing for more complex shapes. One example where this mechanism is used in the bending of wood is Hygroshape, developed by Wood et al. (2021) (see Figure 125 and 126).

Figure 125 - The Hygroshape chair
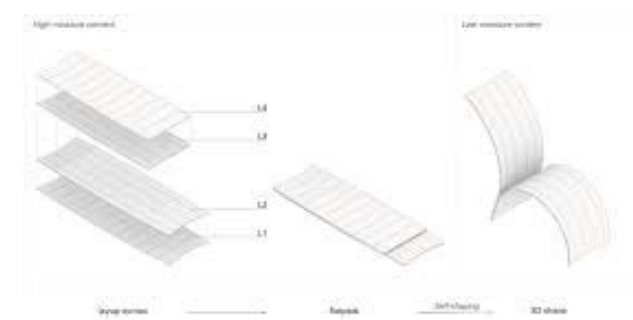
Figure 126 - Graphic visualization of the bending of the wood

Finally, a localised thickness variation allows for adding more active ingredients where more is needed. This allows for the programmability of the habitability of the L.T.M., meaning the livingness of the to be designed artefacts can be adapted to the needs of the user.

3. Conclusion

In this paragraph, the overall conclusions are drawn from the results of testing with the first iteration of a testing setup for CelluShaping.

In the first test, where the overall functioning of the testing setup is evaluated, partial answer on research question D.3. is given. When increasing and decreasing the medium volume with bursts of 8.6mL in 10 seconds, only when subtracting the volume change affects the geometry. The performed test does not include different volume rates and individual increasing and decreasing of the medium volume. Individual increasing and decreasing and a slower volume rate has been tested in the next tests, although with obstructing geometry.

In the second test multiple circular rods with different diameters are tested to answer research question D.4.. Here, no direct answer on the research question could be given, since the smallest geometry did change the geometry of the grown cellulose samples in a stable- and moving air-liquid interface.

In the third test, where multiple single geometries are tested through a moving air-liquid interface, research questions D4., D4.1., D4.2. and D4.6. are partially answered. A limited set of four geometries varying in the x-y plane, as well as in the z-direction have been tested. Here, the main conclusion is that a slanted geometry is needed to release the grown cellulose layer from the obstruction when the vessel's medium volume is decreasing.

In the fourth test, where a combined shape is tested, research questions D2.1., D4., D4.1., D4.3., D4.4., D4.5. and D4.6. are partially tested. Resulting from this test is a first comparison of a modelled B.C. geometry and the outcome. In the model, the bending behaviour is not taken into account, resulting in an overall thickness variation difference. Here, where the model predicted a sample of 8.61mm, the grown B.C.

sample showed a thickness of 2.5mm at its thinnest and 4.5 at its thickest. Also, this caused the indentations made in the grown sample to be slightly different than the modelled sample showed.

4. Recommendations

Resultant from the performed tests with the current setup for CelluShaping, some recommendations for further development of the production method are discussed.

A New Testing Setup
From the discussed points of improvement in Chapter 6.1 a new testing setup is proposed. In Figure X a visualization of this proposed setup is shown. This setup, compared to the used setup, has some key differences.

First of all, the stepper motor operated syringe pump is replaced by a dual leveling system. The inspiration for this system is derived from the filling of multiple connected vessels with medium. When filling one of the vessels, due to them being connected by the silicone tubing, the other vessels also filled up. To speed up this process, I used to lift the already filled vessel up, so the liquid level would be higher than the other vessels, resulting in them filling up more quickly due to hydrostatic pressure generated by gravity. This same principle is used in the proposed setup, where the medium pumping container is placed on a height adjustable platform, also operated by a stepper motor in combination with the used micro-stepping driver and an Arduino. This method of pumping fluid into the vessel allows for more freedom and flexibility in the amount of medium to be transported into and from the vessel(s), while keeping the fine control. Also, instead of translating a volume difference into a liquid level height difference, the changes in height of the pumping volume are directly translated to the height of the air-liquid interface of the vessel.

To seperate the inoculated medium in the vessel(s) from the pumping medium volume, a microbial filter is introduced in the bottom of the vessel. Tests need to be performed if the hydrostatic pressure generated by the pumping mechanism would be enough to overcome the resistance of the filter.

Secondly, the borosilicate glass beaker is replaced by a polycarbonate tube, sandwiched between two aluminium or stainless steel caps connected by threaded rods and bolts. The top cap and bottom cap are different and both have their own purpose.

The top cap consists of two parts. The first part is made to clamp the bottom cap with the polycarbonate tube. This clamping part has a hole in the middle, where the second part slots in. This part, like the designed lid for the current testing setup, is the lid of the vessel and allows for air-flow while keeping out microbes from outside of the vessel. The lid also contains a threaded hole in the bottom, also like the current lid design.

The bottom cap has the same geometry as the top clamping cap, apart from the bottom hole for the valve, the lack of a hole for the lid and four legs to add some height to be able to run the tube in the bottom, which allows for the vessel to be completely emptied. In the threaded hole, a quick-connect valve is screwed in, which allows for deattachment of the vessel from the system, without risk of contamination. The top of the bottom cap consists of a circular groove, which can hold a rubber O-ring, which is used to make the vessel water-tight without the need for glue.

The silicone tubing diameter is increased to 15mm, which allows for more flow of medium and is less prone to clogging. Both sides of the tube are connected to quick connect stainless steel couplers, so all parts of the system can be disconnected without any leakage and risk of contamination.

In the bottom of the vessel a raised microbial filter is placed. There is no difference between the vessel's parts and the medium pump container's parts.

To measure the loss of medium volume due to evaporation more accurately, both the vessel and the pumping volume is placed on seperate load cell sensors. These will allow for accurate monitoring of weight differences in the system, allowing for counteracting evaporation and checking the flow of medium between the containers.

This accuracy of the way of measuring volume, as well as the functioning of the system mainly depends on it being level. Also, some dampening needs to be added to dampen vibrations. Also, it is recommended that the system is placed in a separate incubator to also limit the amount of vibrations during testing.

Re-testing for the current research questions
To improve on the current findings, some tests need to be re-iterated and re-performed. Moving the air-liquid interface without any obstruction at different rates, directions, sequences and durations should be tested first. This will give a first impression on the limitations of the setup. Secondly, more simple obstruction geometries need to be tested above and/or below the air-liquid interface. Multiple variations of geometry conforming Figure X are proposed to be tested in the resulting 'safe' volume sequences from the previously mentioned test. This will provide a better view on the limitations and capabilities of the system. Simultaneous testing is adviced to reduce the amount of time needed.

From these tests, the results should be used to produce a more accurate computational model. Here, a more accurate growth rate for the B.C. layer should be developed, including parameters like nutrient volumes, temperature, humidity, pH and bacterial colony size. Also, physical parameters of the testing setup should be incorporated in the model to predict bending behaviour of the cellulose sample while it is expanding.

Finally, research should be done in the development of an AI model, which could reverse the computational model's function. A model is envisioned where a to be grown 3D model is inserted, resulting from a potential body-scan. The output of this model would be an obstruction geometry, medium volume sequence and growing timeframe.

5. Reflection

In this final paragraph, a reflection is given on the process of this project.

In general, I think I have learned a great deal during this project about what it means to work with a living organism, conducting my own research, the effect of tunnel vision, communication and planning. Also, new skills are acquired regarding lab-work, prototyping, 3D modelling and coding.

I had some difficulties adapting to the more scientific methods needed to perform reliable tests when designing a testing setup. In previous projects, I have been designing products that needed testing to see if the requirements were met and how well the product performs regarding its function. To design a new way of producing geometry with a living organism asked for a different approach. To wrap my head around that and structurise my work, I had to translate my concept of ideas into principles, the product concept into a testing setup and the list of requirements became a list of research questions. When designing a product, smaller prototypes are made to test individual functions and elements in a fast and controlled manner. Working with a living organism meant however that simultaneous testing was not as time effective and more care needed to be put into developing more elaborate tests to test the most simple elements.

In this project, regarding the cooperation between the living organism and me, some issues occurred, which were to be expected. A lot of contaminations occured throughout the process (see Figure X). Some of the contaminations were accounted for, but timewise these setbacks did in the end result in some delay of results. I learned that taking my time in the lab, so working securely when handling the B.C. growing containers, is more time-effective in the long run.

Also, for example unexpected clogging of tubes due to more loose cellulose fibres being formed than usual , or a slower production rate from unexpected causes meant that results from some tests were not as reliable. The instable nature of the organism resulted in some frustration during the project.

Apart from the issues regarding the organism, technical and logistical issues also hampered the process. The ordering of parts from the 3D printing company took more time than advertised, resulting in significant delays of testing. The problem however was that in some cases I could not change to a different production method, since the requirement of sterilization of the parts of the testing setup had to be met. Later in the project, I learned it to be more effective to work with production methods like turning and milling to produce geometry that can be sterilized. I had little experience using these methods, which is why it took me some time to produce the parts. This time was in some cases also needed to work on the report or to prepare a a meeting. However, it was a lot faster than having to wait for the parts for weeks. I would advice anyone who has to produce parts that need to be sterilized to do a course in milling and turning before the project starts.

Regarding the technical issues, a lot of things broke during the project (see Figure X). Breaking equipment is normal in projects, but this project I think I have had the most technical issues than I have had before in one running project.

Unfortunately, lack of communication between me and my mentor and chair sometimes caused some issues. In some weeks I lost oversight, which led to not checking that for example an appointment was set to be the week after. I learned during the project that meeting appointments with my chair, who has a very tight schedule, and mentor I had to check in advance. Also, I learned that it is more effective to have meetings where a onepager has been sent in advance, updating the parties involved on the progress. For some meetings, no time was scheduled to prepare this, which resulted in a more messy meeting from my part.

The ambitions for this project were set high at the beginning, but had to be adjusted during the project. These adjustments were the result of feedback sessions with my mentor and chair, which aided me in getting back on track and to regain focus on the goals of the project. In the beginning, I had expected to deliver a fully tested and iterated prototype for a production method, but in practice the testing of the individual elements of the CelluShaping principle took more time than expected. The testing of the current setup did aid in the production of some interestingly shaped samples and the ideation for a second iteration of the testing setup.

All in all, I think I delivered sufficient results and I am content about the amount of things I have learned in the past half year. I would like to thank all the contributors to this project for their guidance and help.

References

Abeer, M. M., Amin, M. C. I. M., & Martin, C. (2014). A review of bacterial cellulose-based drug delivery systems: their biochemistry, current approaches and future prospects. Journal of Pharmacy and Pharmacology, 66(8), 1047–1061. https://doi.org/10.1111/jphp.12234

Amnuaikit, T., Chusuit, T., Raknam, P., & Boonme, P. (2011). Effects of a cellulose mask synthesized by a bacterium on facial skin characteristics and user satisfaction. Medical Devices : Evidence and Research, 77. https://doi.org/10.2147/mder.s20935

Binelli, M. R., Rühs, P. A., Pisaturo, G., Leu, S., Trachsel, E., & Studart, A. R. (2022). Living materials made by 3D printing cellulose-producing bacteria in granular gels. Biomaterials Advances, 141, 213095. https://doi.org/10.1016/j.bioadv.2022.213095

Bourgeois, J. F., & Barja, F. (2009). The history of vinegar. Archives Des Sciences, 62, 147–160.

Brown, A. J. (1886). XLIII - On an acetic acid ferment which forms cellulose. Journal of the Chemical Society, Transactions, 49, 432–439.

Bungay, H. R., & Serafica, C. G. (1999). Production of microbial cellulose using a rotating disk film bioreactor (Patent No. US5955326A). Rensselaer Polytechnic Institute.

Cannon, R. E., & Anderson, S. M. (1991). Biogenesis of bacterial cellulose. Critical Reviews in Microbiology, 17(6), 435–447. https://doi.org/10.3109/10408419109115207

Chan, C. K., Shin, J., & Jiang, S. K. (2017). Development of Tailor-Shaped Bacterial cellulose textile cultivation Techniques for Zero-Waste Design. Clothing and Textiles Research Journal, 36(1), 33–44. https://doi.org/10.1177/0887302x17737177

Chao, Y., Sugano, Y., & Shoda, M. (2001). Bacterial cellulose production under oxygen-enriched air at different fructose concentrations in a 50-liter, internal-loop airlift reactor. Applied Microbiology and Biotechnology, 55(6), 673–679. https://doi.org/10.1007/s002530000503

Coelho, R. M. D., De Almeida, A. L., Amaral, R. Q. G. D., Da Mota, R. N., & De Sousa, P. H. M. (2020). Kombucha: Review. International Journal of Gastronomy and Food Science, 22, 100272. https://doi.org/10.1016/j.ijgfs.2020.100272

COMSOL. (2015, July 2). The Marangoni Effect: Understanding the Marangoni Effect. Comsol. Retrieved October 24, 2023, from https://www.comsol.com/multiphysics/marangoni-effect

De Azeredo, H. M. C., Da Silva Barud, H., Farinas, C. S., Vasconcellos, V. M., & Claro, A. M. (2019). Bacterial cellulose as a raw material for food and food packaging applications. Frontiers in Sustainable Food Systems, 3. https://doi.org/10.3389/fsufs.2019.00007

Fiedler, S., Fussel, M. B., & Sattler, K. (1989). Gewinnung und Anwendung von Bakteriencellulose. Zentralblatt Für Mikrobiologie, 144(7), 473–484. https://doi.org/10.1016/s0232-4393(89)80037-x

González-García, Y., Meza-Contreras, J. C., Gutiérrez-Ortega, J. A., & Manríquez-González, R. (2022). In vivo modification of microporous structure in bacterial cellulose by exposing Komagataeibacter xylinus culture to physical and chemical stimuli. Polymers, 14(20), 4388. https://doi.org/10.3390/polym14204388

Gutiérrez, E., Burdiles, P. A., Quero, F., Palma, P. V. B., Olate-Moya, F., & Palza, H. (2019). 3D printing of antimicrobial Alginate/Bacterial-Cellulose composite hydrogels by incorporating copper nanostructures. ACS Biomaterials Science & Engineering, 5(11), 6290–6299. https://doi.org/10.1021/acsbiomaterials.9b01048

Gough, P., Yoo, S., Tomitsch, M., & Ahmadpour, N. (2021). Applying Bioaffordances through an Inquiry-Based Model: A Literature Review of Interactive Biodesign. International Journal of Human-Computer Interaction, 37(17), 1583–1597. https://doi.org/10.1080/10447318.2021.1898846

Hestrin, S., & Schramm, M. (1954). Synthesis of cellulose by Acetobacter xylinum. 2. Preparation of freeze-dried cells capable of polymerizing glucose to cellulose. Biochemical Journal. Cellular Aspects, 58(2), 345–352. https://doi.org/10.1042/bj0580345

Hornung, M., Ludwig, M., & Schmauder, H. (2007). Optimizing the production of bacterial cellulose in surface culture: a novel aerosol bioreactor working on a fed batch principle (Part 3). Engineering in Life Sciences, 7(1), 35–41. https://doi.org/10.1002/elsc.200620164

Hospodiuk-Karwowski, M., Bokhari, S. M., Chi, K., Moncal, K. K., Özbolat, V., Özbolat, İ. T., & Catchmark, J. M. (2022). Dual-charge bacterial cellulose as a potential 3D printable material for soft tissue engineering. Composites Part B: Engineering, 231, 109598. https://doi.org/10.1016/j.compositesb.2021.109598

Jang, W. D., Hwang, J. H., Kim, H. U., Ryu, J. Y., & Lee, S. Y. (2017). Bacterial cellulose as an example product for sustainable production and consumption. Microbial Biotechnology, 10(5), 1181–1185. https://doi.org/10.1111/1751-7915.12744

Jonas, R., & Farah, L. F. X. (1998). Production and application of microbial cellulose. Polymer Degradation and Stability, 59(1–3), 101–106. https://doi.org/10.1016/s0141-3910(97)00197-3

Karana, E., Barati, B., Rognoli, V., & Van Der Laan, A. Z. (2015). Material Driven design (MDD): a method to design for material experiences. International Journal of Design, 9(2), 35–54. http://repository.tudelft.nl/islandora/object/uuid:7359026d-57f5-4f63-9835-126c5d23baed/?collection=research

Karana, E., Blauwhoff, D. R. L. M., Hultink, E., & Camere, S. (2018). When the material grows: A case study on designing (with) Mycelium-Based materials. International Journal of Design, 12(2), 119–136. https://pure.tudelft.nl/ws/files/53910160/2918_10991_5_PB.pdf

Karana, E., Barati, B., & Giaccardi, E. (2020). Living Artefacts: Conceptualizing livingness as a material quality in everyday artefacts. International Journal of Design, 14(3), 37–53. https://research.tudelft.nl/en/publications/living-artefacts-conceptualizing-livingness-as-a-material-quality

Kouda, T., Naritomi, T., Yano, H., & Yoshinaga, F. (1997). Effects of oxygen and carbon dioxide pressures on bacterial cellulose production by acetobacter in aerated and agitated culture. Journal of Fermentation and Bioengineering, 84(2), 124–127. https://doi.org/10.1016/s0922-338x(97)82540-8

Krystynowicz, A., Czaja, W., Wiktorowska-Jezierska, A., Gonçalves-Miśkiewicz, M., Turkiewicz, M., & Bielecki, S. (2002). Factors affecting the yield and properties of bacterial cellulose. Journal of Industrial Microbiology & Biotechnology, 29(4), 189–195. https://doi.org/10.1038/sj.jim.7000303

Lahiri, D., Nag, M., Dutta, B., Dey, A., Sarkar, T., Pati, S., Edinur, H. A., Kari, Z. A., Noor, N. H. M., & Ray, R. R. (2021). Bacterial cellulose: production, characterization, and application as antimicrobial agent. International Journal of Molecular Sciences, 22(23), 12984. https://doi.org/10.3390/ijms222312984

Lin, L., Lien, C., Yeh, H., Yu, C., & Hsu, S. (2013). Bacterial cellulose and bacterial cellulose–chitosan membranes for wound dressing applications. Carbohydrate Polymers, 94(1), 603–611. https://doi.org/10.1016/j.carbpol.2013.01.076

Liu, M., Zhong, C., Zhang, Y. M., Xu, Z., Qiao, C., & Shi, J. (2016). Metabolic investigation in gluconacetobacter xylinus and its bacterial cellulose production under a direct current electric field. Frontiers in Microbiology, 7. https://doi.org/10.3389/fmicb.2016.00331

Masaoka, S., Ohe, T., & Sakota, N. (1993). Production of cellulose from glucose by Acetobacter xylinum. Journal of Fermentation and Bioengineering, 75(1), 18–22. https://doi.org/10.1016/0922-338x(93)90171-4 Schramm, M., & Hestrin, S. (1954). Factors affecting production of cellulose at the air/ liquid interface of a culture of acetobacter xylinum. Journal of General Microbiology, 11(1), 123–129. https://doi.org/10.1099/00221287-11-1-123

McQuillan, H., & Karana, E. (2023). Conformal, Seamless, Sustainable: Multimorphic Textile-forms as a Material-Driven Design Approach for HCI. Proceedings of the 2023 CHI Conference on Human Factors in Computing Systems (CHI '23). https://doi.org/10.1145/3544548.3581156

Noh, Y. K., Da Costa, A. D. S., Park, Y. S., Du, P., Kim, I. H., & Park, K. (2019). Fabrication of bacterial cellulose-collagen composite scaffolds and their osteogenic effect on human mesenchymal stem cells. Carbohydrate Polymers, 219, 210–218. https://doi.org/10.1016/j.carbpol.2019.05.039

Park, J. (2009). Bacterial cellulose. In Elsevier eBooks (pp. 724–739). https://doi.org/10.1533/9781845695873.724

Payen, A. (1838). Mémoire sur la composition du tissu propre des plantes et du ligneux. Comptes Rendus Hebdomadaires Des Seances De L'Académie Des Sciences, 7, 1052–1056.

Portal, O., Clark, W., & Levinson, D. J. (2009). Microbial cellulose wound dressing in the treatment of nonhealing lower extremity ulcers. PubMed, 21(1), 1–3. https://pubmed.ncbi.nlm.nih.gov/25904579

Ross, P. S., Mayer, R., & Benziman, M. (1991). Cellulose biosynthesis and function in bacteria. Microbiological Reviews, 55(1), 35–58. https://doi.org/10.1128/mr.55.1.35-58.1991

Sani, A. J., & Dahman, Y. (2009). Improvements in the production of bacterial synthesized biocellulose nanofibres using different culture methods. Journal of Chemical Technology and Biotechnology, 85(2), 151–164. https://doi.org/10.1002/jctb.2300

Shah, A., Raval, A., & Kothari, V. (2016). SOUND STIMULATION CAN INFLUENCE MICROBIAL GROWTH AND PRODUCTION OF CERTAIN KEY METABOLITES. The Journal of Microbiology, Biotechnology and Food Sciences, 5(4), 330–334. https://doi.org/10.15414/jmbfs.2016.5.4.330-334

Sharma, P., Pal, V., Kaur, H., & Roy, S. (2022). Exploring the TEMPO-Oxidized nanofibrillar cellulose and short Ionic-Complementary peptide composite hydrogel as biofunctional cellular scaffolds. Biomacromolecules, 23(6), 2496–2511. https://doi.org/10.1021/acs.biomac.2c00234

Stanisławska A. (2016). Bacterial nonocellulose as amicrobiological derived nanomaterial. Advances in MaterialsScience 16(4), 45-57.

Steel, R., & Walker, T. K. (1957). A Comparative Study of Cellulose-Producing Cultures and Celluloseless Mutants of certain Acetobacter Spp. Journal of General Microbiology, 17(2), 445–452. https://doi.org/10.1099/00221287-17-2-445

Ullah, H., Santos, H. A., & Khan, T. (2016). Applications of bacterial cellulose in food, cosmetics and drug delivery. Cellulose, 23(4), 2291–2314. https://doi.org/10.1007/s10570-016-0986-y

Van Boeijen, A., Daalhuizen, J., Van Der Schoor, R., & Zijlstra, J. (2014). Delft Design Guide: Design Strategies and Methods. Bis Pub.

Wahid, F., & Zhong, C. (2021). Production and applications of bacterial cellulose. In Elsevier eBooks (pp. 359–390). https://doi.org/10.1016/b978-0-12-821888-4.00010-1

Wang, J., Gao, C., Zhang, Y., & Wan, Y. (2010). Preparation and in vitro characterization of BC/PVA hydrogel composite for its potential use as artificial cornea biomaterial. Materials Science and Engineering: C, 30(1), 214–218. https://doi.org/10.1016/j.msec.2009.10.006

Watanabe, K., Tabuchi, M., Morinaga, Y., & Yoshinaga, F. (1998). Structural Features and Properties of Bacterial Cellulose Produced in Agitated Culture. Cellulose, 5(3), 187–200. https://doi.org/10.1023/a:1009272904582

Wiegand, C., Moritz, S., Heßler, N., Kralisch, D., Wesarg, F., Müller, F. A., Fischer, D., & Hipler, U. (2015). Antimicrobial functionalization of bacterial nanocellulose by loading with polihexanide and povidone-iodine. Journal of Materials Science: Materials in Medicine, 26(10). https://doi.org/10.1007/s10856-015-5571-7

Zang, S., Zhang, R., Chen, H., Lu, Y., Zhou, J., Chang, X., Qiu, G., Wu, Z., & Yang, G. (2015). Investigation on artificial blood vessels prepared from bacterial cellulose. Materials Science and Engineering: C, 46, 111–117. https://doi.org/10.1016/j.msec.2014.10.023

Zhong, C. (1996). Method for Edible Fiber Product by Fermentation of Coconut Juice (Patent No. CN1066926C). China National Intellectual Property Administration.

Zhong, C. (2020). Industrial-Scale production and applications of bacterial cellulose. Frontiers in Bioengineering and Biotechnology, 8. https://doi.org/10.3389/fbioe.2020.605374

Zor, E. (2018). Silver nanoparticles-embedded nanopaper as a colorimetric chiral sensing platform. Talanta, 184, 149–155. https://doi.org/10.1016/j.talanta.2018.02.096

Zuo, K., Cheng, H., Wu, S., & Wu, W. (2006). A hybrid model combining hydrodynamic and biological effects for production of bacterial cellulose with a pilot scale airlift reactor. Biochemical Engineering Journal, 29(1–2), 81–90. https://doi.org/10.1016/j.bej.2005.02.020

Żywicka, A., Junka, A., Szymczyk, P., Chodaczek, G., Grzesiak, J., Sedghizadeh, P. P., & Fijałkowski, K. (2018). Bacterial cellulose yield increased over 500% by supplementation of medium with vegetable oil. Carbohydrate Polymers, 199, 294–303. https://doi.org/10.1016/j.carbpol.2018.06.126

Żywicka, A., Ciecholewska-Juśko, D., Drozd, R., Rakoczy, R., Konopacki, M., Kordas, M., Junka, A., Migdał, P., & Fijałkowski, K. (2021). Preparation of Komagataeibacter xylinus Inoculum for Bacterial Cellulose Biosynthesis Using Magnetically Assisted External-Loop Airlift Bioreactor. Polymers, 13(22), 3950. https://doi.org/10.3390/polym13223950

Figures

Figure 1: https://www.e-education.psu.edu/egee439/node/669

Figure 3: https://inhabitat.com/could-bacteria-grown-materials-be-the-future-of-building/

Figure 4: https://mica.bio/project-template-bacterial-cellulose-2/

Figure 6: https://pubmed.ncbi.nlm.nih.gov/36063577/

Figure 7: https://www.sciencedirect.com/science/article/pii/S2772950822003727?via%3Dihub

Figure 89: https://www.icd.uni-stuttgart.de/projects/hygroshape/

Figure 90: https://www.icd.uni-stuttgart.de/projects/hygroshape/

Figure X: https://www.researchgate.net/publication/281701067_Use_of_Bacterial_Cellulose_from_Gluconacetobacter_hansenii_NOK21_as_a_Proton-permeable_Membrane_in_Microbial_Fuel_Cells

Figure X: https://www.sciencedirect.com/science/article/pii/B9780128218884000101#bib28

Appendices

Appendix A: Annotated taxonomy

Oxygen tension

"When oxygen-enriched air was supplied instead of air, the BC production rate increased to 0.093 g/l per h, and the BC yield was enhanced from 11% in air to 18%." (Chao et al., 2001)

Oxygen levels

"The BC production rate was dependent on the oxygen transfer rate, which declined as the broth viscosity increased, accompanied by BC accumulation." (Kouda et al., 1997)

Sound

"Both the sound patterns namelyAhir Bhairav (172-581 Hz) and Piloo (86-839 Hz) were able to significantly affect microbial growth and production of certain keymetabolites by the test microbes." (Shah et al., 2016)

Light

"The polysaccharide production was enhanced 2.28-fold by exposing K. xylinus culture to UV light (366 nm) and 1.7-fold by adding chloramphenicol (0.25 mM) to the medium in comparison to BC control." (González-García et al., 2022)

Agitation rate

"Agitation rate has an impact on the size of the BC. It may decrease the size of BC from 8 mm to <1 mm." (Lahiri et al., 2021)

Electrical charge

"When a DC electric field at 10 mA was applied using platinum electrodes to the culture broth, bacterial cellulose (BC) production was promoted in 12 h but was inhibited in the last 12 h as compared to the control (without DC electric field)." (Liu et al., 2016)

Surface tension

"By supplementing culture media with 1% vegetable oil, we achieved BC yield exceeding 500% over the yield obtained in standard media." (Żywicka et al., 2018)

Temperature

"A temperature range of 25 to 30 °C was found to be best for the production of BC, as a Komagataeibacter sp. Was cultivated at 30 °C for 7 days under static conditions" (Lahiri et al., 2021)

pH

"Thus, pH 4–6 is considered the ideal pH for the fermentation culture medium of BC" (Lahiri et al. 2021)
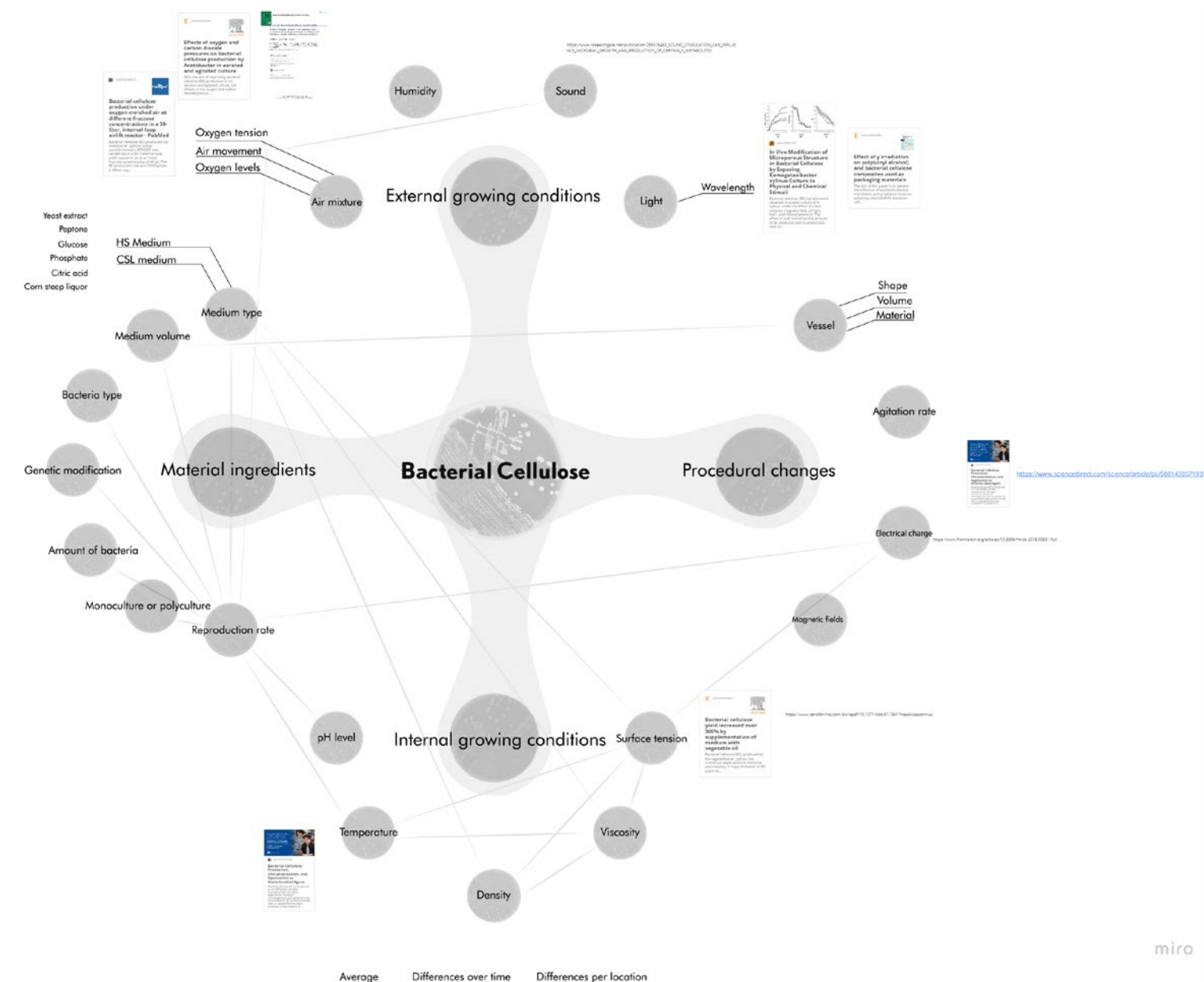
Link to Miro board: https://miro.com/app/board/uXjVMsQDn0M=/

Appendix B: Grasshopper Script

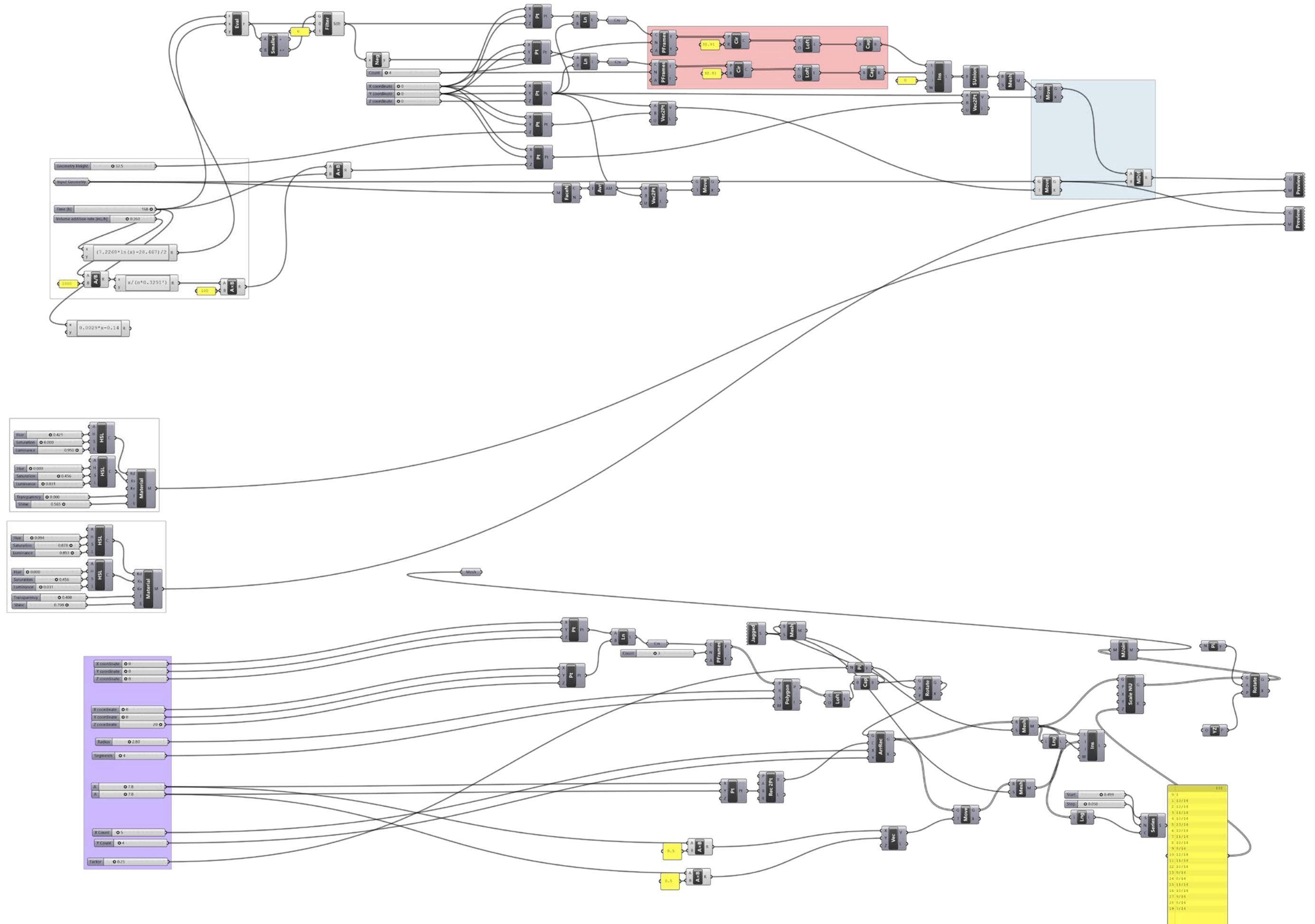# Appendix C- Code for the Time of Flight sensor

```
#include <Adafruit_VL53L0X.h>
// #include <vl53l0x_api.h>
// #include <vl53l0x_api_calibration.h>
// #include <vl53l0x_api_core.h>
// #include <vl53l0x_api_ranging.h>
// #include <vl53l0x_api_strings.h>
// #include <vl53l0x_def.h>
// #include <vl53l0x_device.h>
// #include <vl53l0x_i2c_platform.h>
// #include <vl53l0x_interrupt_threshold_settings.h>
// #include <vl53l0x_platform.h>
// #include <vl53l0x_platform_log.h>
// #include <vl53l0x_tuning.h>
// #include <vl53l0x_types.h>
#include <AccelStepper.h>
#include <MultiStepper.h>
const int stepsPerRevolution = 200;

AccelStepper stepper(AccelStepper::DRIVER, 2, 3);
Adafruit_VL53L0X lox = Adafruit_VL53L0X();

const int numReadings = 10;
const int numReadings2 = 1000;
//const int numExcludedReadings = 8; // Number of readings to exclude at the beginning and end
//float alpha = 0.1;
//float ema = 0;
float totalDistance = 0.0;

bool firstReading = true;
float firstArray = 0;
float firstDistance = 0;
double setpoint = 0;
double kp = 0.1;
double ki = 0.01;
double kd = 0.05;
double error, prevError = 0, integral = 0;
void setup() {
Serial.begin(9600);
stepper.setMaxSpeed(1000.0);
stepper.setAcceleration(500.0);

  while (! Serial) {
    delay(1);
  }

  Serial.println("Adafruit VL53L0X test.");
  if (!lox.begin()) {
    Serial.println(F("Failed to boot VL53L0X"));
    while(1);
  }
  // power
  Serial.println(F("VL53L0X API Continuous Ranging example\n\n"));
  // start continuous ranging
  lox.startRangeContinuous();
}
void loop() {
VL53L0X_RangingMeasurementData_t measure;
  lox.rangingTest(&measure, false);
totalDistance = 0.0;
//if (lox.isRangeComplete()) {
if (firstReading==true) {
  delay (100);
   for (int i = 0; i < numReadings2; ++i) {
    firstArray += lox.readRange();
    //Serial.println(firstDistance);
   }
  firstDistance = round(firstArray / numReadings2);
  Serial.print("First Distance (mm): ");
  Serial.println(firstDistance);
  firstReading = false;
}
  for (int i = 0; i < numReadings; ++i) {
    // pass in 'true' to get debug data
    //if (i >= numExcludedReadings && i < numReadings - numExcludedReadings) {
    //  totalDistance += measure.RangeMilliMeter;
    //}
    totalDistance += lox.readRange();
    //ema = alpha * totalDistance + (1-alpha)*ema;
    // Convert mm to cm
    //Serial.println(totalDistance);
    delay(20); // Delay between readings
  }
//}
float AverageDistance = round(totalDistance / numReadings);
double currentDistance = AverageDistance / numReadings ;
setpoint = firstDistance;
error = setpoint - AverageDistance;
double P = kp * error;
  integral += error;
  double I = ki * integral;
  double derivative = error - prevError;
  double D = kd * derivative;
  double motorSpeed = abs(P + I + D)/10;
```

```
 if (error > 1) {
  stepper.move(stepsPerRevolution);
  stepper.setSpeed(motorSpeed);
  stepper.runSpeed();
 } else if (error < -1) {
  stepper.move(-stepsPerRevolution);
  stepper.setSpeed(-motorSpeed);
  stepper.runSpeed();
 } else {
  stepper.stop();
 }

 Serial.print("Distance: ");
 Serial.println(AverageDistance);
 Serial.print(" mm, Motor Speed: ");
 Serial.println(motorSpeed);

 // Update previous error for derivative term in the next iteration
 prevError = error;

}
```

Appendix D- Code for the pump

```cpp
#include <AccelStepper.h>
#include <Wire.h>
#include <rgb_lcd.h>

// Define the number of steps per revolution for your stepper motor
float STEPS_PER_REV = -83200;
float STEPS_PER_REV2 = 83200;
//float revs = 13;

rgb_lcd lcd;


// Define the pins connected to the stepper motor driver
const int STEP_PIN = 2; // Replace with your pin number
const int DIR_PIN = 3;  // Replace with your pin number

// Create an instance of AccelStepper
AccelStepper stepper(AccelStepper::DRIVER, STEP_PIN, DIR_PIN);

void setup() {
  Serial.begin(115200);
   //lcd.begin(16, 2);
  //lcd.setRGB(0, 128, 64); // Set initial backlight color (R, G, B)

  //lcd.setCursor(0, 0);
  //lcd.print("Revolutions: ");
  // Set the maximum speed and acceleration in steps per second
  stepper.setMaxSpeed(STEPS_PER_REV / 432000);
 // Steps per revolution / time in seconds
  //stepper.setMaxSpeed(STEPS_PER_REV / 5);
  stepper.setAcceleration(STEPS_PER_REV / 2); // Adjust acceleration as needed

  // Set initial speed
  stepper.setSpeed(stepper.maxSpeed());
  delay(50);
  stepper.setMaxSpeed(STEPS_PER_REV2 / 432000);
 // Steps per revolution / time in seconds
  //stepper.setMaxSpeed(STEPS_PER_REV2 / 5);
  stepper.setAcceleration(STEPS_PER_REV2 / 2); // Adjust acceleration as needed

  // Set initial speed
  stepper.setSpeed(stepper.maxSpeed());
  delay(50);
}

void loop() {
  Serial.println("wait");
  //delay(172800000);
  //delay(2000);
  //float totalSteps = STEPS_PER_REV*revs;
  // Move the stepper motor one revolution
  stepper.move(STEPS_PER_REV);
  //Serial.println(stepper.distanceToGo());

  // Run the motor until it reaches the desired position
  while (stepper.currentPosition() != STEPS_PER_REV) {
    stepper.run();
    //  lcd.setCursor(13, 0);
    // lcd.print("  "); // Clear previous count
    // lcd.setCursor(13, 0);
    // lcd.print(STEPS_PER_REV);
    Serial.println(stepper.currentPosition());
  }
  stepper.move(STEPS_PER_REV2);
  //Serial.println(stepper.distanceToGo());

  // Run the motor until it reaches the desired position
  while (stepper.currentPosition() != STEPS_PER_REV2) {
    stepper.run();
    //  lcd.setCursor(13, 0);
    // lcd.print("  "); // Clear previous count
    // lcd.setCursor(13, 0);
    // lcd.print(STEPS_PER_REV);
    Serial.println(stepper.currentPosition());
  }
  // Stop the motor after completing one revolution
  //if(stepper.distanceToGo() == 0) {stepper.stop();}

  // Add a delay before starting the next revolution (if needed)
  //delay(1000); // 1000 milliseconds delay between revolutions
}
```

Appendix D - Unsuccesful Final Test

As a demonstrator, this final test will provide insight in how much contrast can be made in the indentations as well as to provide a more aesthetically pleasing sample.

For this test the following research questions apply:
- How can more contrast in depth of indentations in the cellulose layer be made?
- How does an increased growth time influence the workings of the test setup?
- How does an increased growth time compare to the results of the model?

Method
To best demonstrate the height differences translated in the forming B.C. layer, two models are made. These models contain concentric circular steps, where in model A the step height and width is constant and set to 1.5mm by 5mm. For model B the step height and width vary for every step. In Figure X a section view is shown of both models, depicting the dimensions.

These models are made alongside iterative testing with the computational model. In the model's settings, the B.C. growth rate as well as the feed rate of the medium is set the same as the previous test, being:

$h_{B.C.}(t) = 7.2268\ln(t)-28,467;$
$h_{A.L.I.}(t) = 0.1058t+58.78;$

where t is time in hours and $h_{B.C.}$ is height of the B.C. layer and $h_{A.L.I.}$ is the height of the air liquid interface, both in mm.

After 5 days at the same rate the same amount of volume is removed from the vessel, changing the $h_{A.L.I.}$ formula to:

$h_{A.L.I.}(t) = -0.1058t+71.48;$

Height above the air-liquid interface of both geometries are set the same, being [...] from the bottom of the geometry to the initial air-liquid interface height.

To fabricate both models, first the models were sent to Oceanz Plastics, where it can be SLS 3D printed in PA12 like the designed lids for the vessel. However, due to a slow production time, the parts would not be fabricated in time to be able to test with them within the timeframe of the project. It was thus decided that the models would be fabricated by hand, using a machining process called turning, which was also used in the fabrication of the geometries in paragraph 3 of this chapter. Although time consuming, this method allows for higher precision with tolerances of +-0.01mm.

SECTION c-c SCALE 2:1
SECTION B-B SCALE 2:1